BACHELOR THESIS & COLLOQUIUM – ME184841

FAILURE AND CRACK PROPAGATION PREDICTION ANALYSIS OF A STEAM TURBINE BLADES

FADILAH KURNIA

NRP. 04211541000046

SUPERVISOR:

Ir. Amiadji, M.Sc.
Irfan Syarif Arief, S.T., M.T.

DOUBLE DEGREE PROGRAM
DEPARTMENT OF MARINE ENGINEERING
FACULTY OF MARINE TECHNOLOGY
INSTITUT TEKNOLOGI SEPULUH NOPEMBER
SURABAYA
2019

BACHELOR THESIS & COLLOQUIUM – ME184841

FAILURE AND CRACK PROPAGATION PREDICTION ANALYSIS OF A STEAM TURBINE BLADES

FADILAH KURNIA
NRP. 04211541000046

SUPERVISOR :

Ir. Amiadji, M.Sc.
Irfan Syarif Arief, S.T., M.T.

DOUBLE DEGREE PROGRAM
DEPARTMENT OF MARINE ENGINEERING
FACULTY OF MARINE TECHNOLOGY
INSTITUT TEKNOLOGI SEPULUH NOPEMBER
SURABAYA
2019

“This page intentionally left blank”

APPROVAL FORM

FAILURE AND CRACK PROPAGATION PREDICTION ANALYSIS OF A STEAM TURBINE BLADES

BACHELOR THESIS

Submitted to Comply One of The Requirement to Obtain a Bachelor Engineering Degree

On

Marine Manufacturing & Design (MMD)
Bachelor Program Department of Marine Engineering
Faculty of Marine Technology
Institut Teknologi Sepuluh Nopember

Prepared by:

FADILAH KURNIA
NRP. 04211541000046

Approved by Supervisor:

Ir. Amiadji, M.Sc. ( )

Irfan Syarif Arief, S.T., M.T. ( )

“This page intentionally left blank”

APPROVAL FORM

FAILURE AND CRACK PROPAGATION PREDICTION ANALYSIS OF A STEAM TURBINE BLADES

BACHELOR THESIS

Submitted to Comply One of The Requirement to Obtain a Bachelor Engineering Degree

On

Marine Manufacturing & Design (MMD)
Bachelor Program Department of Marine Engineering
Faculty of Marine Technology
Institut Teknologi Sepuluh Nopember

Prepared by:

FADILAH KURNIA
NRP. 04211541000046

Approved by

Head of Department of Marine Engineering

Dr. Eng. Muhammad Badrus Zaman., ST., MT.
NIP. 199708022008011007

“This page intentionally left blank”

APPROVAL FORM

FAILURE AND CRACK PROPAGATION PREDICTION ANALYSIS OF A STEAM TURBINE BLADES

BACHELOR THESIS

Submitted to Comply One of The Requirement to Obtain a Bachelor Engineering Degree

On

Marine Manufacturing & Design (MMD)
Bachelor Program Department of Marine Engineering
Faculty of Marine Technology
Institut Teknologi Sepuluh Nopember

Prepared by:

FADILAH KURNIA
NRP. 04211541000046

Approved by

Representative of Hochschule Wismar in Indonesia

Dr.-Ing. Wolfgang Busse

“This page intentionally left blank”

DECLARATION OF HONOR

I hereby who signed below declare that:

This bachelor thesis has written and developed independently without plagiarism act, and confirm consciously that all data, concepts, design, references, and material in this report own by Marine Manufacturing & Design (MMD) in Department of Marine Engineering ITS which are the product of research study and reserve the right to use for further research study and its development.

Name	: Fadilah Kurnia
NRP	: 04211541000046
Bachelor Thesis Title	: Failure and Crack Propagation Prediction Analysis of a Steam Turbine Blades
Department	: Marine Engineering

If there is plagiarism act in the future, I will fully responsible and receive the penalty given by ITS according to the regulation applied.

Surabaya, 2019

Fadilah Kurnia

“This page intentionally left blank”

FAILURE AND CRACK PROPAGATION PREDICTION ANALYSIS OF A STEAM TURBINE BLADES

Name : Fadilah Kurnia
NRP : 04211541000046
Department : Marine Engineering
Supervisor I : Ir. Amiadji, M.Sc.
Supervisor II : Irfan Syarif Arief, S.T., M.T.

ABSTRACT

Steam turbine blade are an important component in power plant since its function of converting steam flow energy into mechanical energy through rotary shaft. Blades in low pressure (LP) turbine play a critical role in power generation. It is common to find defect in LP turbine’s blade due to critical operating condition and its significant geometry compare to blades in other stages. Failure in turbine blades commonly caused by high cycle fatigue induced by high steam force and centrifugal force. A large number of high-stress cycle may accumulated in certain area which will caused a crack initiation/propagation if there is no any further action. A failure and crack propagation prediction analysis is perform on last stage blades of 670 MW LP steam turbine. Induced force on the body of blade, determined using Computational Fluid Dynamics (CFD) analysis. A crack model is applied to the blade to observe the stress distribution, fatigue life and crack propagation on each crack variations. Finite Element Method (FEM) is done in this present thesis. Analysis result revealed that the highest stress concentration accumulated in bottom tip of leading edge. Number of cycles before a damage occur on the normal condition blade were calculated. Crack growth rate were also calculated.

Key Word: Failure Analysis, Fatigue, Crack Propagation, Steam Turbine Blades, Finite Element

“This page intentionally left blank”

ANALISA PREDIKSI KEGAGALAN DAN PROPAGASI RETAKAN PADA SUDU TURBIN UAP

Nama : Fadilah Kurnia
NRP : 04211541000046
Departemen : Marine Engineering
Pembimbing I : Ir. Amiadji, M.Sc.
Pembimbing II : Irfan Syarif Arief, S.T., M.T.

ABSTRAK

Sudu turbin uap merupakan komponen yang penting pada pembangkit energi karena fungsinya yang mengubah energi aliran uap menjadi energi mekanik melalui poros yang berputar. Sudu pada turbin tekanan rendah (LP) memiliki peranan penting pada pembangkit listrik. Menemukan kerusakan pada sudu turbin uap tekanan rendah (LP) merupakan hal yang umum dikarenakan kondisi operasi yang kritis serta ukuran geometri dari sudu terkait yang signifikan dibandingkan sudu pada stage lain. Kegagalan pada sudu turbin umumnya disebabkan oleh kelelahan siklus tinggi yang diinduksi oleh tingginya gaya kerja uap dan gaya sentrifugal. Sejumlah besar siklus tegangan tinggi dapat terakumulasi pada area tertentu yang kemudian akan menyebabkan inisiasi/propagasi retakan jika tidak dilakukan penanganan lebih lanjut. Analisa prediksi kegagalan dan propagasi retakan dilakukan pada sudu di stage terakhir dari turbin uap LP berkapasitas 670 MW. Gaya yang terinduksi pada sudu ditentukan menggunakan analisa *Computational Fluid Dynamics* (CFD). Model retakan diaplikasikan pada sudu untuk mengamati persebaran tegangan, ketahanan kelelahan dan propagasi retakan pada setiap variasi retakan. *Finite Element Method* (FEM) dilakukan pada tesis ini. Hasil analisa menunjukan bahwa konsentrasi tegangan tertinggi terakumulasi di ujung bawah tepi depan. Jumlah siklus sebelum kerusakan muncul pada sudu kondisi normal dihitung. Tingkat pertumbuhan retakan juga dihitung.

Kata Kunci: Analisa Kegagalan, Kelelahan, Propagasi Retakan, Sudu Turbin Uap, *Finite Element*

“This page intentionally left blank”

PREFACE

Author would like to praise and thanks to the almighty and merciful Allah SWT for giving knowledge, strength and fortune to work and complete the studies and bachelor thesis. This bachelor thesis is expected to be useful and beneficial for all parties who interested in related studies and field.

Author would like give his warmest regard, gratitude and appreciation for those who have directly or indirectly helped and contributed by guiding, providing knowledge, and supporting author to complete this bachelor thesis.

1. Author's beloved family, Bapak Kukun Kurnia, Ibu Endah Sulistyaningrum, Latifha Kunen Kurnia and Halida Kurnia who never tired of giving support and praying for the best for their youngest son and brother.
2. Dr. Eng, M. Badrus Zaman, ST., M.T. as the Head of Marine Engineering Department, Marine Technology Faculty of Institut Teknologi Sepuluh Nopember
3. Mr. Ir. Amiadji, M.Sc. and Mr. Irfan Syarif Arief, S.T., M.T. as the supervisor who guide and provide knowledge, motivation and encouragement from the beginning to the very last day of this bachelor thesis completion.
4. Mr. Achmad Baidowi S.T., M.T. as laboratory lecturer for the help and contribution of guiding and motivating author during the time in the Marine Manufacturing & Design laboratory.
5. Mr. Rokhmad as Senior Plant Engineer and Mr. Tri Kuswijayanto as Plant Engineer of Paiton Operation & Maintenance Indonesia for helping by providing thesis material and giving author a tremendous knowledge along motivation regarding power generation industry.
6. Mrs. Safina Pahlawani as part of Community and HR Department of Paiton Operation & Maintenance Indonesia for helping author in order to done research and material data collection in related power plant.
7. Desta Rifky Aldara S.T., B.Eng. as author senior in Marine Engineering Department for the time and patience in guiding and helping author.
8. Amelia Nurfitri Fadlilah as author best friend who has been around since day one of university life.
9. Danang Setiabudi and Risdiana Izzaty as author closest friend for giving both physically and mentally support who have been hanging in here long before university life.
10. Best friends, fellow colleagues which I cannot mention who have giving full support in ups and downs from the very beginning of university life.

Author realizes that this thesis remains far away from perfect. Therefore, every constructive suggestions and idea from all parties are highly expected by author to improve this bachelor thesis in the future. Author hope this bachelor thesis can be advantages for all parties who interested in related field.

Author

“This page intentionally left blank”

TABLE OF CONTENT

“This page intentionally left blank”

LIST OF FIGURE

“This page intentionally left blank”

LIST OF TABLE

“This page intentionally left blank”

CHAPTER I

INTRODUCTION

1.1 Overview

Electricity is one of the most essential thing in the history of human being. Not only is electricity one of the foundations of a modern developed society, electricity is also capable of nourishing the advancement of a society. In consequence, electricity supply is a key element of human survival and development.[1]

Power plants worked by converting the heat energy released by a combustion of diesel, natural gas, fuel oil or coal into electricity. The risk of failure in power generation industry is high due to the extreme working operation and condition. It is essential to understand the working principle and behavior of the plant in order to avoid failure(s). Failure generally leads to economic loss due to interruptions in production, consequential failure and required repairs; in addition, they can pose a threat to human health and safety.

Turbine blade are the critical components in power plant which convert the steam flowing into rotary shaft. Steam turbine blades in low-pressure (LP) system are the most important part of all types of the turbine and therefore play an important role in power generation.[11] It is common to find defect or damage in the LP turbine's blade. The failure mechanism of blades may cause by high cycle fatigue induced by high stresses vibrations. Blades vibrations are generally excited by the fluid flow and they may become severe when resonances occur. The forced vibrations may enlarge the stresses resulting in degradation of the blades, which referred as high cycle fatigue. Furthermore, a large number of high-stress cycle are accumulated in the blades during startup of turbines.[19] This phenomenon will caused a crack growth if there is no any further action which known as crack propagation.

In past years, failure and crack propagation analysis in last stage turbine blades have been conducted by many parties.[11,16,17,19] In the present thesis, the failure prediction analysis is perform on last stage blades of 670 MW steam turbine and as the comparison purpose, author will also analyze the first stage blades. There has been no major failure or crack case found in the field which author decide to do a prediction analysis to study the methodology. First of all, the induced force on turbine blade need to determine which in the present paper will done using Computational Fluids Dynamics (CFD) Analysis. From that result, the pressure distribution will generate to get the induced force for Finite Element Analysis. Analysis of turbine blades focused on normal condition and flawed condition, which are analyzed using static structure analysis. Modeling is implemented as the tools to generate the prototype of the real blades. Finite Element Analysis are used to determine the stress distribution, deformation, damage prediction and the life-span of the blade itself. Griffith's–Irwin's formula and Paris-Erdogan Law are used to calculate the crack propagation during the cycle.

1.2 Research Problems

Based on background mentioned above, it can be conclude that problems of this final project are:

a. How is the stress distribution on normal blade and flawed blade of the last stage of a steam turbine plant?
b. How many number of cycles before crack occur in the blades of the last stage of a steam turbine plant?
c. How does the crack propagation behavior on the blade of the last stage of a steam turbine plant?

1.3 Research Limitations

This final project can be focused and organized, with limitations on problem which are:

a. Research object is generic model of last stage blades of 670 MW LP steam turbine.
b. Steam turbine operating condition data such as steam total pressure, total temperature, total amount of mass flow and rotation speed is obtained from certain Power Plant.
c. This research use model initial crack as the input in the FEA analysis.
d. This research use Computational Fluids Dynamic (CFD) as the tools to determine the induced force on turbine blade.
e. This research use Finite Element Method (FEM) as the tools to analyze the structural load distribution and crack propagation.
f. Operating parameters demonstrated to be out range such as the implosions particle phenomenon.
g. The software for modelling the prototype is NUMECA AutoBlade.
h. The software for CFD Analysis is NUMECA Fine Turbo.
i. The software for FEA is Ansys Research 19.
j. Numerical simulations are perform in ASUSTek Computer G501VW Intel ® Core ™ i7-6700HQ CPU @ 2.60 GHz with installed 7.9 GB memory (RAM).
k. This research does not perform metallographic analysis.

1.4 Research Objectives

Based on research problems, the objective of this final project are:

a. To know the stress distribution on normal blade and flawed blade of the last stage of a steam turbine plant.
b. To acknowledge the number of cycles before crack occur in the blades of the last stage of a steam turbine plant.
c. To know the crack propagation behavior on the blade of the last stage of a steam turbine plant.

1.5 Research Benefits

This final project is expected to give benefits for various parties such as academics (Institution) and professional community in related study field. The benefits that can be obtained are:

a. Provides data regarding the stress distribution on normal blade and flawed blade of the last stage of a steam turbine plant.
b. Provides result of the number of cycles before crack occur in the blades of the last stage of a steam turbine plant.
c. Provides result related to the crack propagation behavior on the blade of the last stage of a steam turbine plant.

1.6 Systematics of Writing

The systematics of writing in this thesis are:

- **CHAPTER I INTRODUCTION**
  In this section the authors explain the background of the problem of research to be done, the formulation of the problem, the objectives to be achieved in the experiment, the benefits of future research, scope the problem that limits in doing research, and systematical writing the final task.

- **CHAPTER II LITERATURE STUDY**
  In this section the author explains some basic theories, information from previous papers and journal that support the failure and crack propagation prediction analysis of a steam turbine blades in this final project.

- **CHAPTER III RESEARCH METHODOLGY**
  In this section the authors describe and explain the methodology of the research in form of flow chart steps which arranged systematically.

- **CHAPTER IV ANALYSIS OF RESULT AND DISCUSSION**
  In this section the author describe the process and result regarding failure and crack propagation prediction diagnostic of last stage's blades in a steam turbine plant.

- **CHAPTER V CONCLUSION**
  In this section the authors draw conclusions based on the goals to be achieved in this final project, as well as provide development advice for further research.

“This page intentionally left blank”

CHAPTER II

LITERATURE STUDY

2.1 Steam-Powered Electricity Generation

Electricity is at the root of everything that human think as a modern-being. Not only is electricity one of the foundations of a modern developed society, electricity is also capable of nourishing the advancement of a society. Something as simple as the availability of electric lighting can lead to enormous benefits in terms of levels of life quality.[1] From that simple statement, it can conclude that electricity is one of the most essential thing in the human life history. World energy consumption in 2014 are showed in **Figure 1**.[3] This chart showed how huge the amount of electricity which human used in the modern era.

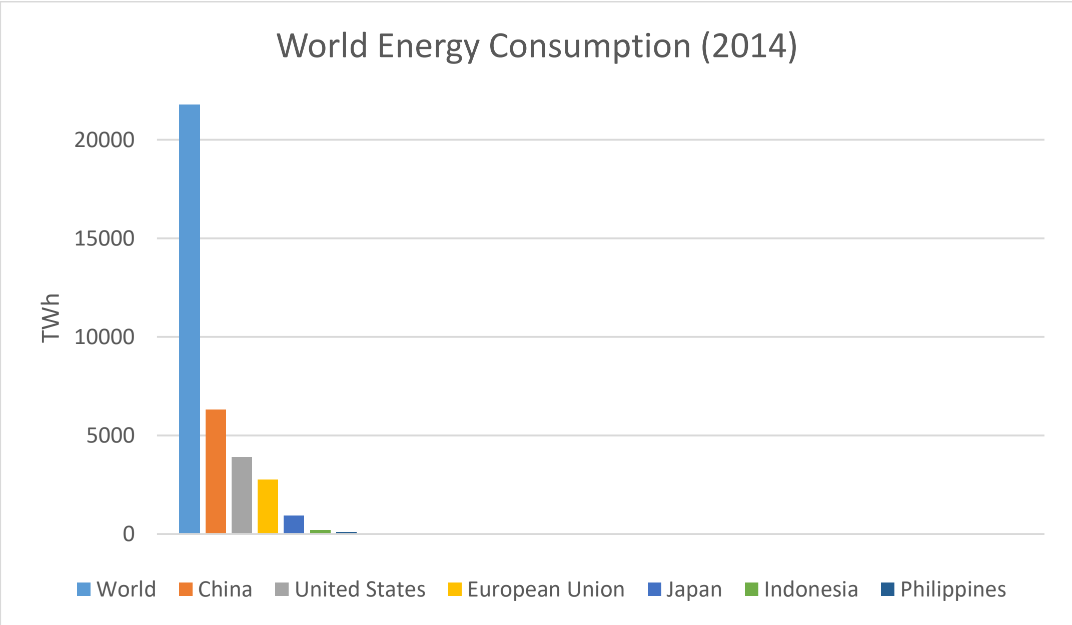

Figure 1 World Energy Consumption (2014) [3]

Power plant concepts are based on the Laws of Thermodynamics, which depict the relationship among heat, work and various properties of the system.[2] Steam is the most important and utilized substance in the beginning time of electricity generation. Steam power was at this stage based on reciprocating steam engines, similar concept to piston engine. These engines were not ideal for the purpose because they could not easily develop the high rotational speeds needed to drive a generator effectively. This difficulty was eventually overcome with the invention of the steam turbine by Sir Charles Parsons in 1884.[1]

Fuel for steam plants was usually coal which used to raise steam in a boiler. Coal is the most important source of electrical power in the world today. At the end of the first decade of the 21st century it was responsible for over 40% of world electricity production, an annual output of around 8100 TWh out of global total of 20,000 TWh in 2010, according to the U.S. Energy Information Administration.[4]

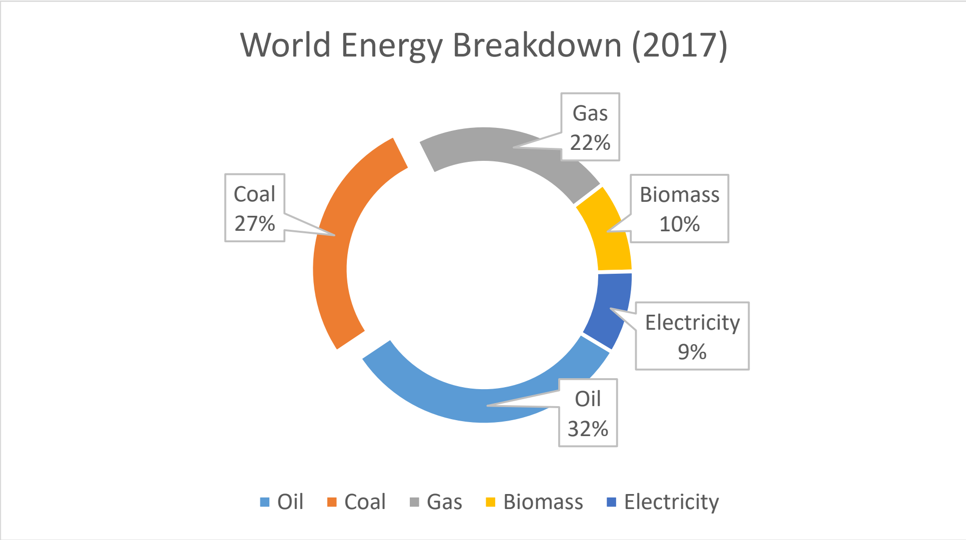

Figure 2 World Energy Breakdown (2017) [5]

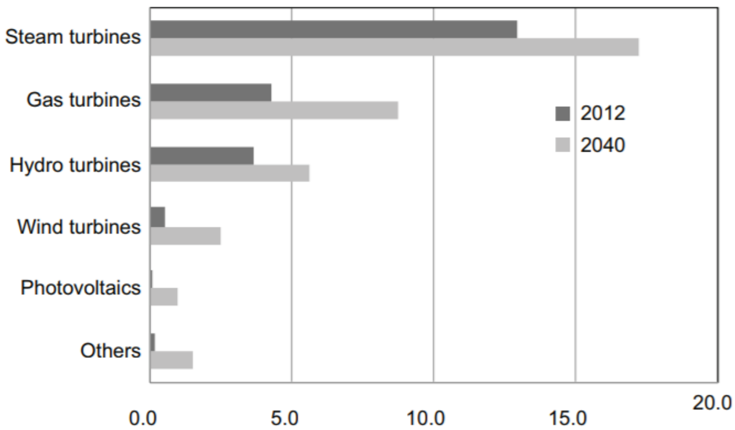

Figure 3 World Electricity Generation in 2012 and 2040 (trillion kWh) [7]

From **Figure 2** and **Figure 3**, it can understand that coal and oil which mostly used steam turbine as the conversion media still take a huge role in the world energy generation and will continue to do so in the future. The power generation percentage by prime movers in all power stations was 60% from steam turbines, 20% from gas turbines, 17% from hydro turbines, 2.4% from wind turbines and 0.5% from PVs in 2012, and is forecast as 47% from steam turbines, 24% from gas turbines, 15% from hydro turbines, 6.7% from wind turbines and 2.6% from PVs in 2040.

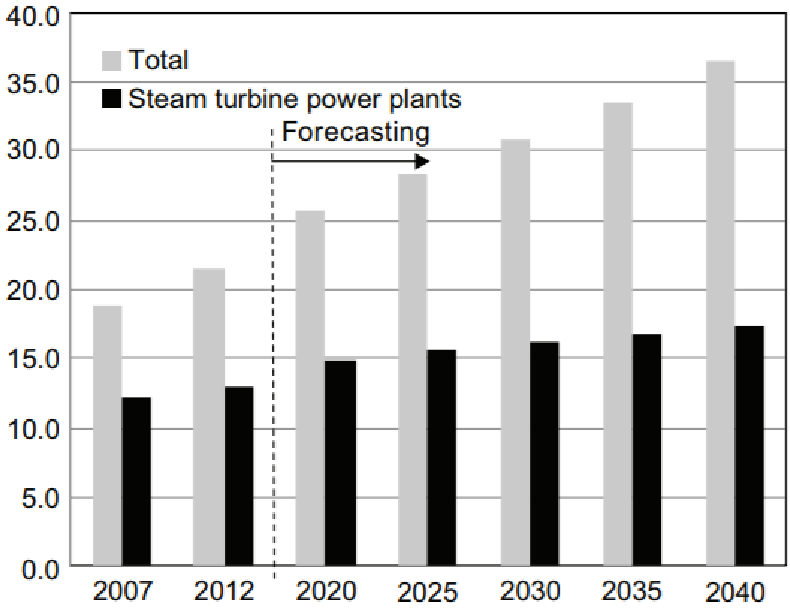

Figure 4 World Power Generation of Steam Turbine Power Plants (trillion kWh) [7]

Figure 4 shows the world power generation of steam turbine power plants calculated using world net electricity generation by fuel (power generation ration of steam turbines, gas turbines, hydro turbines, wind turbines, PVs, and others, by each fuel). The data for 2007 and 2012 are factual, while the data for 2020-2040 are forecast of demand. The electricity generation of steam turbine power plants was 12.1 trillion kWh in 2007, 12.9 trillion kWh in 2012, and 17.3 trillion kWh in 2040.

Steam power plant as a heat engine is a cyclically operating system across whose boundary is a cyclically operating system across which only heat and work flow. This definition incorporates any device operating cyclically and its primary purpose is transformation of heat in form of superheated-steam into work.[2] Referring to **Figure 5**, the heat enters the boiler and leaves at the condenser. The difference between those equals work at the turbine and pump. The working medium is water and it undergoes a cycle of processes. Passing through the boiler and transforming to steam, it goes to the turbine and then to the condenser where it changes back into water and goes to the feed pump, and finally to the boiler again to its initial state.[2]

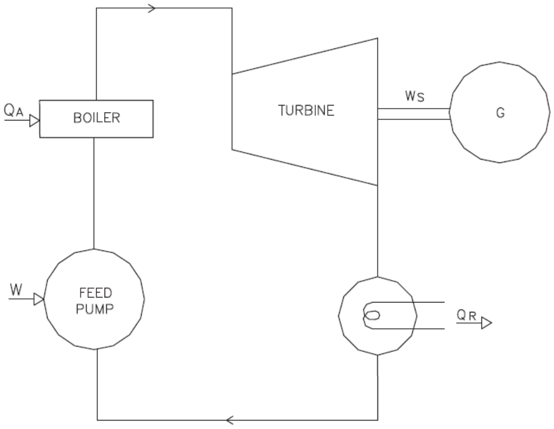

Figure 5 Power Plant as Basic Heat Engine [2]

2.2 Steam Turbine Plant

2.2.1 Steam Turbine Plant History

The modern steam turbine was invented in 1884 by Sir Charles Parson, whose first model connected to a dynamo. The invention of Parsons's steam turbine made cheap and plentiful electricity possible and revolutionized marine transport and naval warfare. Parsons' design was a reaction type.[6]

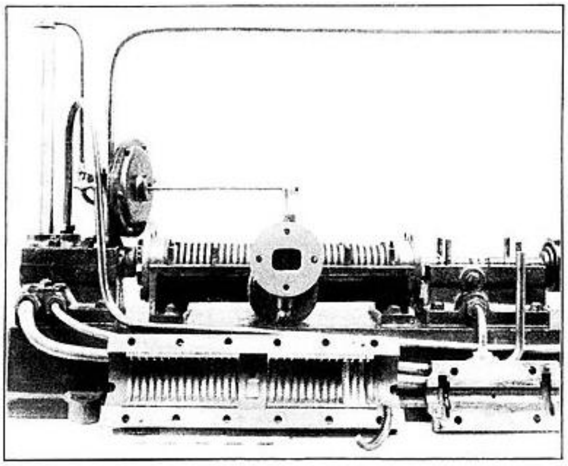

Figure 6 The First Parsons' Turbine [6]

The Brown-Curtis turbine, an impulse type which had been originally developed and patented by the U.S. company, International Curtis Marine Turbine Company. It was developed in the 1900s in conjunction with John Brown & Company.

Steam turbines have been key components of electrical power generation since the 19th century and are one of the distinctive outcomes of the industrial revolution. Steam turbines have played a major role in power-generation industries, upgrading technology innovations for more than 130 years, and they continue to do so today.[7]

2.2.2 Classification of Steam Turbine

Steam turbines are made in a variety of sizes ranging from small units used as mechanical drive for pumps, compressor and other shaft driven equipment, to huge units used to generate electricity. Turbine are consist of two basic components, blades and nozzles. Blade move entirely due to the impact of steam on them and their profiles do not converge. This results in a steam velocity drop and essentially no pressure drop as steam moves through the blades. There are two major classification for steam turbines based on the principle to rotate turbine wheel through the blade which shown in **Figure 7**.

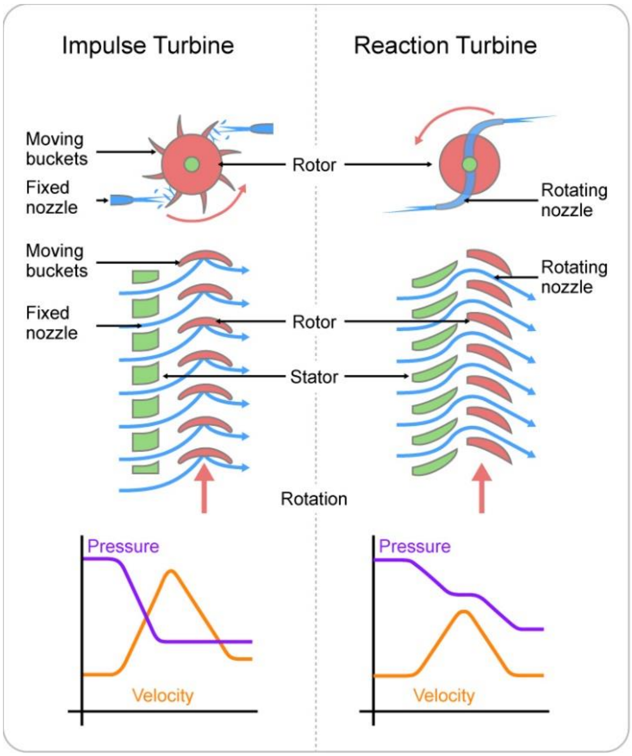

Figure 7 Schematic Diagram of Impulse and Reaction Turbines [8]

Based on the direction of the fluids, steam turbine is classified into two which are axial turbine and radial turbine. Axial turbine work with steam flow direction parallel to the axis of the shaft as it shown in **Figure 8**. Radial Turbine work with steam flow direction perpendicular to the axis of the shaft as it shown in **Figure 9**.

Based on the value of the pressure, steam turbine can divided into 4 category which are low pressure turbine, medium/intermediate pressure turbine, high pressure turbine, and super critical pressure turbine.

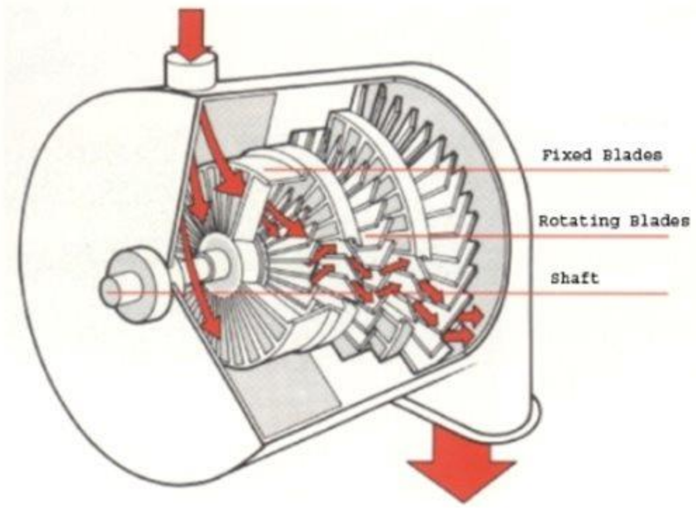

Figure 8 Axial Turbine
(Source: https://www.turbinesinfo.com/wp-content/uploads/2011/07/Schematic-Diagram-of-Parson-Type-Steam-Turbine.jpg)

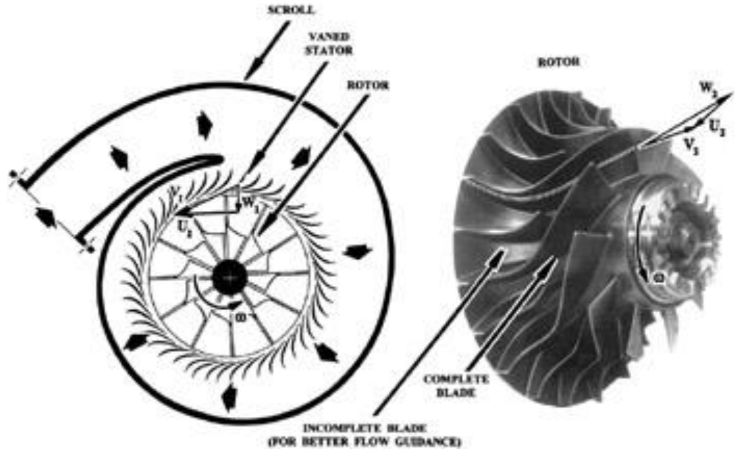

Figure 9 Radial Turbine
(Source: http://images.books24x7.com/bookimages/id_15431/fig418_01.jpg)

2.2.2.1 Impulse Turbine

An impulse Turbine has fixed nozzles that orient the steam flow into high speed jest. These jets contain significant kinetic energy which later converted into shaft rotation by the bucket-like shaped rotor blades as the steam jet changes direction. A pressure drop occurs across the stationary blades with a net increase in steam velocity across the stage. As the steam flows through the nozzle its pressure falls from inlet pressure to the exit pressure. Due to this high ratio of expansion of steam, the steam leaves the nozzle with a very high velocity. The steam leaving the moving blades has a large portion of the maximum velocity of the steam when leaving the nozzle. The loss of energy due to this higher exit velocity is commonly called the carry over velocity or leaving loss.[8]

2.2.2.2 Reaction Turbine

In the reaction turbine, the rotor blades themselves are arranged to form convergent nozzles. This type of turbine makes use of the reaction force produced as the steam accelerates through the nozzles formed by the rotor. Steam is directed onto the rotor by the fixed vanes of the stator. It leaves the stator as a jet that fills the entire circumference of the rotor. The steam then changes direction and increases its speed relative to the speed of the blades. A pressure drop occurs across both the stator and the rotor, with steam accelerating through the stator and decelerating through the rotor, with no net change in steam velocity across the stage but with a decrease in both pressure and temperature, reflecting the work performed in the driving of the rotor.[8]

2.2.3 Principle of Operation of Steam Turbine Plants

Steam generated in the boiler is carried to a steam turbine that is designed to extract as much heat energy as possible from the gas. In a large power station the steam turbine is likely to be composed of at least three elements: a high-pressure (HP) turbine, an intermediate-pressure (IP) turbine, and one or more low-pressure (LP) turbines. Steam passes from one to the next in sequence. Higher efficiency can often be achieved by reheating the steam between the HP and IP turbines by returning it through a special stage of boiler called a re-heater. To extract the maximum amount of energy from the steam, a condenser is fitted to the output of the LP turbine(s) to condense the steam back into water. The colder the cooling water used in the condenser, the higher the efficiency will be. The water is then returned to the boiler and passes around the cycle again.[1]

Conversion the hot steam into electricity relies on the Rankine thermodynamics cycle. Conversion efficiency depends on the temperature and pressure of the steam (more accurately the temperature and pressure drop that is achieved between steam turbine inlet and outlet), so the development of the power plant technology is directed at producing steam at the highest temperature and pressure possible. From an energy viewpoint, therefore, the two most important components of a steam turbine plant are the boiler, which produces high-temperature, high-pressure steam, and the steam turbine, which must then convert the energy carried by that steam into electrical energy.[1]

2.2.3.1 Rankine Cycle

Rankine cycle closely describes the process by which steam-operated turbines. Power depends on the temperature difference between a heat source and cold source. The higher the differences, the more mechanical power can be extracted out of heat energy. The efficiency of Rankine cycle is limited by the high heat of vaporization of the working fluids. The working fluids in Rankine cycle follows a closed loops and is reused constantly. The water vapor with condensed water droplets is created by the cooling systems. The exhaust heat which represented by the "Q_{out}" flowing out of the system shown in the **Figure 10**.

Cooling towers operates as the condenser by absorbing the heat of the working fluids and simultaneously evaporating cooling water to the atmnosphere.

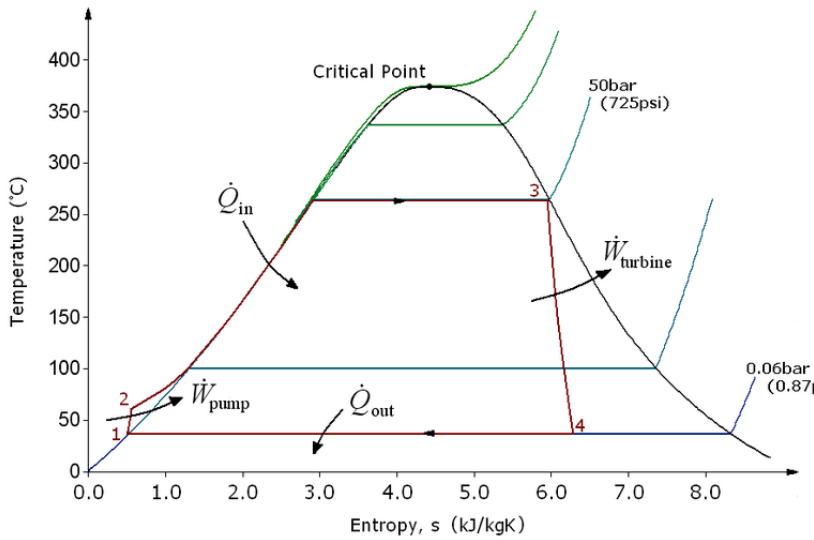

Figure 10 Rankine Cycle
(Source: https://upload.wikimedia.org/wikipedia/commons/thumb/b/be/Rankine_cycle_Ts.png/800px-Rankine_cycle_Ts.png)

There are four processes in the Rankine cycle. These states can be observe in the **Figure 10**.

- **Process 1-2**: The working fluid is pumped from low to high pressure. As the fluids is in a liquid stage, the pump requires an energy input.
- **Process 2-3**: The high pressure liquid enters boiler, where it is heated at constant pressure by an external heat source to become a dry saturated vapor.
- **Process 3-4**: The dry saturated vapor expands through a turbine, generating power by moving the generator. This decreases the temperature and pressure of the vapor, and some condensation may occur.
- **Process 4-1**: The wet vapor then enter the condenser, where it is condensed at a constant pressure to become saturated liquid.

2.3 Failure Analysis

Failure analysis is a process of observation in a structure when a failure or defects occurred, measures shall be taken to prevent similar case by investigating and analyzing the failure. The common objectives of this analysis are to improve the reliability of plant, reduce maintenance cost and reduce risk of accident and pollution.[20]

From an economic perspective, products are manufactured to function reliably and safely during the period for which they are expected to operate. Despite careful design and manufacturing, as well as testing it is not always possible to avoid defects and failure, even when intended manned of operation is implemented. Failure generally leads to economical loss due to interruption in production, consequential failure and required repairs, in addition, they can pose a threat to human health and safety.

2.3.1 Fundamentals and Performance of Failure Analysis

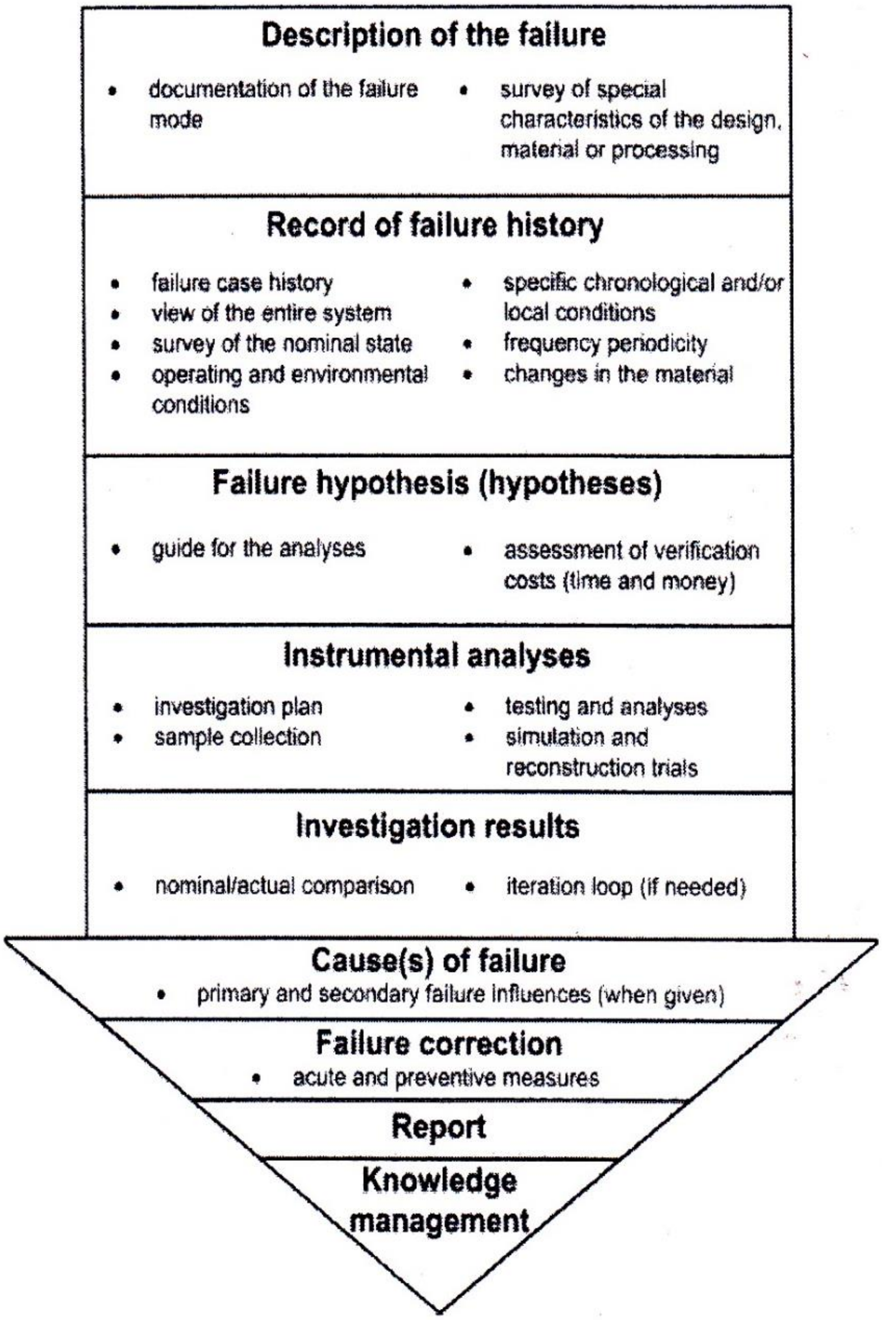

Figure 11 Performance of Failure Analysis Chart
(Source: VDI Guidelines 3822 – Failure Analysis)

According to VDI Guidelines 3822, there are eight steps to perform failure analysis which are:

1. **Failure Description**
   The first step in the whole evaluation of a failure is the description of the failure mode itself. In this conjunction, the failure must be documented by means of photograph or a sketch, and all available operating data must be secured. All visually recognizable abnormalities are to be noted and listed.
2. **Record of Failure History**
   In the process of recording the failure history, background information and framework conditions related to the failure should be identified. This record of failure history is, therefore, of central importance, because the result of later analytical investigation to test the failure hypothesis must always be placed in the context of real framework conditions. Hence, the failure history must be recorded carefully and comprehensively and also take background information into consideration that cannot or yet be brought into an obvious casual connection to the failure. Insufficient failure history record can make failure analysis more difficult or even lead to the analysis in the wrong direction.
   A record of the failure history initially involves recording general information on the product such as description of product, description of functionality, function of the product within the system, description of the effect external factor under operating conditions, history of defective components attempt to reconstruct how the failure occurred, and date of audits, revision or external monitoring certification of any test conducted.
3. **Failure Hypothesis**
   In very few cases is it possible to determine the causes of the failure by using only the description of the failure and the record of failure history. The failure hypothesis shall cite conditions that tend to promote failure and differentiate between consequential failures and potential failures.
   Failure hypothesis must assessed, on the one hand, by comparing them to record of failure history regarding the probability of their occurrence and, on the other hand, with regard to whether they can be proved and/or the effort involved in proving them.
4. **Instrumental Analysis**
   There are many investigation and testing methods available to study failures. The appropriate selection is determined by the available samples, the material to be evaluated and the properties of this material on which the focus is placed by the failure hypothesis adopted, as well as what seems to be a reasonable expenditure of efforts and resources for investigation.
5. **Assessment of the Findings and the Analysis**
   The result of the investigations and test must be viewed in relation to the failure hypothesis. In addition, an independent evaluation should be undertaken to

determine whether the result give rise to new acknowledge or conclusions, were not formulated in the failure hypothesis.

6. **Determination of the Cause(s) of Failure**
   In order to determine the causes of failure, the failure description, the failure history and findings of the instrumental analysis must be logically combined with one another. Depending on the complexity of the case of failure, the result does not always give a clear conclusion to be drawn regarding the causes of failure. The goal of this process is to procure sufficiently secured information regarding one or often a number of possible cause of failure.
7. **Failure Correction**
   The goal of failure analysis is not limited solely to the clarification of the cause of a failure. On the contrary, acute measures to remedy the failure as well as for general failure prevention, should also be developed. In this conjunction, it is important that experience from similar cases of failure comes to bear. The measure that are adopted are used to remedy failure and can be include aspects related to the manufacture design, process, selection of the material and manner of operation.
8. **Report**
   The report on the failure analysis shall be formulated concisely, yet include all of the details that are important for determining the cause, these shall be documented by illustrations and testing data. Recommendations for measures for failure correction and prevention shall also be included. This report will store in the failure record of history which will become an important supporting document if another case happen in the future.

Failure prediction analysis is categorize as the process number four which is the instrumental analysis. This analysis can be conducted even before the occurrence of the failure/defect itself. One of the form of this process is simulation test, the condition and environment are created to be as real as possible so that the result will have a minimum error. In the present day, software based test is commonly used for this process. This kind of test has advantages which one of those is, instead of using physically real prototype, this test uses a modelling process which save huge amount of time and cost yet this simulation test involve a long period of time therefore in some cases impossible to carry out in an emergency situation.

2.3.2 Fundamentals Causes of Failures

Failures occurs when a component or equipment are no longer can perform its intended function safely. This situation can lead to several harmful consequences whether it's technically, environmentally or economically.

Premature failure happens when a defect occurs within the timeframe of design life of the component. Design life is a design criteria understood statistically which means that the expected dispersion of the components' useful life shall be take into account. Design life commonly is related to certain specific types of failure modes, any other occurrence is considered abnormal. This concept does not applicable to components designed for infinite life.

The root cause of a failure is the fundamental reason which made the failure possibly occurs. Multiple root causes are more likely happen when dealing with machinery failures. An effective failure analysis selects the root causes that most effectively avoid repetition pf the failure and in which some action is feasible.

The various types of root causes can be classified in several ways, which are:[20]

1. **Manufacture Design Failures**
   This kind of failure cause are born on the drawing board and such failures can only be avoided through redesign of the failed component/equipment. Design modification can result in unexpected failures if the process is not done carefully. A huge amount of consideration shall be done before creating the new design so that a possible future case will not happen repeatedly.

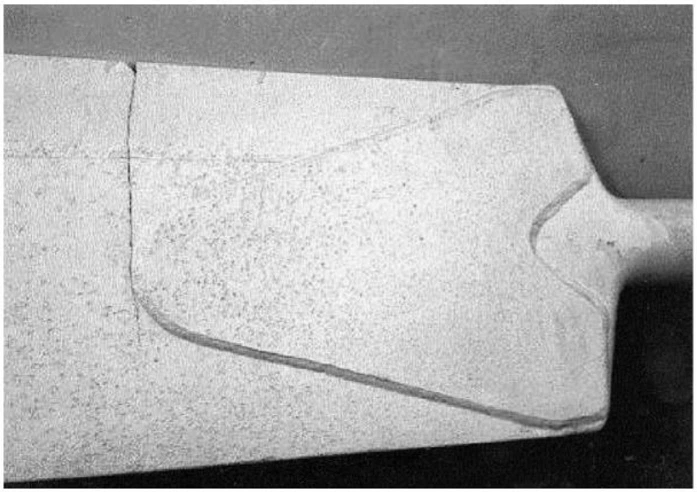

Figure 12 Fatigue Crack Initiated at a Stress Concentration Spot of a Fan Blade [20]

   Manufacture defects also occur due to early process such as machining operation, heat treatment, and welding.

2. **Material Selection Deficiencies**
   A material selection-related failure can also classified as a design failure, as the materials are selected during the process of designing components. This type of causes can be avoided by selecting new material of the components' part.

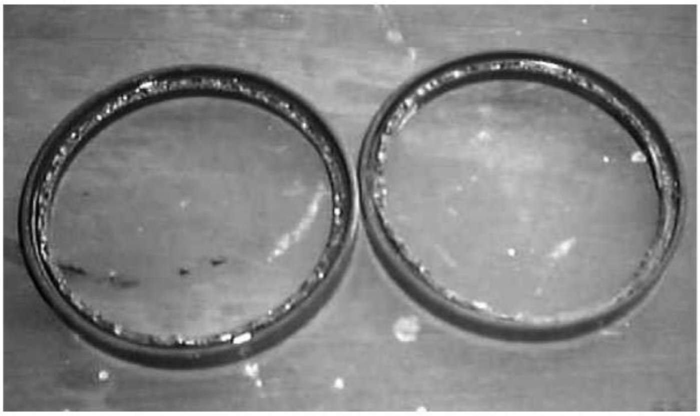

Figure 13 Reciprocating Compressor Oil Scrapper Rings Damaged due to High Temperature [20]

Contributing factors include consequences of selecting certain type of material which has specific properties. Structural material normally are selected for mechanical strength. High strength commonly followed by less ductility of less corrosion resistance. Failure may arise due to these or other properties of the material. Unexpected failure modes also may force a change in material properties. Material imperfection may also be the origin of the machinery failures. Such defects are closely connected to the processing of the raw material during fabrication. Common examples include casting process such as voids, cold shots and pores, forging process, and lamination process.

3. **Assembly and Installation Errors**
   Human imagination is the only limit to the variety of assembly and installation errors. Most of the time, there are the direct consequence of a human error and frequently can be found anywhere. This type of error can be avoided with carefully written procedures, thorough training, correct tools and auditing.
4. **Maintenance and Operation Errors**
   Process machinery often operate under severe and critical conditions, which means that their maintenance and operation shall be conduct with highest quality. Operation process outside of the design conditions not only may reduce the length of the equipment's life but also be dangerous.
   Equipment startup and shutdown is a very critical condition because the machine is subject to conditions which categorize not normal operation including transient loads, flows, temperatures etc. The machine and system design shall allow adequate requirement during these periods.

Figure 14 Gear Coupling with Signs of Severe Wear due to Lack of Lubrication [20]

Analyzing a failure is likely as simple as looking for the reason for what happened at the end of the history. However, commonly the failure analysis process does not contain any record of all events at the disposal. Although the investigation can bring to light most of the history, quite often some parts of it remain unknown.

2.3.3 Failure Caused by Mechanical Working Conditions

2.3.3.1 Failure Designation of Forced Fractures

Forced fracture is a fracture which occurs due a static load. Forced fractures that exhibit a macroscopically visible deformation of the component are designated as ductile forced fractures and this type of fracture commonly occurs in long period of time.

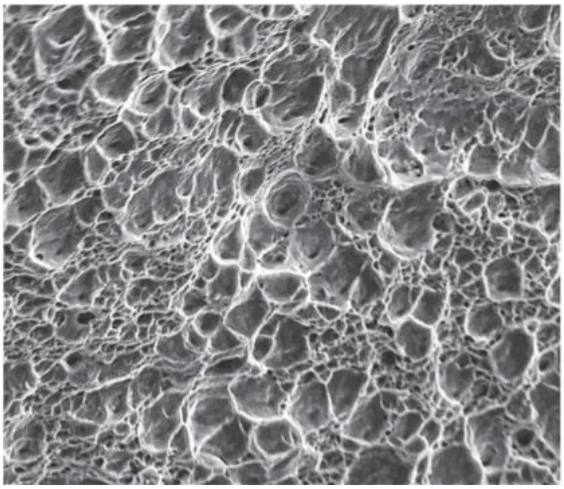

Figure 15 Surface of Ductile Fracture
(Source: K.P. Balan, Fracture Metallugical Failure Analysis, 2018)

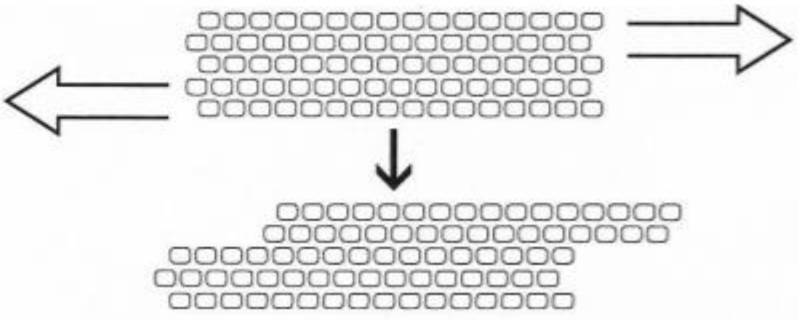

Figure 16 Ductile Fracture Mechanism [20]

Conversely, brittle forced fractures is defined as the forced failure of a component without previous, macroscopically visible deformation and unlike the ductile fracture it commonly occur in very short period of time. Fractured surfaces often exhibit areas of both ductile and brittle forced fracture in close proximity to each other.

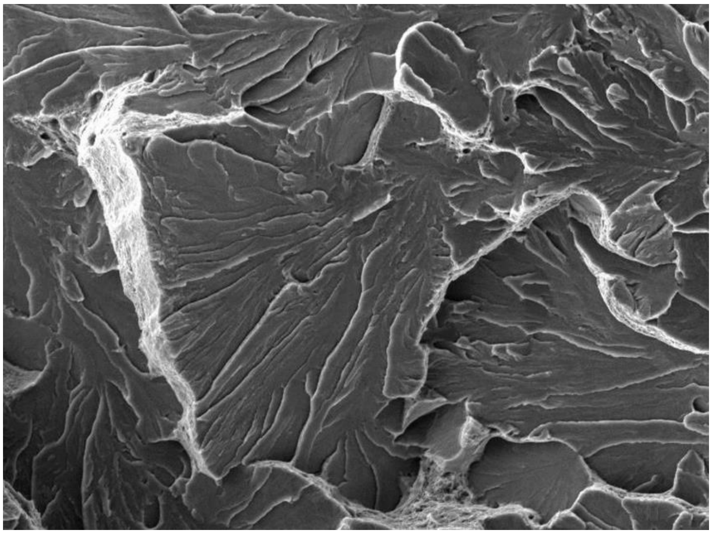

Figure 17 Surface of Brittle Fracture
(Source: http://vgoinc.com/general/fractures-in-the-sem)

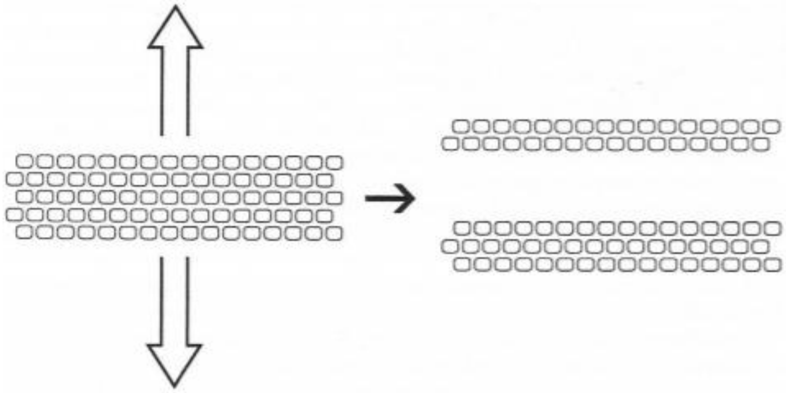

Figure 18 Brittle Fracture Mechanism [20]

2.3.3.2 Failure Designation of Fatigue Fractures

Similar to the case with forced fractures, fatigue fractures can also be designated according to the macroscopic appearance of the failure and the type of load condition that effects it externally. Microscopically, the fatigue fractures can also expand in both a ductile and a brittle manner. The difference with forced fracture is the fatigue fracture occurs due to cyclic loading which can be happen in a zero-based or fully reverse process.

2.4 Fatigue Fractures

Fatigue phenomenon is likely occurs in rotating machineries. This is due to oscillating/cyclic loads present when the machineries operates. According to H.O Fuchs and R.I. Stevens, Fatigue is a progressive and localized process which cause permanent structural modifications in the material. This process occurs due to conditions that cause fluctuating stresses and strains in one or more locations and can result in the formation of cracks and the complete rupture of the component after a sufficient number of cycles. This statement explain that fatigue develop in a certain period of time, a single defect/crack can affect the whole process which implies to worsen the condition, complete rupture means there a crack growth after certain critical condition until the final fracture. Fatigue failure commonly initiate at locations/points with highest stresses such as discontinuities. [21]

High cycle fatigue is the term used to designate the process of final rupture in the cycle-frame of 1,000 to 10,000. In this case commonly the average working stresses are below the yield strength of the material. Contrarily, the term of low cycle fatigue is used for the opposite process which is a smaller number cycles occur until the final rupture and the working stresses are higher than the yield strength of the material. A component categorized to has a finite life when it has remaining life below 10^6 cycles. Vice versa, when it has remaining life above ^{6}, then it categorized to has an infinite life.

2.4.1 Fatigue Fracture Mechanism

Fatigue fracture process commonly divided into three stages [20]:

1. **Crack Nucleation**
   This first stage related to crack formation from the accumulation of shear stresses in certain critical point. This stage require high number of stress cycles to complete and the presence of stress concentrators may greatly reduce the duration of the phase. This stage take most of the load cycles.
2. **Crack Growth**
   The second stage related to the crack growth perpendicular to the main tensile stress. The fracture surface presence is visibly observe with naked eye and it has a beach marks pattern. The second stage can influence most of the fracture surface but not the load cycles.
3. **Final Rupture**
   This stage occur in the very last load cycle. It happens when the crack reaches its final critical crack size. The final fracture area corresponds to the applied mean stress, which means that greater loads normally lead to a greater final fracture area. Sensitivity of the material to crack propagation also play a huge role.

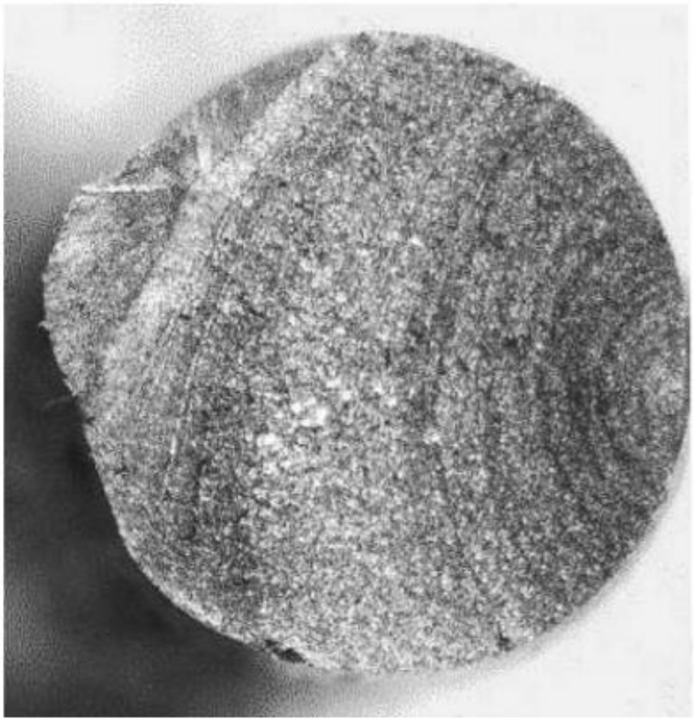

Figure 19 Fatigue Fracture Surface (Beach Marks) [20]

2.4.2 Influenced Factors of Fatigue Strength

The first contribute element in fatigue fracture is the number of cycles which the component exposed with. In some cases, reduction of stress below certain magnitude helps prevent fatigue failure of a component, this is understood as fatigue strength. **Figure 20** illustrates the relation between number of cycles and stress which cause fatigue failure in form of S-N curve.

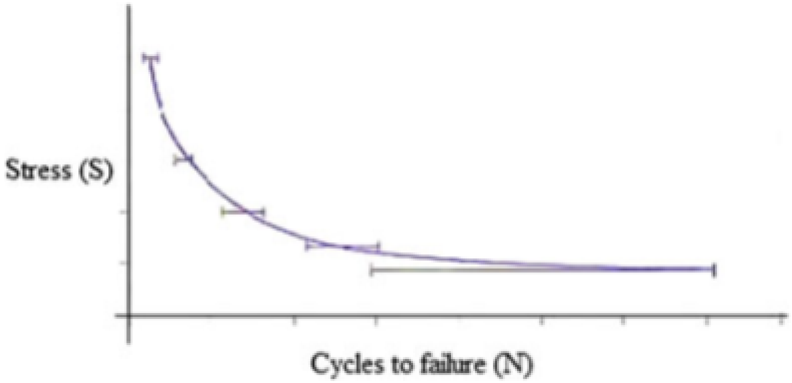

Figure 20 Schematic of S-N Curve Showing Increase in Fatigue Life with Decreasing Stresses (Source: M.A. Maleque, Materials Selection and Design, 2013)

It can conclude that the first factor is fluctuate loads. Then, there is geometry which obviously affect the stress concentration. The last one is environment influence, it can be corrosion, critical temperature, or radiation.

2.4.2 Fatigue Life Methods

Fatigue failure is a complicated occurrence compare to static failure due much complicating factors are involved. Fatigue life methods has an objective to determine the life (number of loading cycles) of an element until failure.

There are three major fatigue life methods where each is more accurate for some types of loading or for some materials. Those methods are the stress-life method, the strain-life method, and the linear-elastic fracture mechanics method. [21]

The stress-life method relates the fatigue life to the alternating stress level causing failure. The data of stress distribution which obtained from simulation or test are used to generate the fatigue strength vs. fatigue life diagram which known as the S-N diagram. For steel alloys the low-cycle fatigue and the high-cycle fatigue can be recognized as having different slopes on the curve in the diagram. **Figure 21** shown the corresponding slopes.

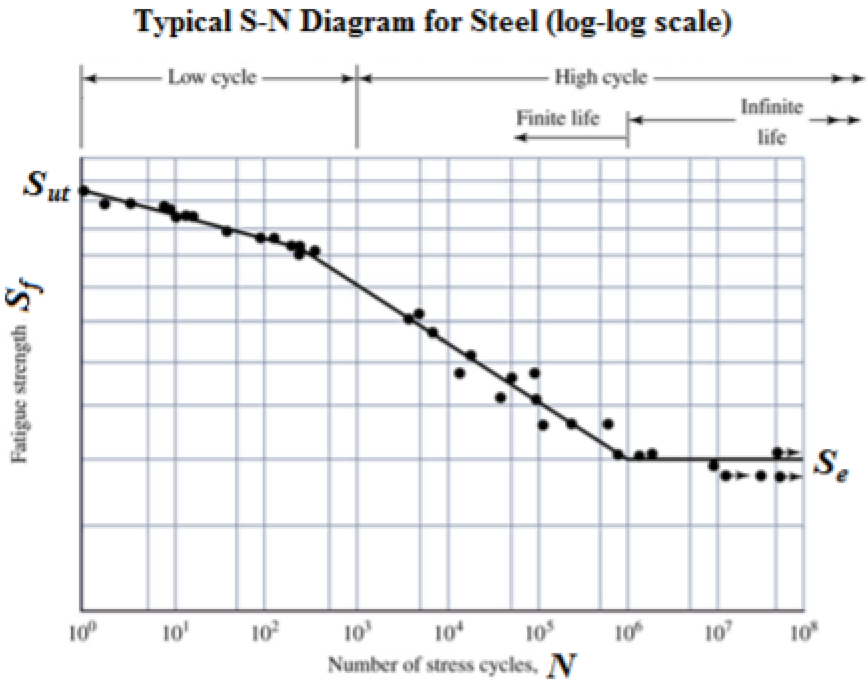

Figure 21 Typical S-N Diagram for Steel [21]

According to the **Figure 21**, if the stress magnitude is reducing then the component will reach to a stress level which it will never fail, and this value of stress is known as the endurance limit (S_e).

The determination of endurance limit is important for designing machinery components which are subjected to high-cycle fatigue. The common practice when designing such elements is to make sure that the fatigue stress level of the elements is below the endurance limit of the material being used. The relationship between the endurance limit and ultimate strength for steel is given as:

$$S_e = \begin{cases} 0.5\, S_{ut} & for\ S_{ut} \leq 1400\ MPa \\ 700\ MPa & for\ S_{ut} > 1400\ MPa \end{cases}$$

Factors which influence the value of endurance limit is considered many and only can obtain by testing a material. Those factors are size, surface finish, correspondent loading, temperature, reliability, and all other factor.

In general, fluctuating stress is categorized into two types which are zero-based and fully-reversed.

σ_m : Mean or average stress, $\sigma_m \frac{\sigma_{max}+\sigma_{min}}{2}$ **[1]**

σ_r : Stress range, $\sigma_r = \sigma_{max} - \sigma_{min}$

[2]

σ_m : Stress amplitude

(half of the stress rang), $\sigma_a \frac{\sigma_{max}-\sigma_{min}}{2}$ **[3]**

Figure 22 shows the illustration of mean stress, stress range, and stress amplitude. **Figure 23** shows the two types of fluctuating stress/load.

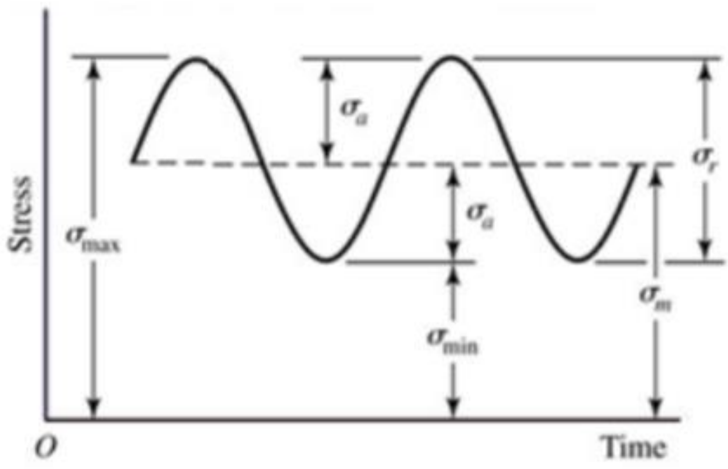

Figure 22 Stress Components [21]

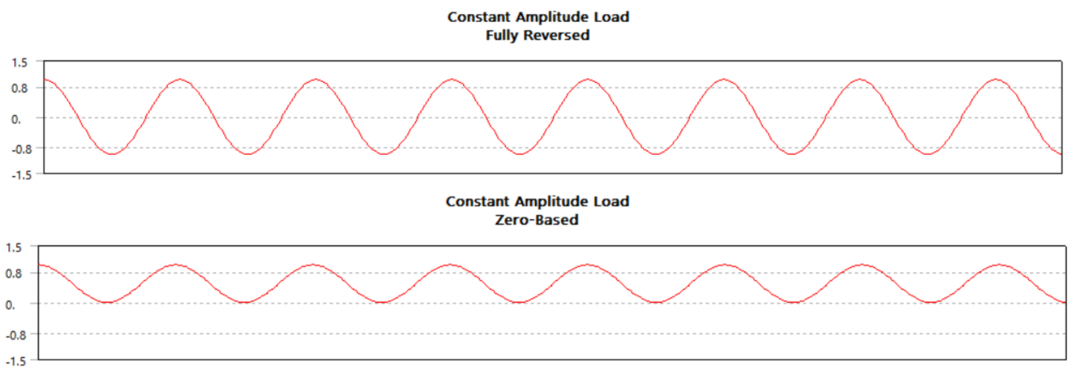

Figure 23 Types of Fluctuating Stress

Goodman theory/line which proposes a failure line which extends from endurance limit on the vertical axis to the ultimate strength on the horizontal axis. It consider failure due to static to be at S_{ut} , it connects S_e on σ_a axis with S_{ut} on σ_m axis using straight line. [22]

$$\frac{\sigma_a}{S_e} + \frac{\sigma_m}{S_{ut}} = \frac{1}{n}$$

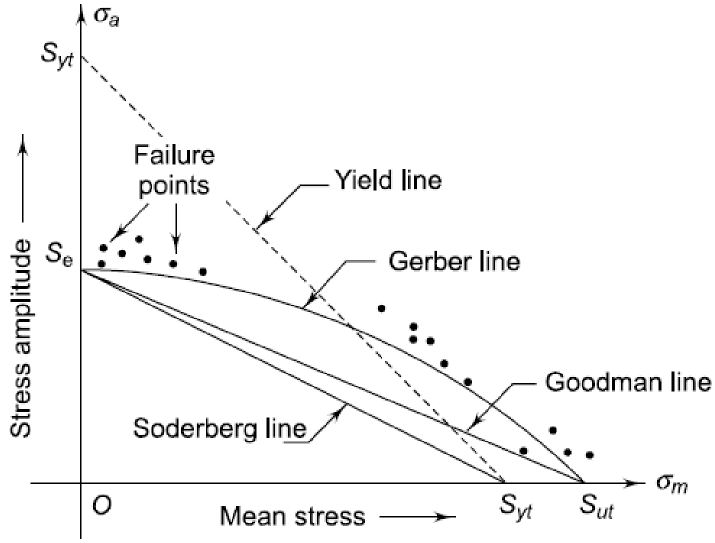

Figure 24 Stress Line Theory
(Source: http://www.ques10.com/p/21916/write-onsoderberg-and-goodman-design-criteria)

2.5 Finite Element Method

The Finite Element Method (FEM), is a numerical method for solving problems of engineering and mathematical physics. Typical problem areas of interest include structural analysis, heat transfer, fluid flow, mass transport, and electromagnetic potential. The analytical solution of these problems generally require the solution to boundary value problems for partial differential equations. The finite element method formulation of the problem results in a system of algebraic equations. The method yields approximate values of the unknowns at discrete number of points over the domain.[18]

FEM is best understood from its practical application, known as finite element analysis (FEA). FEA as applied in engineering is a computational tool for performing engineering analysis. It includes the use of mesh generation techniques for dividing a complex problem into small elements, as well as the use of software program coded with FEM algorithm.[18]

In certain case like turbine failure analysis, FEA can perform to observe the high stress concentration, life-span, and the specific location of the damage which will occur on the object generated by steam pressure and centrifugal load.

2.6 Computational Fluid Dynamics (CFD)

Computational Fluid Dynamics (CFD) is a branch of fluid mechanics that uses numerical analysis and data structures to solve and analyze problems that involve fluid flows. Computers are used to perform the calculations required to simulate the interaction of liquids and gases with the surfaces defined by boundary conditions.

In the simulation process there are three steps that must be done; pre-processing, solving and post-processing.

1. Pre-processor
   Pre-processor is the initial stage in Computational Fluid Dynamics (CFD) which is the stage of data input that includes the determination of domain and boundary condition. At this stage, meshing is also done, where the analyzed object is divided into number of specific grids.
2. Processor
   The next step is the processing or solving stage. At this stage, is done the process of calculating data that has been entered using iterative related equations until the result obtained can reach the smallest error value.
3. Post-processor
   The last step is the post-processing stage. The result of the calculations at the processing stage will be displayed in pictures, graphs and animations.

2.7 Fracture Mechanics

Fracture mechanics was developed during World War I by English aeronautical engineer, A. A. Griffith, to explain the failure of brittle materials.[12]

Fracture mechanics is a subject of engineering science that deals with failure of solids caused by crack initiation and propagation. A fundamental concept of fracture mechanics is to accept the theoretical stress singularity at the crack tip but not use the stress directly to determine failure/crack extension. This is based on the fact that the tip stress is limited by the yield stress or the cohesive stress between atoms and singular stresses are the results of linear elasticity. It is also recognized that the singular stress field is a convenient representation of the actual finite stress field if the discrepancy between the two lies in a small region near the crack tip.[9]

The stress intensity factor K is a measure of the severity of the defect in a given cracked region and its determination is normally the first step in the process of deciding the maximum allowable crack size or stress.[10] The mathematical equation that describe the behavior of the crack propagation is **Eq. 4**[11].

$$K = \beta_{BFS}\beta_{FFS}\beta_{w}\beta_{CFC} * \sigma\sqrt{\pi a} \quad [MPa\sqrt{m}] \tag{4}$$

In which K is Stress Intensity Factor (SIF), β is the geometry factor relationship with consistent structural dimensions. The σ is the nominal stress away from crack. The symbol π is a mathematical constant and a is crack size. The various boundary effects are due to back free surface (BFS), front free surface (FFS), width (w), and crack front curvature (CFC). These boundary effects are neglected and then **Eq. 5**[11] is.

$$K = \beta\sigma\sqrt{\pi a} \quad [MPa\sqrt{m}] \tag{5}$$

where $\beta = 1$

This mathematical equation is the Irwin's modification of Griffith work.[13]

Paris-Erdogan law relates the SIF range to sub critical crack growth under a fatigue stress regime. As such, it is the most popular fatigue crack growth model used in materials science and fracture mechanics.[14]

Certainly in aircraft, but also in other structures as well, it is vital that engineers be able to predict the rate of crack growth during load cycling, so that the part in question be replaced or repaired before the crack reaches a critical length. A great deal of experimental evidence supports the view that the crack growth rate can be correlated with the cyclic variation in the SIF.[15]

$$\frac{da}{dN} = A\Delta K^m \quad [mm/cycle] \tag{6}$$

where da/dN is the fatigue crack growth rate per cycle, $\Delta K = K_{max} - K_{min}$ is the stress intensity factor range during the cycle, and A and m are parameters that depend the material, environment, frequency, temperature and stress ratio which can identified in **Table 1**. This is sometimes known as the "Paris-Erdogan Law" and leads to plots similar to this graphic shown in **Figure 25**.

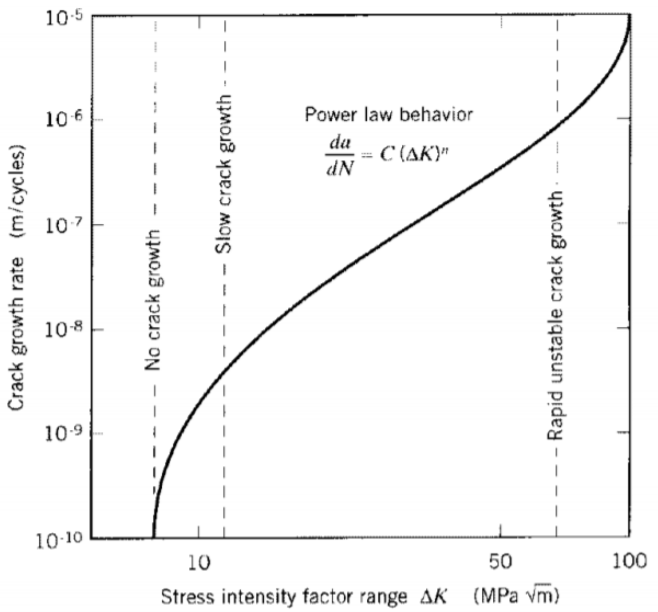

Figure 25 The Paris Law for Fatigue Crack Growth Rates [15]

Table.1 Numerical Parameters in the Paris Equation

No.	Alloy	m	A
1.	Steel	3	10^{-11}

2.	Aluminum	3	10^{-12}
3.	Nickel	3.3	4×10^{-12}
4.	Titanium	5	10^{-11}

CHAPTER III

RESEARCH METHODOLOGY

3.1 Methodology Flow Chart

The methodology flow chart shows all of steps for this final project research. The steps are shown in **Figure 26.**

Figure 26 Methodology Flow Chart

Explanation of the steps of this methodology is as follows:

3.2 Definition of Methodology Flow Chart

1. **Identification & Statement of Problems**
   The first stage is identifies the problems in certain steam turbines failure case(s). There are various types of failure which makes the factors also different. Failure and crack propagation analysis shall perform to determine the number of cycle before crack grows to critical condition.
2. **Literature Study**
   The next study is to conduct a literature study with aim to explaining the depth of review, summarizing the basic theory, general and specific reference, and obtaining various other supporting information related to the final project research. In this final project, the authors conducted a study related to Power Generation, Failure Analysis, Acoustical Engineering and Fracture Mechanics. The resources including Guidelines, Books, Journals, Articles and Websites.
3. **Collecting Data**
   The data needed for the steam turbine blades failure analysis in this final project research is quantitative data. The data including:
   a. Steam Turbine General Dimension
   b. Steam Turbine Operating Condition Data
   c. History and Record of Inspection
4. **Modeling Process**
   Modeling process is conduct to ease the analysis. The model is generated based on general dimension of the real object and shaped as precise as possible.
5. **Computational Fluid Dynamics**
   This process is done to determine the induced force on surface of turbine blades by analyze the interaction of fluids on object's body.
6. **Structural Analysis of Normal Blade**
   This analysis aims to map the stress distribution on normal blade's surface which later used in determining the area where critical condition is occur due to fatigue phenomenon.
7. **Structural Analysis of Cracked Blade**
   This analysis aims to map the stress distribution on cracked blade's surface which later used in determining the area where critical condition is occur due to fatigue phenomenon.
8. **Determination of Critical Condition**
   This process is done by analyzing the result from previous steps. This process show where exactly the area with highest value of stress concentration and minimum remaining life where damage may possibly occur.
9. **Crack Propagation Analysis**
   The stress distribution from previous result will become the input data to Griffith-Irwin formula and the output the value of SIF. This SIF will become the input data

to Paris-Erdogan Law. From this law, it can be observe the crack propagation growth rate.

“This page intentionally left blank”

CHAPTER IV
DATA ANALYSIS

4.1 3D Modeling of 670 MW LP Steam Turbine

In this sub chapter author will explain the process of determination each dimension of the turbine, drawing of the turbine and how the mesh generated in the body of each blades in steam turbine. NUMECA Autoblade software is used to draw the blades in each stages and for mesh generation, author used NUMECA AutoGrid as the tool.

4.1.1. Steam Turbine General Dimension Determination

Data obtained from research in certain power plant are consist of general dimension of the steam turbine, the steam turbine general layout, the number of blades in last stage, the length of blades in last stage blade. From here, the author process the data into model of the turbine itself.

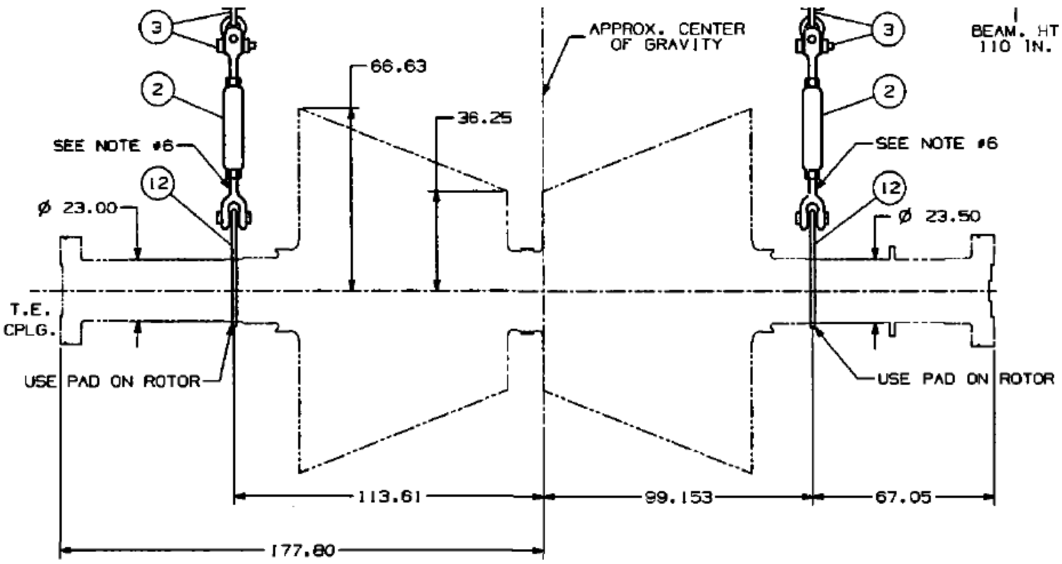

Figure 27 LP Steam Turbine General Dimension
(Source: Author's Data Collection)

Figure 27 show the arrangement and the general dimension of the LP steam turbine. This data will become the parameter of drawing process. Meanwhile, **Figure 28** show the layout inside the LP Turbine, which from there we can determine the number of stages on the plant. Based on those data, the total length of rotor is 71.153 inch (1.807 metre) with total 6 stages consist of 6 rotors and 6 stators.

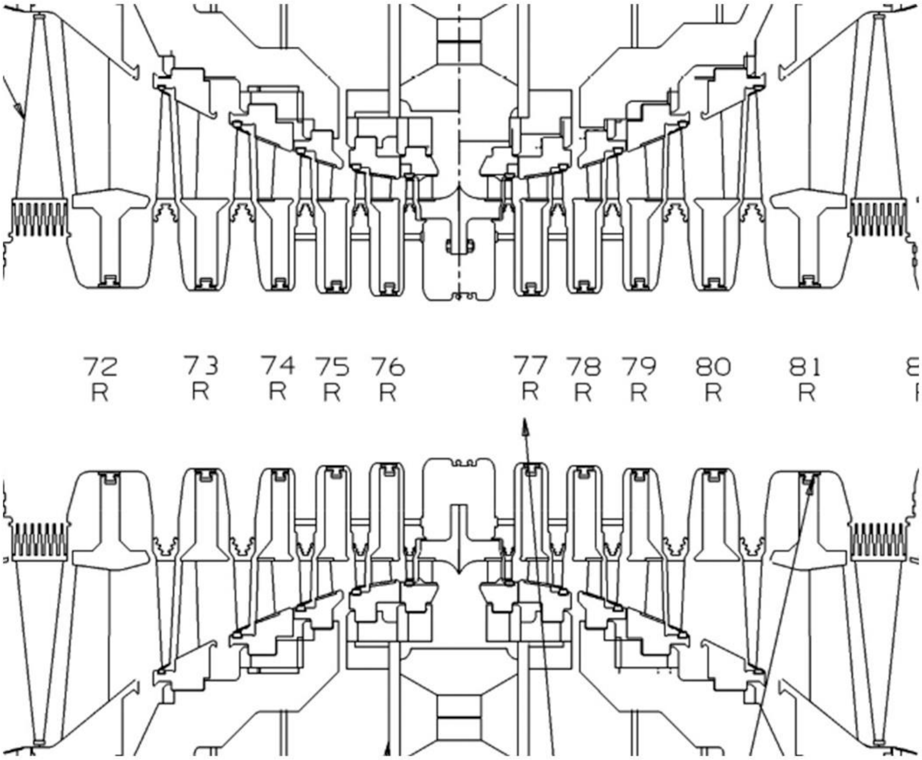

Figure 28 Layout of Steam Turbine
(Source: Author's Data Collection)

From available data, it obtained the length of the blades in the last stage (stage 6th) is 33.5 inch (0.838 metre) and the total number of blades is 94 units. Since the degree of each stage is 0, so the number of blades in the next series of stages is considered same with the last stage. The length of blades in each stages is determined by plotting the layout on drawing software and measured one by one with the main parameter is the last stage data. The process is shown in **Figure 29** and result is shown in **Table 30**

Table 2 Measurement of Blades in each Stages

		Number of Blades	Blade Length in inch	Blade Length in metre
Stage 1st	Stator 1	94	6	0.152
	Rotor 1	94	6.1	0.155
Stage 2nd	Stator 2	94	6.6	0.168
	Rotor 2	94	7.1	0.180
Stage 3rd	Stator 3	94	8.7	0.221
	Rotor 3	94	9.6	0.244
Stage 4th	Stator 4	94	12.5	0.318
	Rotor 4	94	14	0.356
Stage 5th	Stator 5	94	18	0.457

	Rotor 5	94	20.2	0.513
Stage 6th	Stator 6	94	28.3	0.719
	Rotor 6	94	33.5	0.851

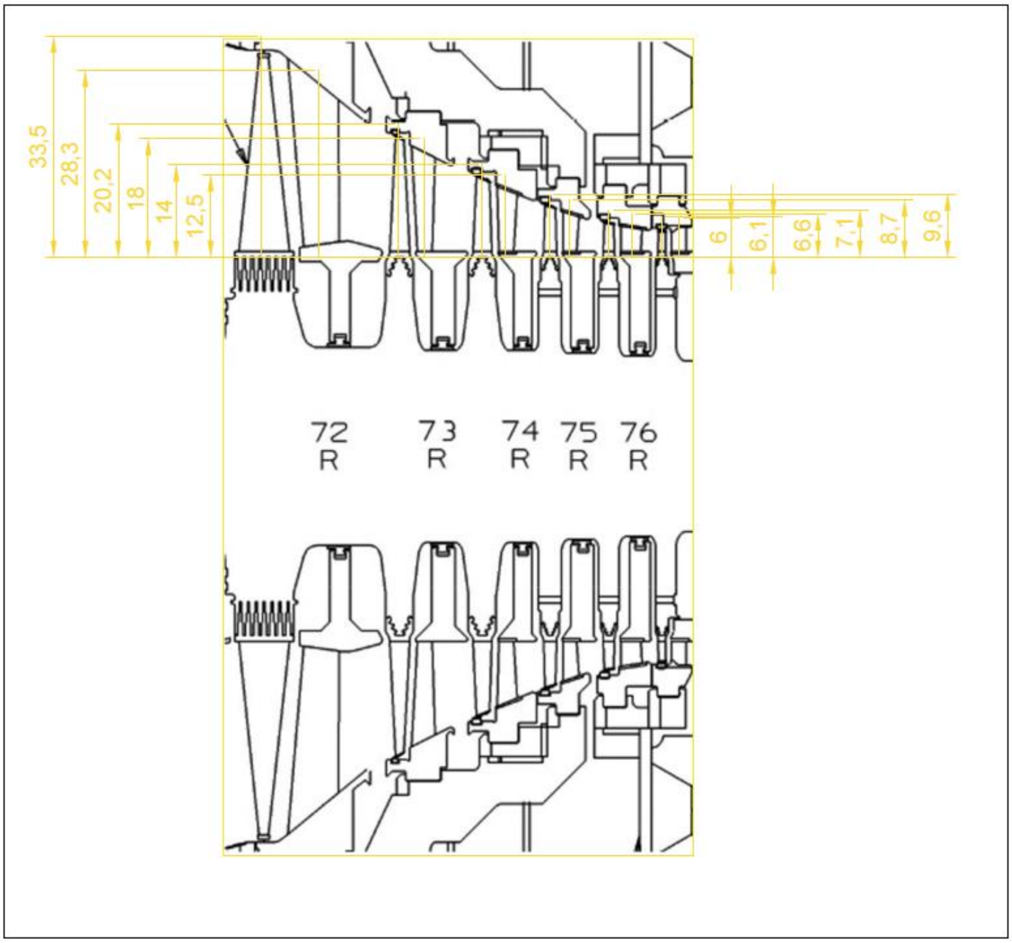

Figure 29 Plotting of Layout in Drawing Software (Blade Length Measurement)

The distance of each stages is also measured with the same method of using plotting in drawing software. **Table 3** is show the result of distance measurement of each stages. The point where lead to the first stage is considered as “Z0” and the end point is considered as “Zn”. The total length from Z0 to Zn is 71.153 inch (1.807 metre).

The shroud and bucket radius also determined in this chapter using the data of general dimension showed in **Figure 27** and the last stage measurement become the main parameter for another stages. The shroud radius of the last stage (stage 6th) from the centerline is 66.65 inch (1.693 metre) and the hub radius of the last stage from the center line is 33.15 inch (0.842 metre). The radius of hub of each stages is considered the same since the degree from one stage to another is 0 and the dovetail point of every stages are in-line. The shroud radius is calculated by adding the value of hub radius and blade length. The result of shroud and hub radius measurement process can observe in **Table 4**.

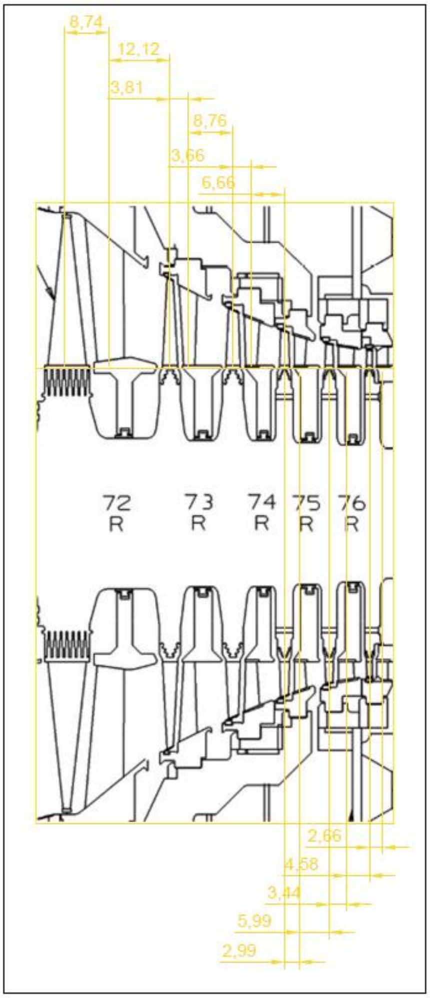

Figure 30 Plotting of Layout in Drawing Software (Stages Distance Measurement)

Table 3 Measurement of Distance each Stages from Z0

		Distance from Z0 in inch	Distance from Z0 in metre
Stage 1st	Stator 1	7.743	0.197
	Rotor 1	10.403	0.264
Stage 2nd	Stator 2	14.983	0.381
	Rotor 2	18.423	0.468
Stage 3rd	Stator 3	24.413	0.620
	Rotor 3	27.403	0.696
Stage 4th	Stator 4	34.063	0.865

	Rotor 4	37.723	0.958
Stage 5th	Stator 5	46.483	1.181
	Rotor 5	50.293	1.277
Stage 6th	Stator 6	62.413	1.585
	Rotor 6	71.153	1.807

Table 4 Measurement of Hub and Shroud Radius

		Hub Radius in inch	Hub Radius in metre	Shroud Radius in inch	Shroud Radius in metre
Stage 1st	Stator 1	33.15	0.842	39.15	0.994
	Rotor 1	33.15	0.842	39.25	0.997
Stage 2nd	Stator 2	33.15	0.842	39.75	1.010
	Rotor 2	33.15	0.842	40.25	1.022
Stage 3rd	Stator 3	33.15	0.842	41.85	1.063
	Rotor 3	33.15	0.842	42.75	1.086
Stage 4th	Stator 4	33.15	0.842	45.65	1.160
	Rotor 4	33.15	0.842	47.15	1.198
Stage 5th	Stator 5	33.15	0.842	51.15	1.299
	Rotor 5	33.15	0.842	53.35	1.355
Stage 6th	Stator 6	33.15	0.842	61.45	1.561
	Rotor 6	33.15	0.842	66.65	1.693

4.1.2. Drawing Process of Steam Turbine

Drawing and 3D modeling of research object is done to ease the next process which is a numerical simulation. This section will explain about the drawing process in the NUMECA AutoBlade software. The input of this process are values that obtained in the previous section which are radius of hub, radius of shroud, distance of each stages and the number of blades in each stages. Stator and rotor are drawn one by one. Steps in this section including hub and shroud endwalls definition, stream surface definition, main blade and construction plane.

4.1.2.1. Hub and Shroud Endwalls Definition

Hub and shroud endwalls surfaces defined by 2 curves (Z and R), where Z and R are the coordinate point of axial and radial directions. Both hub and shroud can be defined separately. In this process, the value of Z and R is inputted based on the previous result of plotting the inside layout of steam turbine. In **Figure 4.5**, it shown the hub and shroud curve type of turbine design. The value of Z and R are shown in **Figure 4.6**.

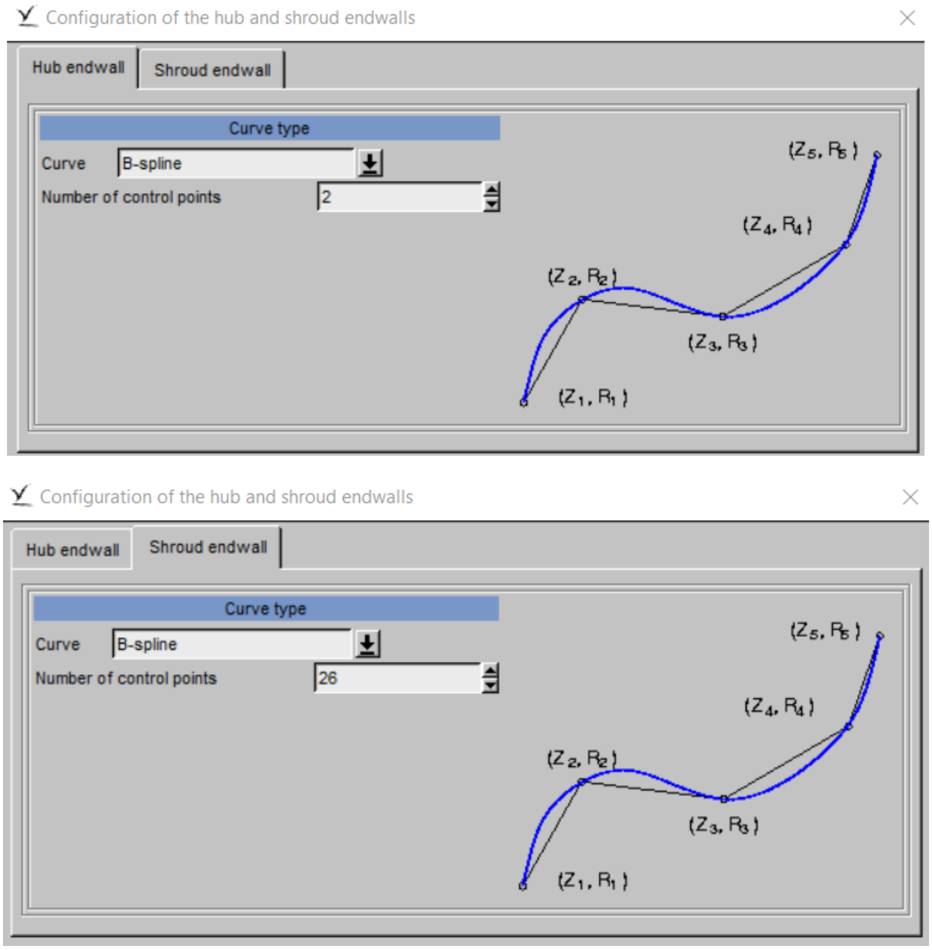

Figure 31 Configuration of Hub and Shroud Endwalls

List of parameters currently in use

Group: endwalls   Filter:

Name	Lower bound		Expression	Value	Upper bound	Reference
HUB_Z1	0			0	0	0.001
HUB_R1	0.842			0.842	0.842	0.001
HUB_Z2	1.807			2	1.807	0.001
HUB_R2	0.842			0.842	0.842	0.001
SHROUD_Z1	0			0	0	0.001
SHROUD_R1	0.994			0.994	0.994	0.001
SHROUD_Z2	0.11688729220			0.197	0.26306556608	0.001
SHROUD_R2	0.88244116245			0.994	1.02861943633	0.001
SHROUD_Z3	0.26444821086			0.247	0.36555497021	0.001
SHROUD_R3	0.96667461846			0.994	1.06778137782	0.001
SHROUD_Z4	0.36829913194			0.264	0.45497587406	0.001
SHROUD_R4	0.94896197127			0.997	1.03563871339	0.001
SHROUD_Z5	0.45576953854			0.314	0.54034312272	0.001
SHROUD_R5	1.00419654573			0.997	1.08877012991	0.001
SHROUD_Z6	0.54300144127			0.381	0.64180648522	0.001
SHROUD_R6	0.99456327217			1.01	1.09336831612	0.001
SHROUD_Z7	0.64318102561			0.431	0.69881583915	0.001
SHROUD_R7	1.04550176287			1.01	1.10113657641	0.001

Figure 32 R and Z value

4.1.2.2. Stream Surface Definition

For this section is define the stream surface type, the rulings and the spanwise location of their traces in the meridional plane. The primary sections is defined the stream surface type which in axial turbine commonly use cylindrical for surface set up. The radius of hub and shroud which inputted on the software are following the values from previous steps on each stages. The number of Z control points in shroud part is determined to be 26 points with each value of Z is slightly modified in order to meet mesh generation requirement, this also aims to plot the steam path for the mesh generating process and CFD simulation. **Figure 33** shown the configuration of steam surfaces and **Figure 34** shown the meridional plane of the blades.

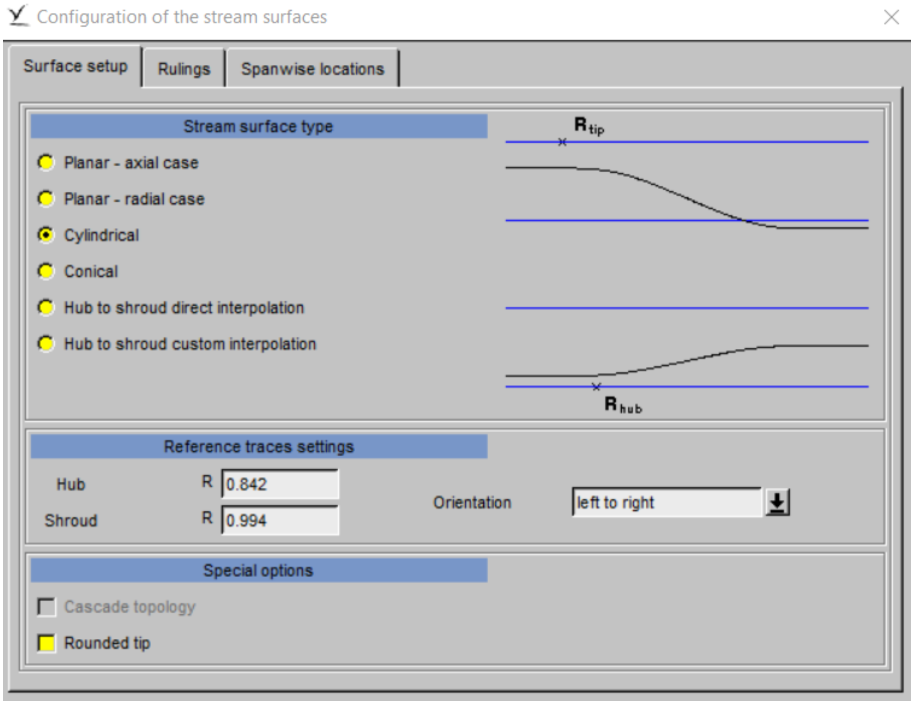

Figure 33 Configuration of Stream Surfaces

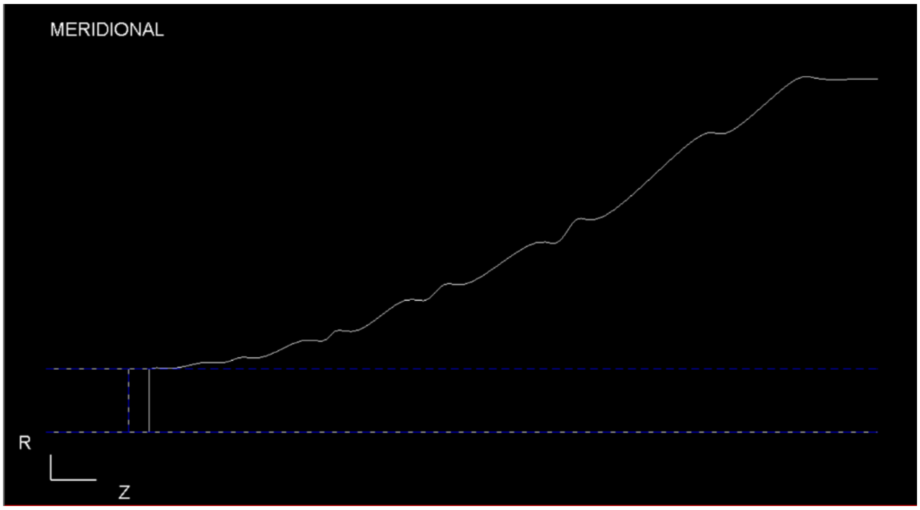

Figure 34 Meridional Plane

4.1.2.3. Main Blade Construction

After the stream surface are defined, the primary blade section can be constructed and placed on the stream surface. In the software, blades are generated from a camber curve which placed in a 2D construction plane. The parameter for rotor blades are shown in **Figure 35** and the parameter for stator blades are shown in **Figure 36.**

Name	Lower bound		Expression	Value	Upper bound	Reference
S1_CAMBER_GAMMA	-89			-40	89	1
S1_CAMBER_BETA1	-89			5	89	1
S1_CAMBER_BETA2	-89			-70	89	1

Figure 35 Parameter of Rotor Blade

Name	Lower bound		Expression	Value	Upper bound	Reference
S1_CAMBER_GAMMA	-89			40	89	1
S1_CAMBER_BETA1	-89			0	89	1
S1_CAMBER_BETA2	-89			70	89	1

Figure 36 Parameter of Stator Blade

The projection value of above parameter can be observe in the camber view which shown in **Figure 37** and **Figure 38.**

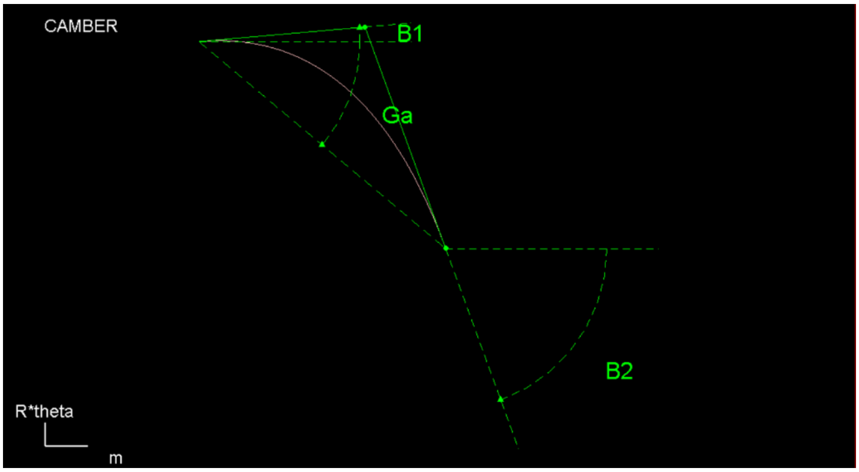

Figure 37 Camber View of Rotor Blades

The final 3D model of each rotor and stator model is shown in **Figure 39** and **Figure 40**.

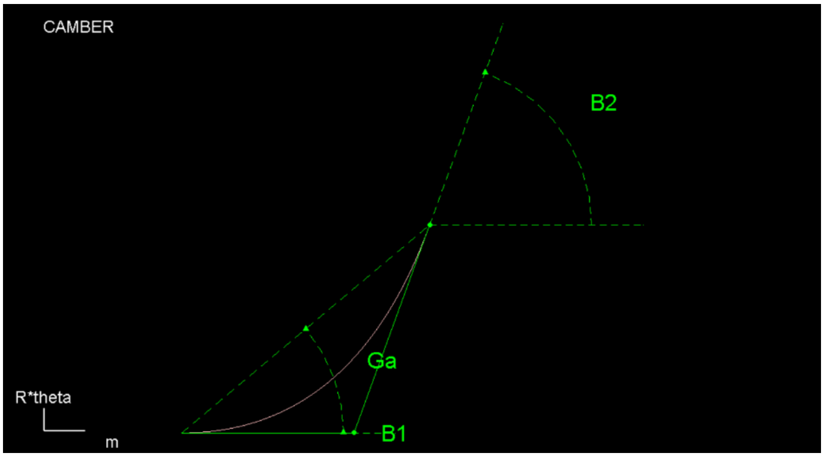

Figure 38 Camber View of Stator Blade

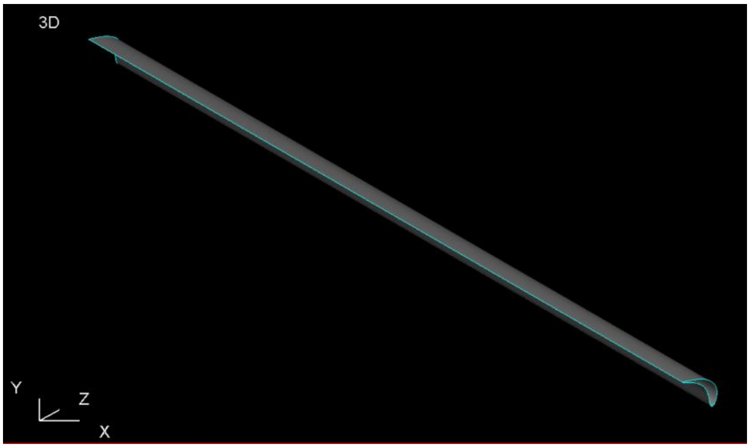

Figure 39 Rotor Blade in 3D View Option

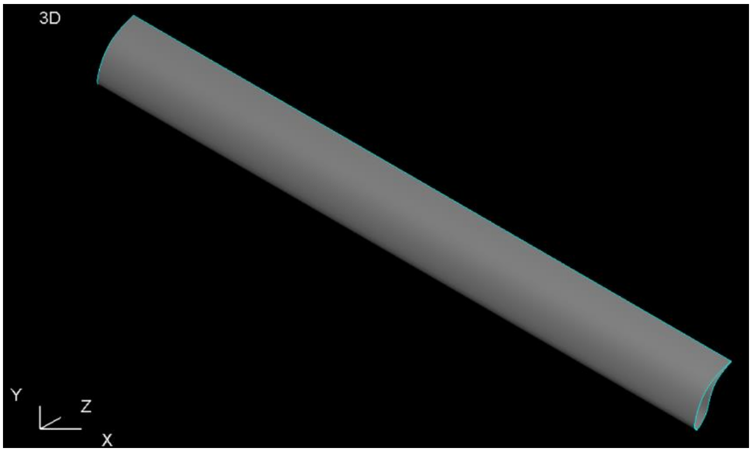

Figure 40 Stator Blade in 3D View Option

4.1.3. Mesh Generation

Mesh generation is the last step of 3D modeling an object. This process is done to ease the next process which is CFD and Finite Element Analysis. Mesh generation also defined as the pre-processing in CFD process which consist of determining the geometrical description of the object model and the discretization of the object domain. This process is done using NUMECA AutoGrid. This software has a user interface which includes multiple windows showing the model visualization as shown in **Figure 41.**

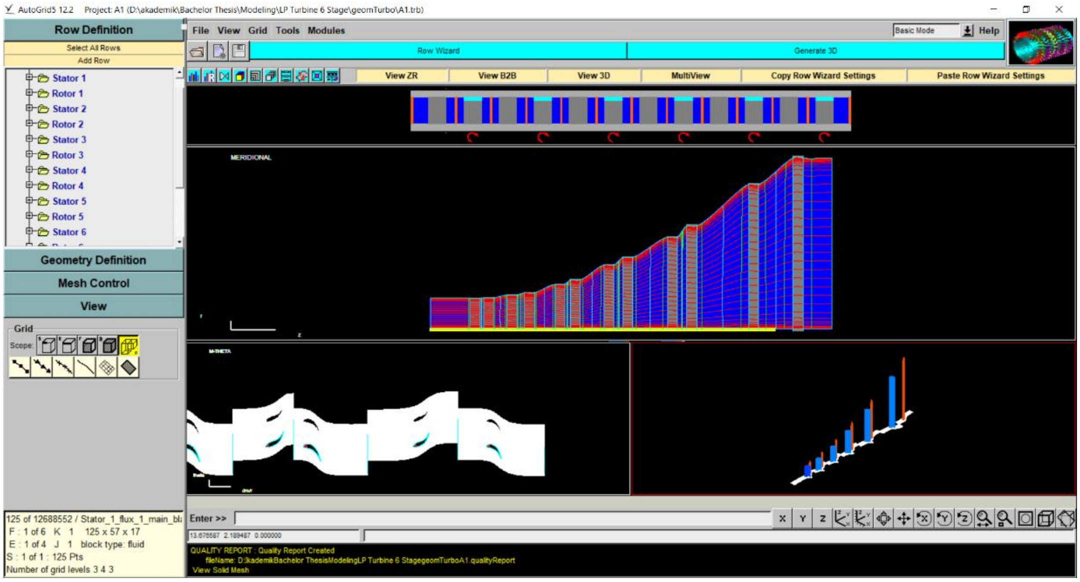

Figure 41 AutoGrid User Interface

The first process in mesh generation is to import stator and rotor file which have been built in previous process. For the file to be able to read in AutoGrid, the file need to be exported as ".geomTurbo" extension. Then manually, one by one the blade whole body need to be define which is the hub, shroud, trailing and leading edge. When the geometry input is correct then a window will pop up as it inform that the process is done.

After the geometry check is done then the software will demand the type of the blades row, the number of blades on each stage and the rotational speed. The type of the row is axial turbine. As defined in the previous process, the number of blade on every stages is 94 units. The rotational speed of rotor is determined by 3000 rpm.

In **Figure 44**, it can be seen the meridional plane of the steam turbine after the mesh generated all the way from stator 1st to rotor 6th.

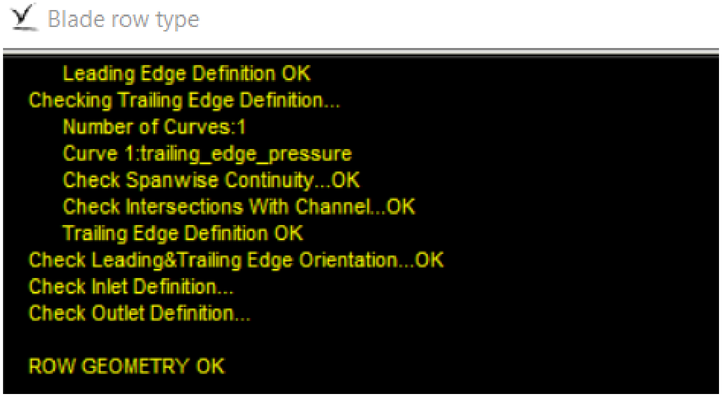

Figure 43 Geometry Check Window

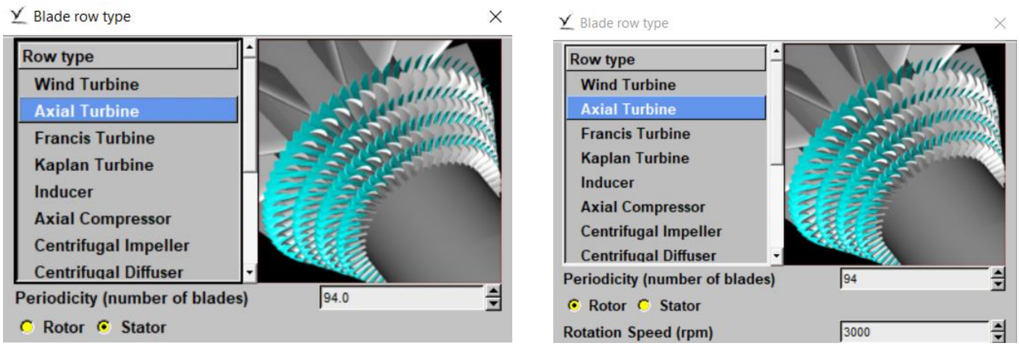

Figure 42 Different Parameter for Stator and Rotor

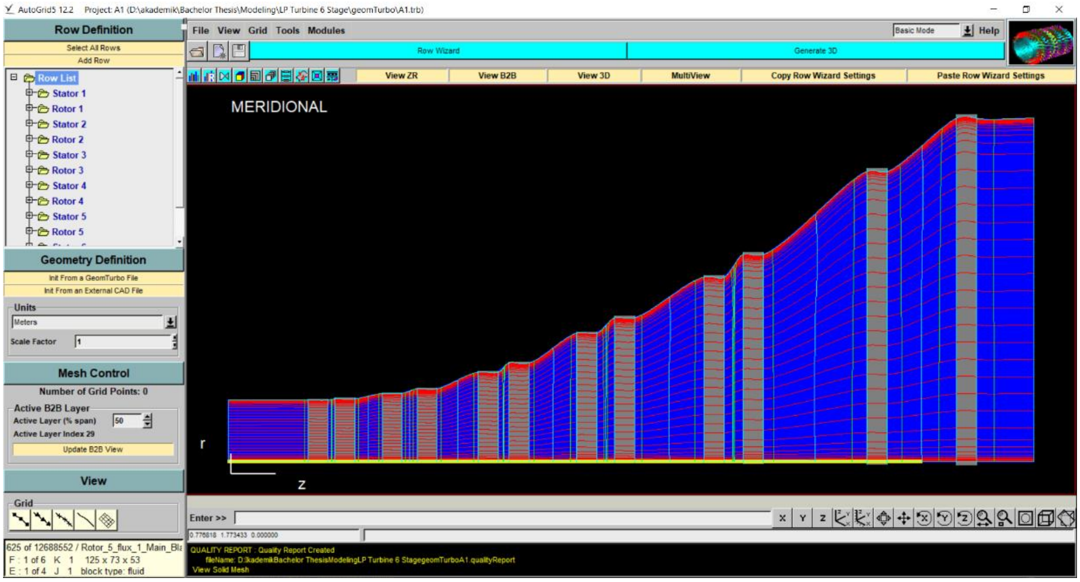

Figure 44 Merdional Plane After Mesh Generated

After the mesh is generated in 3D shape, it is possible to check the grid quality in AutoGrid as it shown in **Figure 45**. It is known that 12688552 points have been generated in approximately 7 minutes of meshing process.

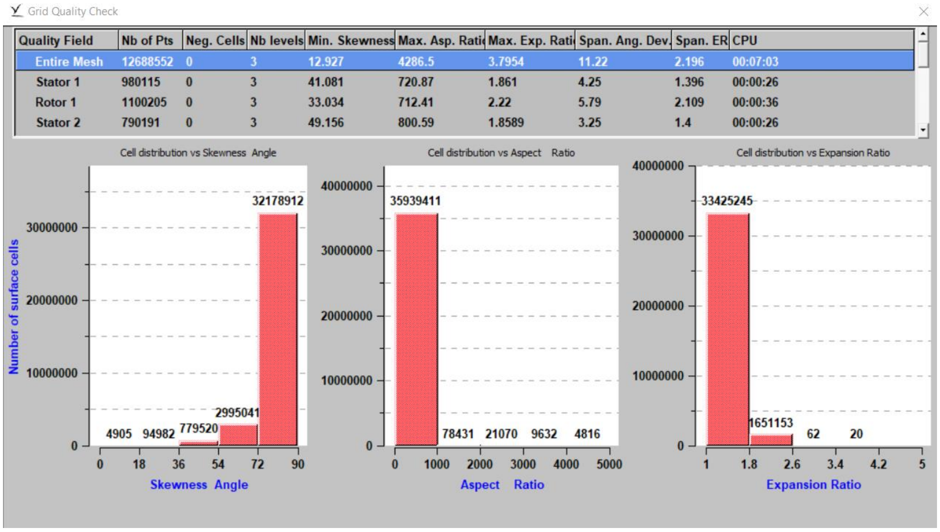

Figure 45 Grid Quality Report

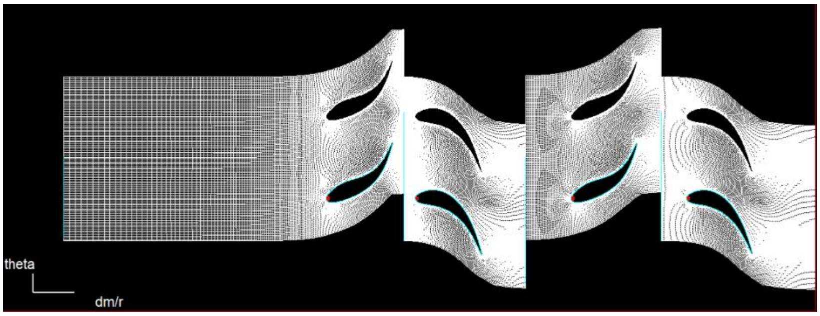

Figure 46 Transverse View of the Stage 1st and 2nd

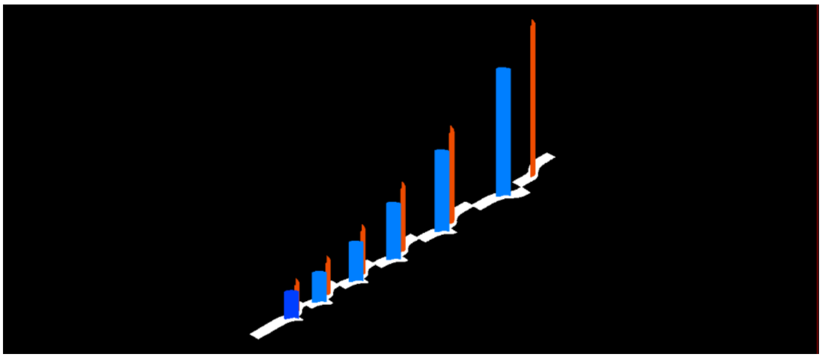

Figure 47 3D Model of Single Blade on each Stage

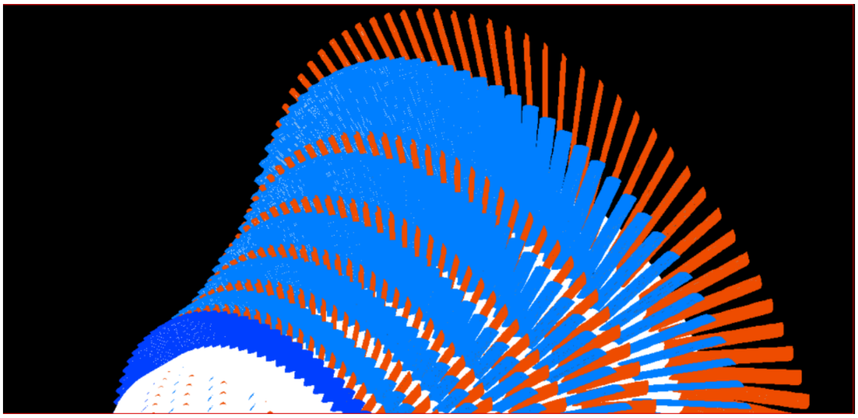

Figure 48 3D Model of the Whole Blade

4.2 Computational Fluid Dynamics Analysis

In this process, author uses NUMECA FINE/Turbo as the software/tool to determine the value of induced steam pressure on the surface of last stage blade of the turbine. Basically the Computational Fluid Dynamics (CFD) process in NUMECA is divided into 3 steps which are grid generation, flow computation and final visualization. The grid generation already done in the previous section. The next step is flow computation which requires several inputs. In the **Table 5**, it can be seen the operating data obtained from several source including certain power plant which later become the inputs for flow computation process.

Table 5 Operating Data of 670 MW LP Steam Turbine

Data	Value	Units
Fluid Type	Condensable Water Steam	
Operating Rotation Speed	3000	rpm
Mass Flow Rate	1480246	kg/hr
Inlet Pressure	148	kPa
Outlet Pressure	30.5	kPa
Inlet Enthalpy	3150.7	kJ/kg
Inlet Temperature	350	□ C

First of all, the grid mesh result needs to input to the current software. Several condition needs to be determine which are fluid model, flow model, rotating machinery, and inlet-outlet boundary condition.

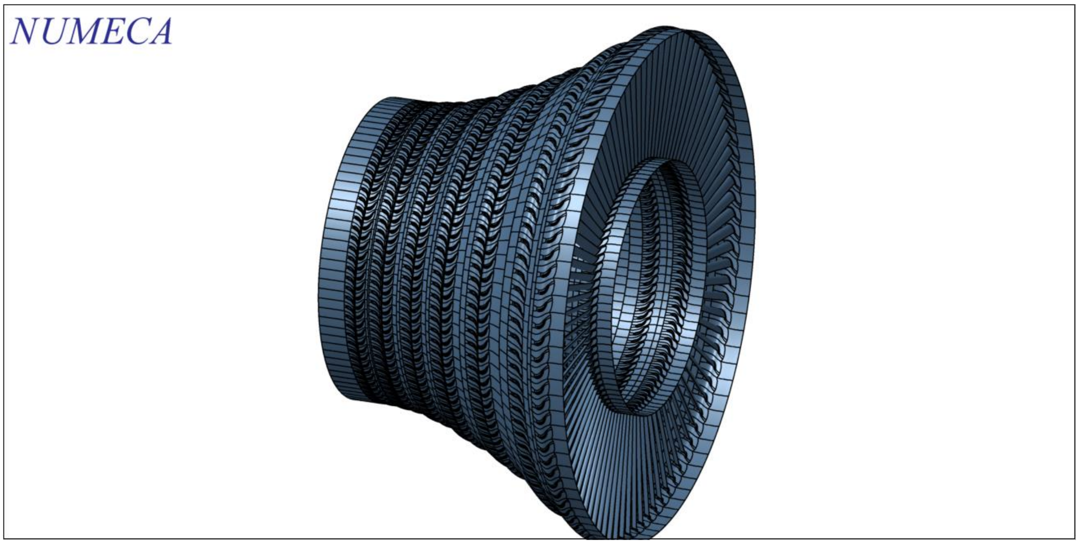

Figure 49 View of All Blocks of the Steam Turbine

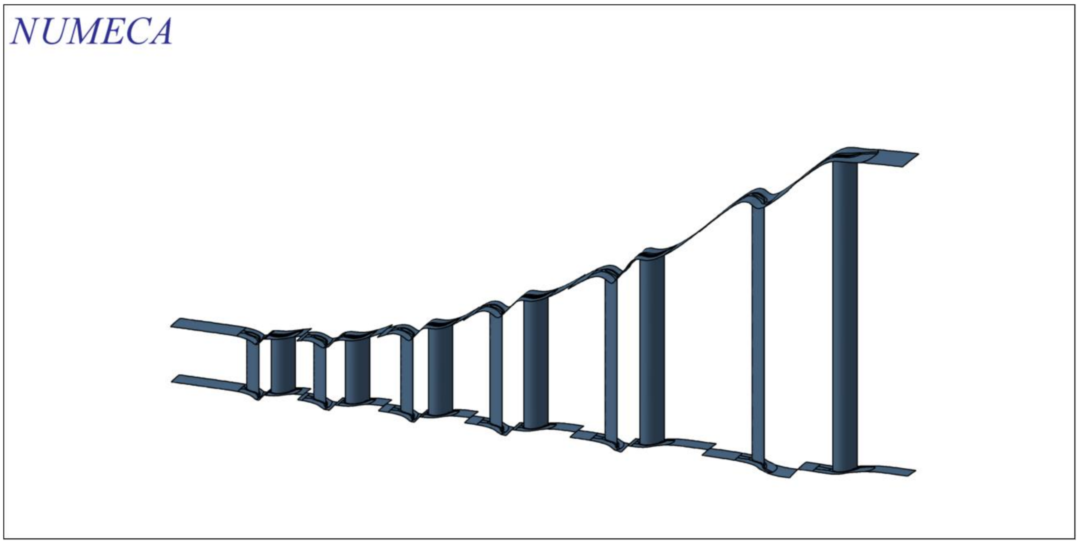

Figure 50 View of One Block of the Steam Turbine

In fluid model, it shows several type of fluids which can selected and in this case condensable water steam is chosen. In the boundary conditions, it shows options that can pick to analyze fluids on the turbine. Based on the availability of the operating condition data, the total quantities imposed is selected on inlet side and on the outlet side it is the pressure imposed that selected. It shown on the **Figure 49** and **Figure 50**.

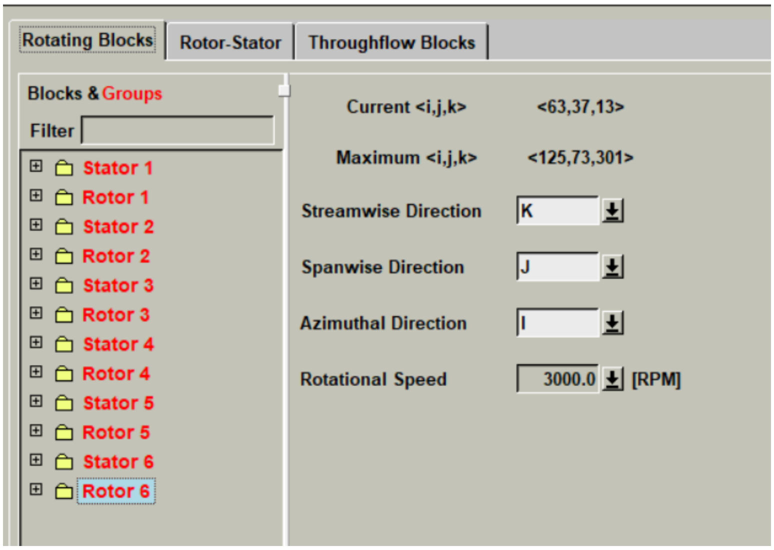

Figure 51 Rotating Blocks of Steam Turbine

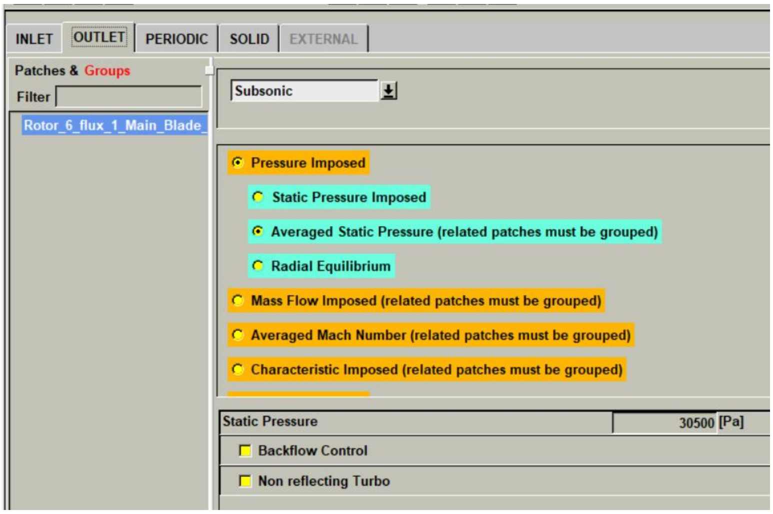

Figure 52 Inlet Boundary Conditions

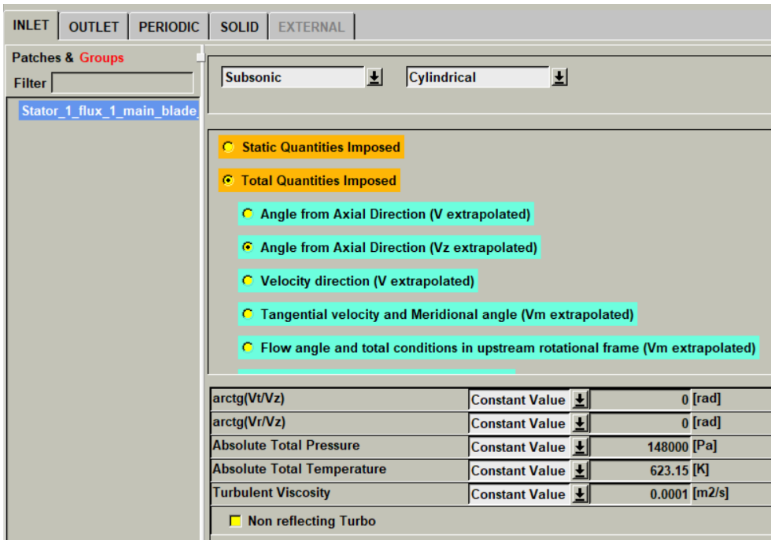

Figure 53 Outlet Boundary Conditions

For this fluid simulation, the output quantities which selected are static pressure, total relative pressure and total absolute pressure.

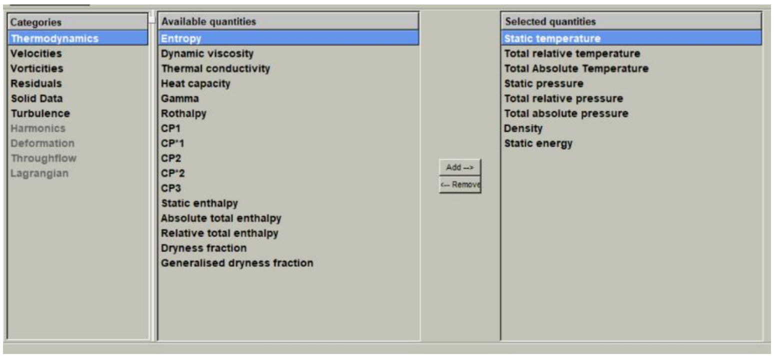

Figure 54 Selected Output Quantities

The iteration process is carried out until stable/converge condition, in this case means the value of mass flow in and out shall balance. This process take 1093 cycles of iteration to reach the balanced condition and the end result is 0.038% error on the mass flow in and out. Mass flow graphic can be seen on **Figure 55**.

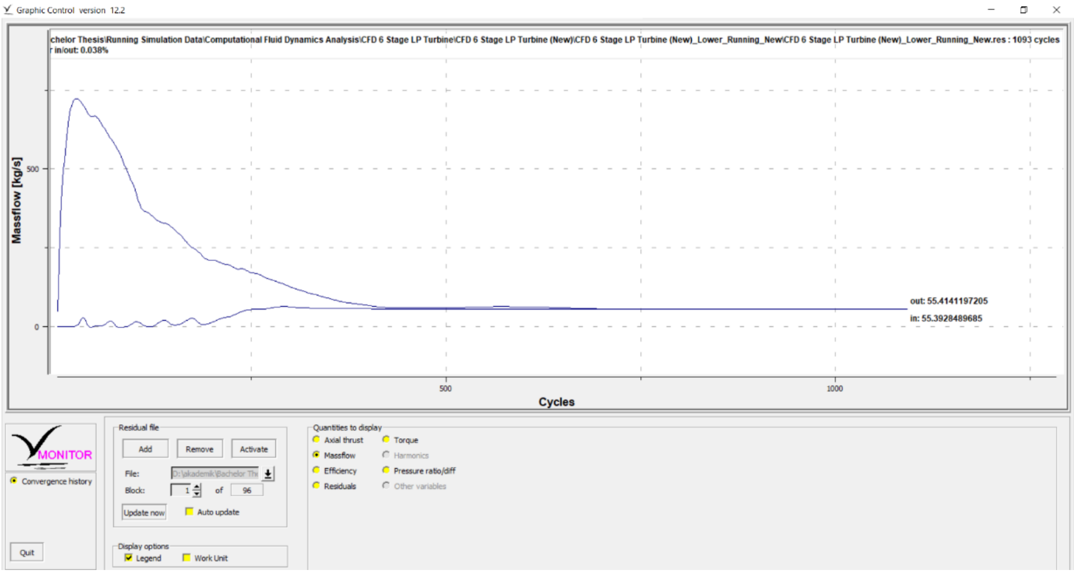

Figure 55 Mass Flow Fluctuation Graph

The next step is the final visualization on CFView. In this software, it is possible to observe the distribution of output quantities which are determined before. To obtain the near-real value of the induced steam force, the total absolute pressure results are chosen because this value represent the pressure which act on the body of the turbine blade and the atmospheric pressure where the turbine itself operate. The contour of pressure distribution can be seen on **Figure 56**.

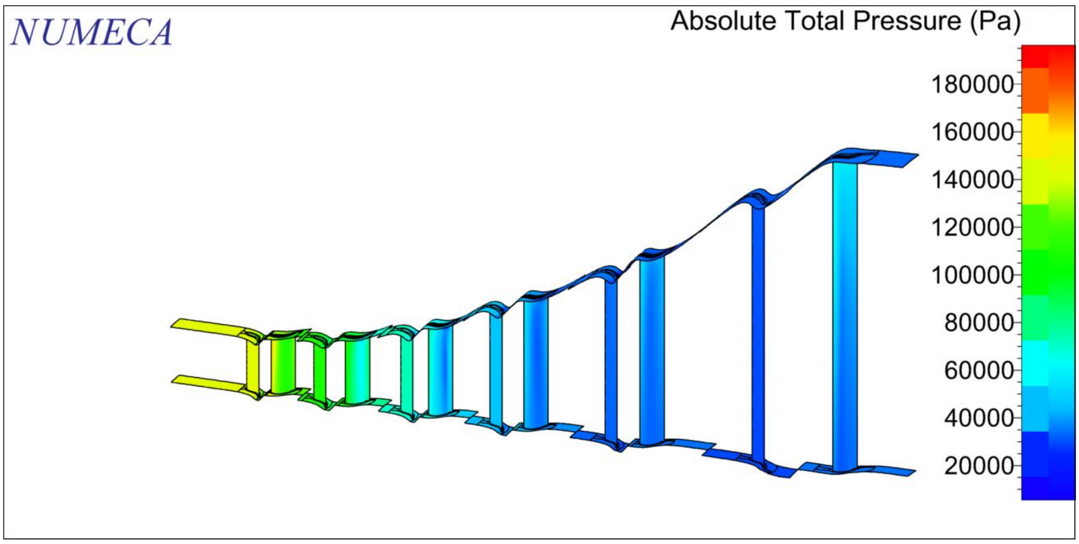

Figure 56 Pressure Distribution

It obvious that the first stage receive the most pressure value of all stages while the last stage receive less with the lowest value of 5696.29 Pa and the highest value of 196131 Pa. The induced force can be obtained by multiply the value of local pressure with the local area which those pressure work. 37 local values is collected all the way from the dovetail to the tip of the blade with the distance of each point is 0.023 m. The series of pressure value which act on the blade can be seen on the **Table 6** and **Table 7**.

Table 6 Pressure of Last Stage Blade

No.	Value in MPa	Value in Pa
1	3.09	30900
2	3.16	31600
3	3.2	32000
4	3.25	32500
5	3.32	33200
6	3.36	33600
7	3.39	33900
8	3.43	34300
9	3.5	35000
10	3.54	35400
11	3.58	35800
12	3.61	36100
13	3.69	36900
14	3.72	37200
15	3.76	37600
16	3.8	38000
17	3.87	38700
18	3.91	39100
19	3.95	39500
20	4	40000
21	4.09	40900
22	4.13	41300
23	4.18	41800
24	4.24	42400
25	4.36	43600
26	4.42	44200
27	4.49	44900
28	4.57	45700
29	4.72	47200
30	4.8	48000
31	4.89	48900
32	4.97	49700
33	5.15	51500
34	5.3	53000
35	5.45	54500

36	5.65	56500
37	5.9	59000

Table 7 Pressure of First Stage Blade

No.	Value in MPa	Value in Pa
1	1.47	147000
2	1.48	148000
3	1.49	149000
4	1.49	149000
5	1.5	150000
6	1.51	151000
7	1.51	151000
8	1.52	152000
9	1.52	152000
10	1.52	152000
11	1.53	153000
12	1.53	153000
13	1.54	154000
14	1.55	155000
15	1.55	155000
16	1.56	156000
17	1.56	156000
18	1.57	157000
19	1.57	157000
20	1.57	157000
21	1.57	157000

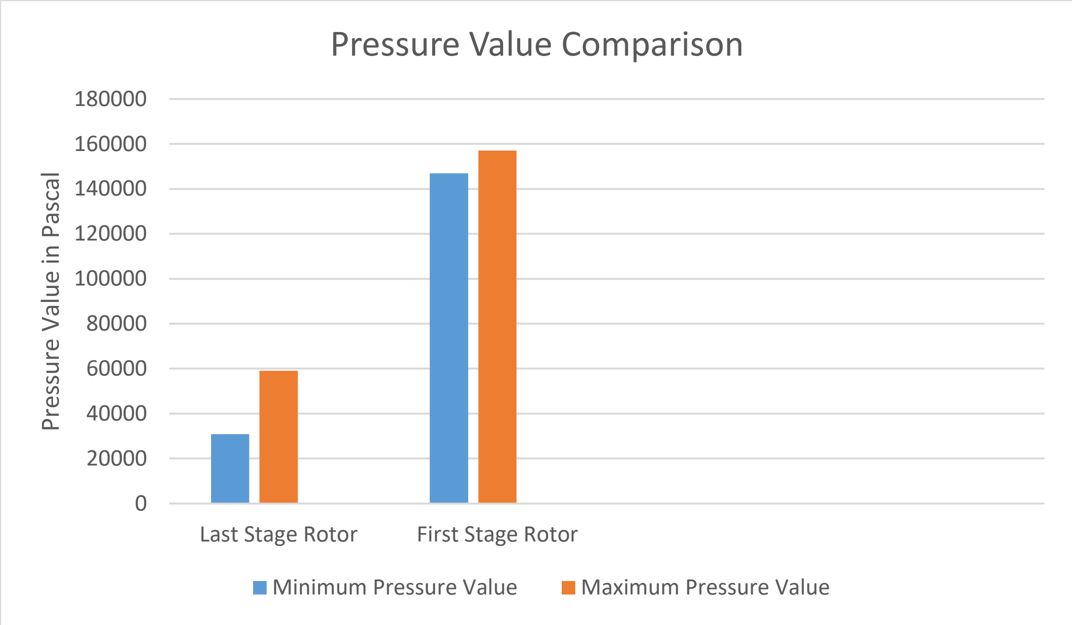

Figure 57 Pressure Value Comparison

4.3 Determination of Induced Force

The method to determine the magnitude and position of the resultant of distributed forces is analytical method. This method requires the value of forces at each points and the length of the beam which in this case is the turbine blade.

The total area which induced by steam pressure is divided into 9 section to ease the plotting process, this area value will be the multiplier of the pressure value so that the induced force on the certain location can be obtained. **Table 8** shown the value of force on first stage and last stage blade.

Table 8 Value of Force on First Stage and Last Stage Blades

No.	Force on Last Stage Blade in Newton
1	203.185
2	207.788
3	210.418
4	213.706
5	218.308
6	220.939
7	222.911
8	225.542
9	230.144
10	232.775
11	235.405

No.	Force on First Stage Blade in Newton
1	316.991
2	319.147
3	321.304
4	321.304
5	323.460
6	325.616
7	325.616
8	327.773
9	327.773
10	327.773
11	329.929

12	237.378
13	242.638
14	244.611
15	247.241
16	249.871
17	254.474
18	257.104
19	259.734
20	263.022
21	268.940
22	271.570
23	274.858
24	278.804
25	286.694
26	290.640
27	295.242
28	300.503
29	310.366
30	315.627
31	321.545
32	326.805
33	338.641
34	348.504
35	358.368
36	371.519
37	387.958

12	329.929
13	332.086
14	334.242
15	334.242
16	336.398
17	336.398
18	338.555
19	338.555
20	338.555
21	338.555

From here, the magnitude and position of the resultant which represent the distributed forces needs to calculated. **Figure 58** shown the force distribution plot, with the horizontal line is the length of the turbine blade itself and the vertical lines is the force value. To find the representative force, the total area of the plot shall divided by the length of the beam and the position will be the centeroid/center of mass of the plot.

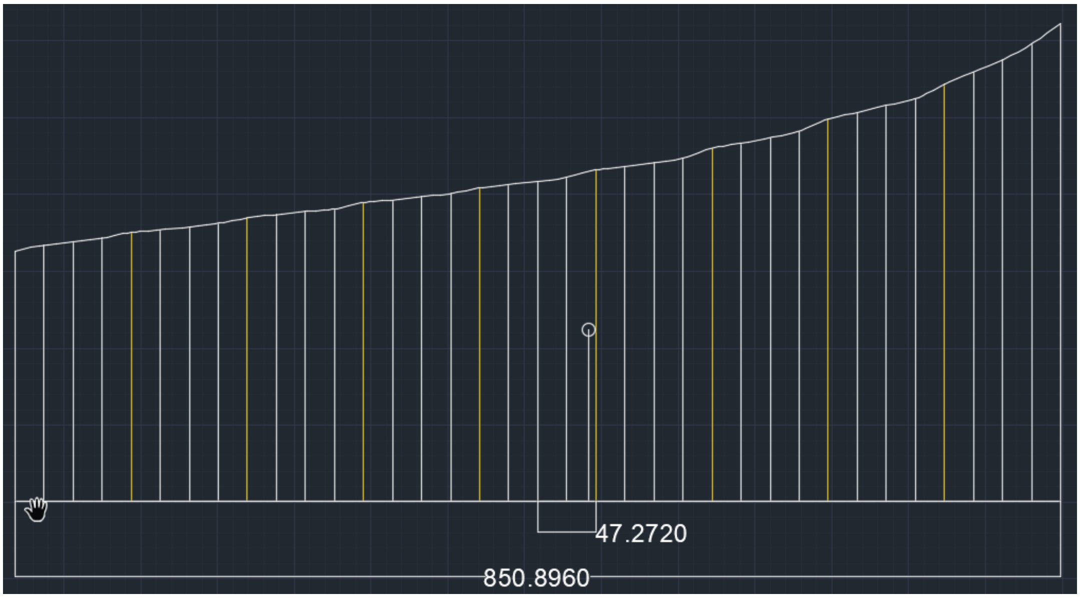

Figure 58 Force Distribution Plot of Last Stage Blade

Based on the process, it obtained that the representative value is 270.242 N and located 47.272 mm from the center of blade towards the tip which in the section 5.

4.4 Finite Element Analysis

This analysis performs on normal blade and flawed blade which determine before the simulation. The crack dimension and location which applied on the normal blade are to be assumed based on the analysis result of normal blade.

Table 9 Crack Variation Model Dimension

No.	Depth (mm)	Height (mm)	Length (mm)	Location
1	1	1	4.242	Leading Tip
2	5	1	8.596	Leading Tip
3	10	1	10.965	Leading Tip
4	1	1	1.161	Trailing – 3% from dovetail
5	5	1	1.787	Trailing – 3% from dovetail
6	10	1	2.657	Trailing – 3% from dovetail
7	5	1	8.596	Leading Tip
	5	1	1.787	Trailing – 3% from dovetail

Material data which used in this simulation is based on author research, available data on Ansys 19, and ASTM standards. Material which used for the blade is Stainless Steel (ASTM A479 Type 403 C2).

Table 10 Stainless Steel (ASTM A479 Type 403 C2) Properties

Material Properties	Value	Units

Density	7800	kg/m^3
Young's Modulus	2×10^{11}	Pa
Poisson's Ratio	0.3	-
Ultimate Tensile Strength	760	MPa
Yield Strength	585	MPa
Paris' Law Material Constant C	6.31×10^{9}	-
Paris' Law Material Constant m	3	-

4.3.1. Structural Analysis of Normal Blade

This simulation process aims to analyze and observe the quantities which related to the structure. The quantities are the stress distribution, damage prediction and fatigue-life cycle. The object which analyze here is the last stage blade and the first stage blade as the comparison.

Before jumping into the simulation, the meshing process needs to be performed. The mesh method which uses here is tetrahedrons with patch conforming algorithm with sizing of 2.5 mm each element. The total number of nodes are 368,833 and elements are 244,793. **Figure 59** shown the result of the normal blade mesh.

The input of this process is the representative force from previous step with magnitude of 270.242 N for last stage blade and 329.83 N for first stage blade. The solution that selected are equivalent stress and fatigue tool such as life, damage and fatigue sensitivity. Fatigue analysis which perform here is fully reverse type and based on stress distribution. Goodman mean stress theory also use in this present analysis. **Table 11** shown the analysis result of normal blade.

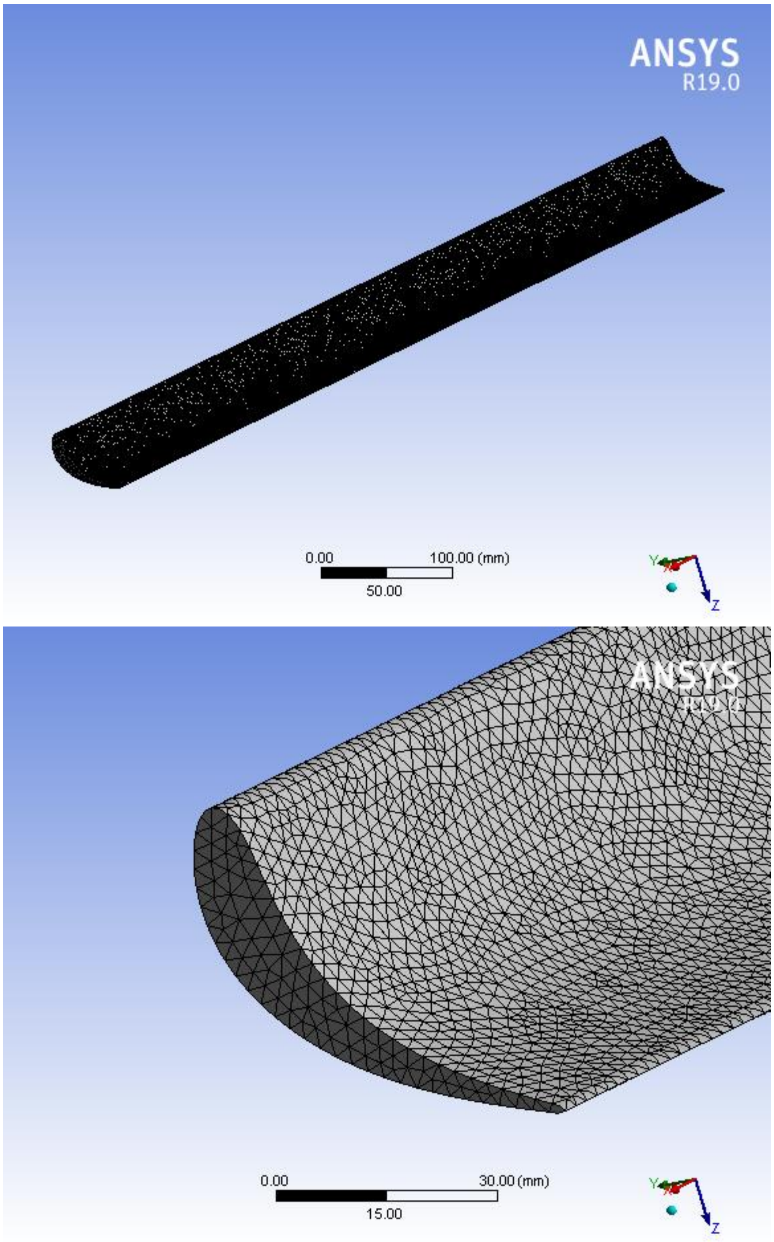

Figure 59 Mesh Result of Normal Blade

Table 11 Analysis Result of Normal Blade

Quantities	Last Stage Rotor	First Stage Rotor
Max. Equivalent Stress (Mpa)	91.925	19.164
Min. Equivalent Stress (MPa)	1.864×10^{-10}	3.229×10^{-4}
Average Equivalent Stress (MPa)	7.293	2.748
Design Life (Cycles)	10^9	10^9
Maximum Remaining Life (Cycles)	10^6	10^6
Minimum Remaining Life (Cycles)	7.179×10^5	10^6
Average Remaining Life (Cycles)	10^6	10^6
Predicted Damage Location	Leading Tip	Undetected

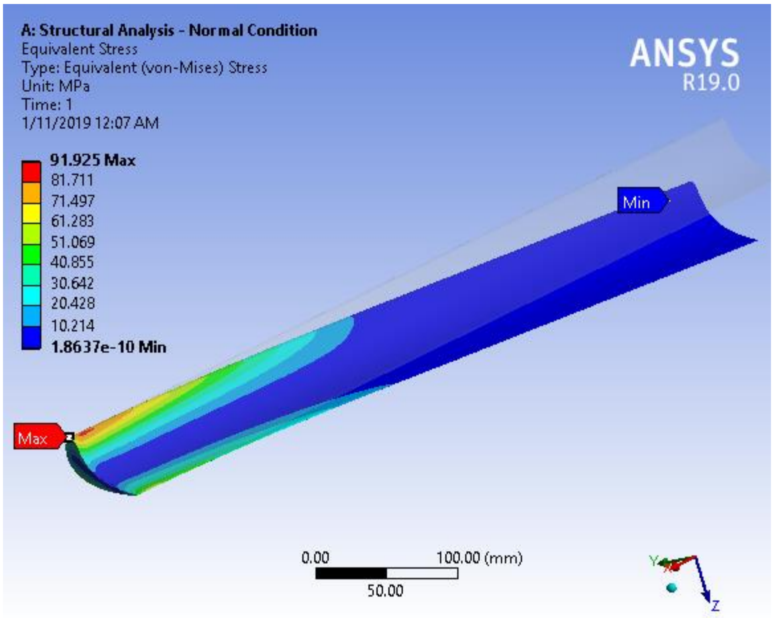

Figure 60 Stress Distribution on Last Stage Blade

Based on the stress distribution result on the normal blade, the highest stress concentration located in the bottom tip of leading edge with value of 91.925 MPa. Stress distribution also appear in the trailing edge but the value is considerably lower compare to the leading edge. However, the highest stress value recorded still far below the yield and ultimate tensile strength of the material.

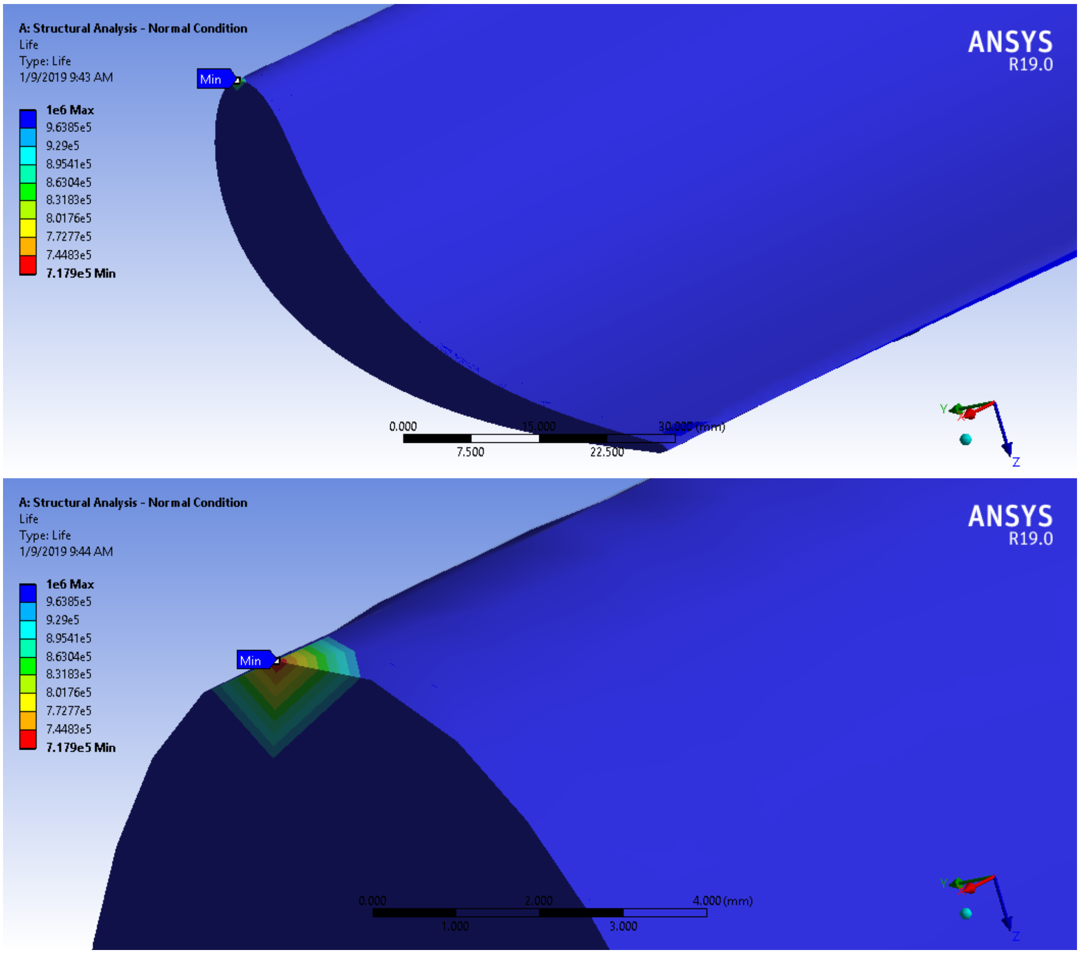

Figure 61 Damage Prediction Location of Last Stage Blade

In the fatigue analysis result, a very minor damage prediction with size of less than 0.2 mm appear in the tip of leading edge. In certain area, the minimum remaining life is recorded 7.179 x 10^5 cycles which means a damage may occur after this life cycle.

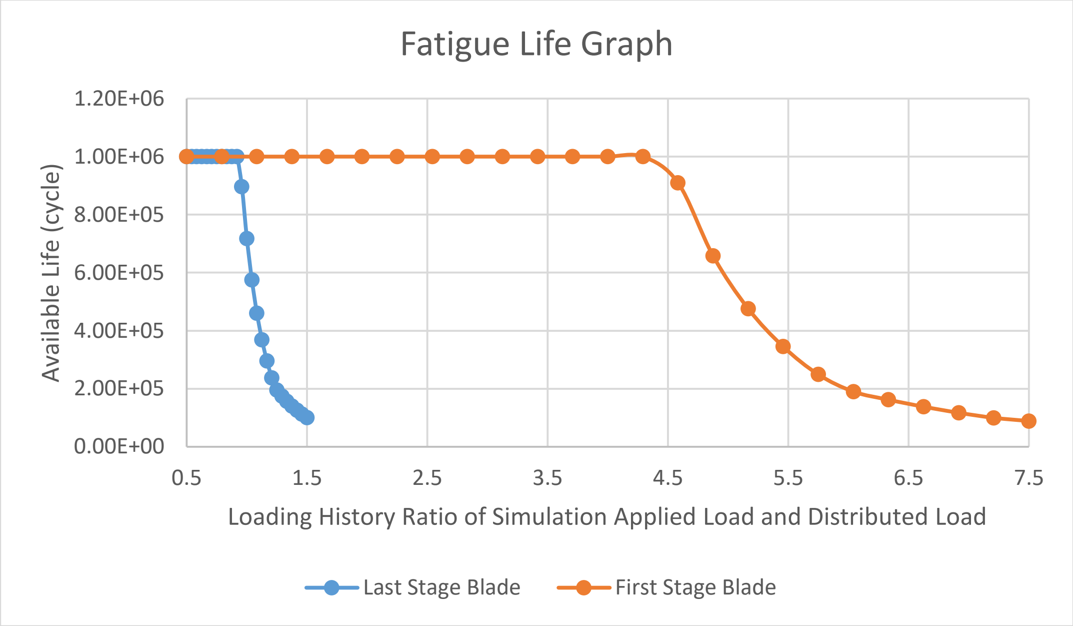

Figure 62 Fatigue Life Graph of Last Stage and First Stage Blade

For comparison, the analysis also perform on the first stage rotor. The result, show that the stress value is very low compare to the last stage blade with highest value of 19.164 MPa and in the fatigue analysis result, damage does not occur or detected. **Figure 62** shows the fatigue life comparison between last stage and first stage blade, there it can be observe that first stage blade have comparably longer life due to lower stress concentration value.

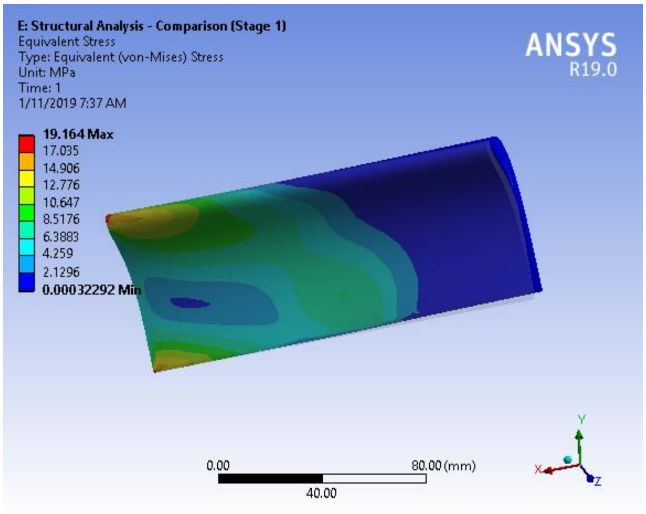

Figure 63 Stress Distribution on First Stage Blade

Figure 63 shows the stress distribution on the first stage blade. The highest value located on the bottom tip of leading blade just like the result of last stage blade. However, the stress concentration also detected on the trailing edge. The minimum value of stress concentration here comparably higher than value on the last stage blade, this occurs due to higher pressure condition in the first stage.

4.3.2. Structural Analysis of Flawed Blade

Initial crack models are applied to the normal blade to observe the quantities and as the comparison with the normal blade result.

The mesh method which uses here is tetrahedrons with patch conforming algorithm with sizing of 2.5 mm. On the crack area, a refinement is applied in order to achieve minimum error result. The sizing on the crack area is 0.35 mm. **Table 12** shows the statistics mesh result of each flawed blade.

Table 12 Statistics Mesh Result of Flawed Blades

Flawed Blade Variations	Number of Nodes	Number of Elements
Leading Tip 1 mm	381,991	254,070
Leading Tip 5 mm	453,492	305,767
Leading Tip 10 mm	540,166	368,937
Trailing Edge 1 mm	369,339	245,209
Trailing Edge 5 mm	376,475	250,127
Trailing Edge 10 mm	429,419	287,535
L 5 mm – T 5 mm	463,193	312,675

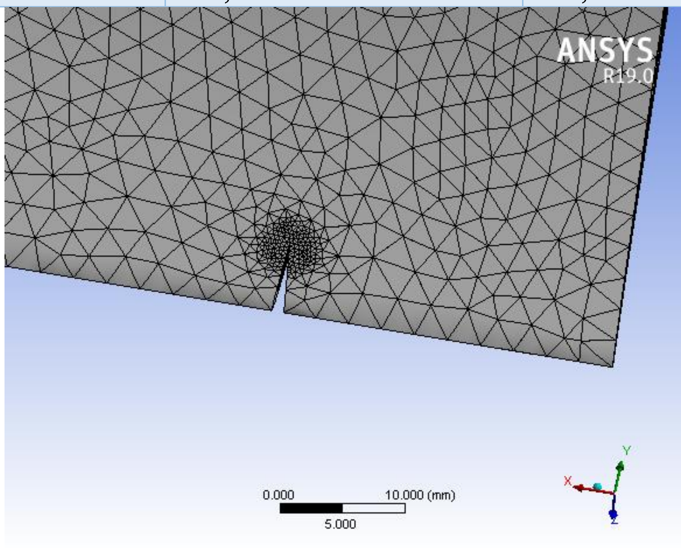

Figure 64 Mesh Result around Crack Area

It can be seen on **Figure 64**, the mesh on the area where crack occur have smaller elements and have a curvature pattern. This aims to obtain more accurate result with lower error and this type of mesh is the best method for analyzing component with crack.

Table 13 Analysis Result of Flawed Blade with Size of 1 mm

Quantities	Leading Tip 1 mm	Trailing Edge 1 mm
Max. Equivalent Stress (Mpa)	165.2	114.06
Min. Equivalent Stress (MPa)	2.025×10^{-10}	3.844×10^{-10}
Average Equivalent Stress (MPa)	9.268	7.4193
Design Life (Cycles)	10^9	10^9
Maximum Remaining Life (Cycles)	10^6	10^6
Minimum Remaining Life (Cycles)	56,217	199,700
Average Remaining Life (Cycles)	9.991×10^5	10×10^5
Location of Minimum Remaining Life	Crack Edge	Crack Edge

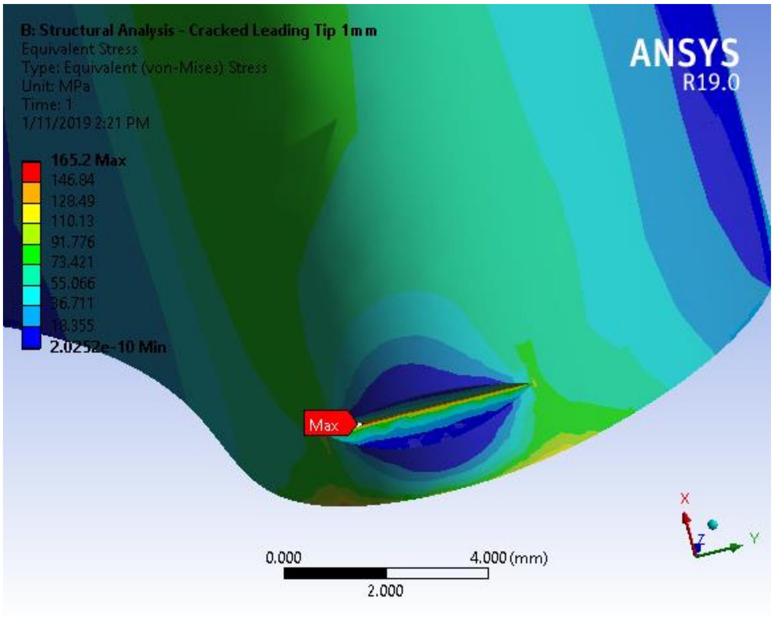

Figure 65 Stress Concentration on 1 mm Leading Crack

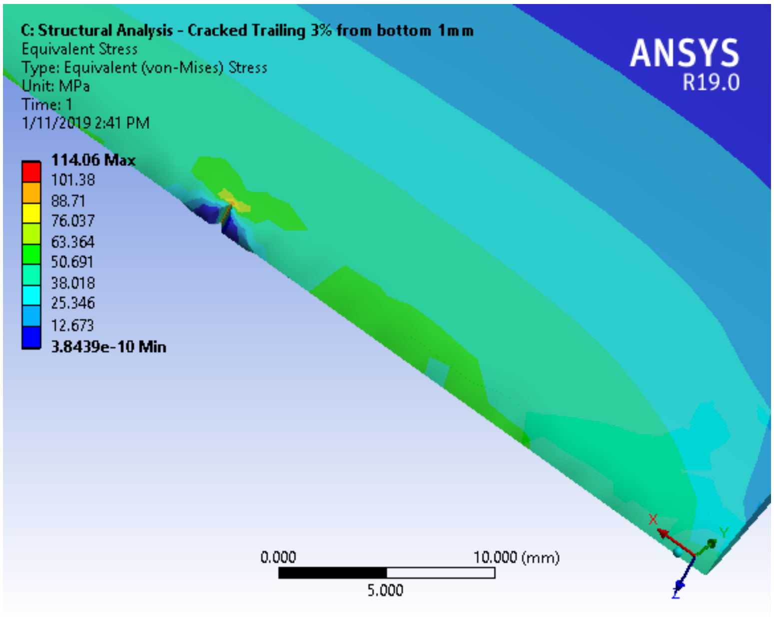

Figure 66 Stress Concentration on 1 mm Trailing Crack

Table 14 Analysis Result of Flawed Blade with Size of 5 mm

Quantities	Leading Tip 5 mm	Trailing Edge 5 mm
Max. Equivalent Stress (Mpa)	212.66	182.64
Min. Equivalent Stress (MPa)	3.852×10^{-10}	1.949×10^{-10}
Average Equivalent Stress (MPa)	15.553	8.185
Design Life (Cycles)	10^9	10^9
Maximum Remaining Life (Cycles)	10^6	10^6
Minimum Remaining Life (Cycles)	20,577	38,858
Average Remaining Life (Cycles)	9.92×10^5	9.995×10^5
Location of Minimum Remaining Life	Crack Edge	Crack Edge

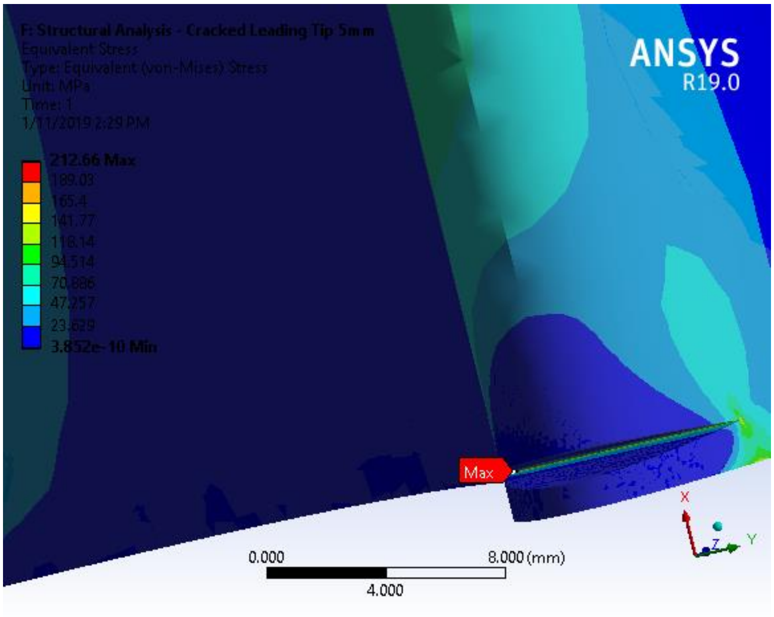

Figure 67 Stress Concentration on 5 mm Leading Crack

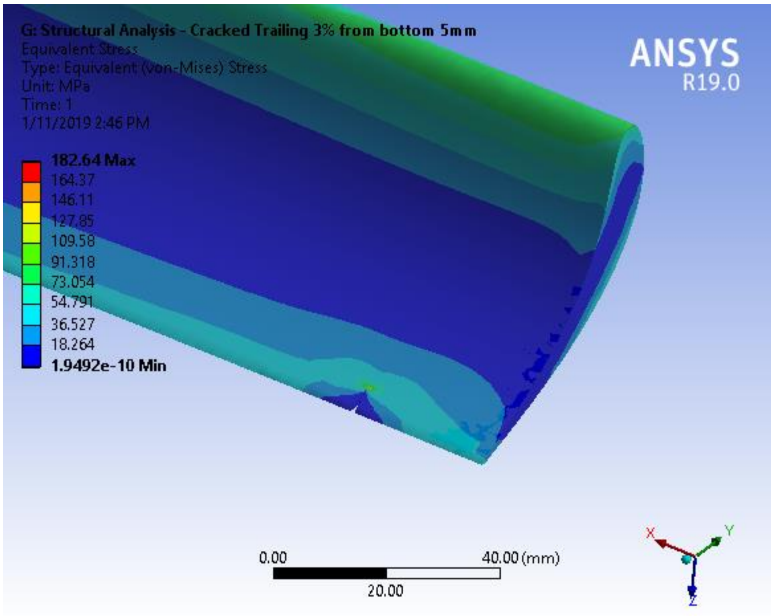

Figure 68 Stress Concentration on 5 mm Trailing Crack

Table 15 Analysis Result of Flawed Blade with Size of 10 mm

Quantities	Leading Tip 10 mm	Trailing Edge 10 mm
Max. Equivalent Stress (Mpa)	318.89	184.52
Min. Equivalent Stress (MPa)	2.343×10^{-10}	2.529×10^{-10}
Average Equivalent Stress (MPa)	21.883	10.711
Design Life (Cycles)	10^9	10^9
Maximum Remaining Life (Cycles)	10^6	10^6
Minimum Remaining Life (Cycles)	5,995.7	37,341
Average Remaining Life (Cycles)	9.708×10^5	9.994×10^5
Location of Minimum Remaining Life	Crack Edge	Crack Edge

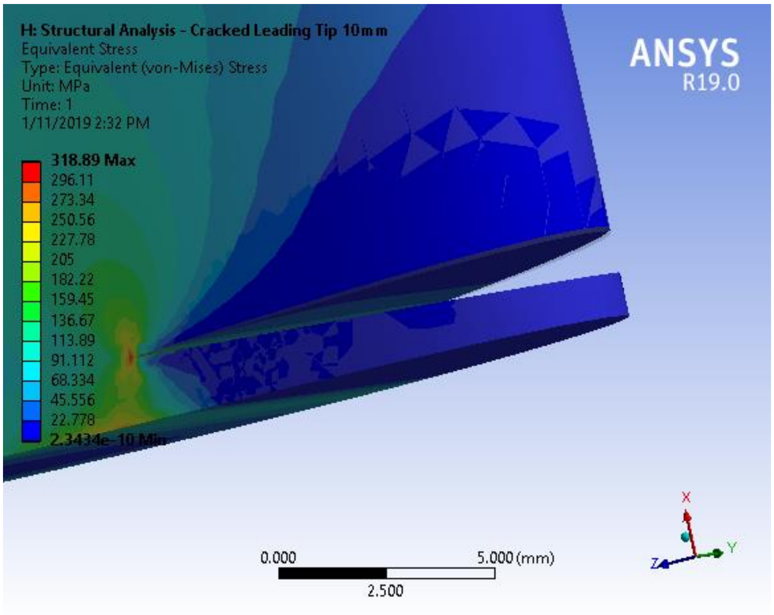

Figure 69 Stress Concentration on 10 mm Leading Crack

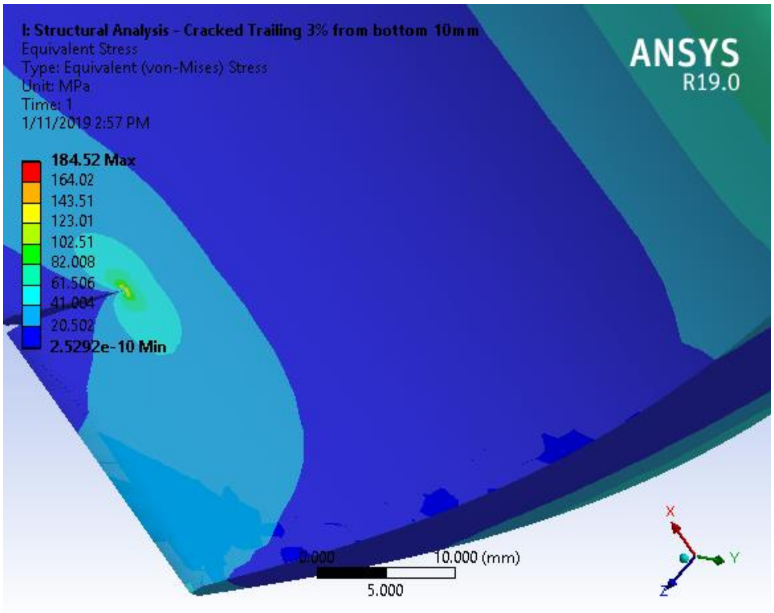

Figure 70 Stress Concentration on 10 mm Trailing Crack

Table 16 Analysis Result of Flawed Blade with Combination Crack Location

Quantities	L 5 mm – T 5 mm
Max. Equivalent Stress (Mpa)	219.62
Min. Equivalent Stress (MPa)	2.446×10^{-10}
Average Equivalent Stress (MPa)	16.478
Design Life (Cycles)	10^9
Maximum Remaining Life (Cycles)	10^6
Minimum Remaining Life (Cycles)	18441
Average Remaining Life (Cycles)	9.904×10^5
Location of Minimum Remaining Life	Leading Crack Edge

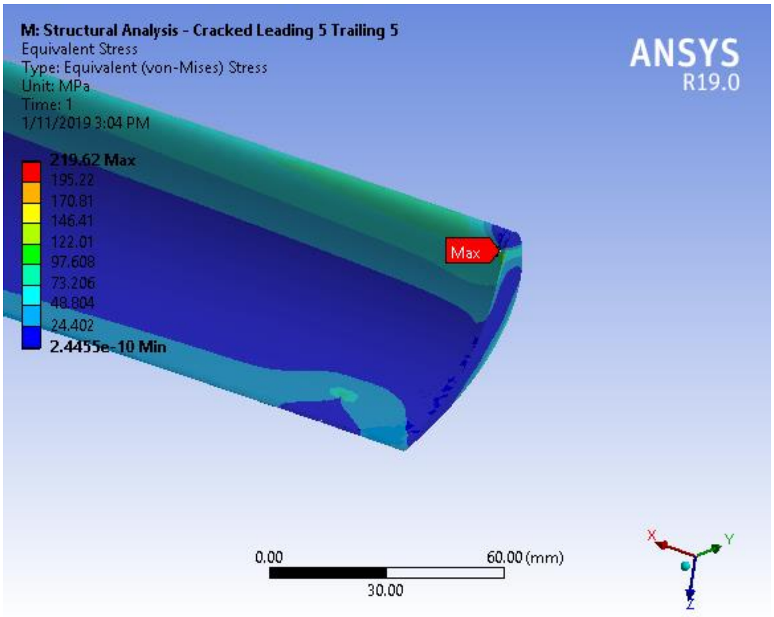

Figure 71 Stress Concentration on Flawed Blade with Combination Crack Location

From the analysis result of flawed blade, it can be observe on **Figure 72** that the working stress value is increasing as the crack dimension expanding with the highest value of 318.89 MPa for the blade with 10 mm crack located on leading tip. The lowest value of working stress is recorded on blade with 1 mm crack located on trailing edge. The number of available life cycle is decreasing from the smallest to greatest crack dimension. The location of minimum remaining life is all the same which is on the surface of crack edge. Compare to crack on the trailing edge, crack on the leading edge considerably more critical due higher value of stress concentration. This proved by the analysis result of blade with combination of crack, the location of minimum remaining life is recorded on the leading side.

From **Figure 73**, it can be observe that blade with crack size of 1 mm on trailing edge has the longest life and blade with crack size of 10 mm on leading tip has the shortest life.

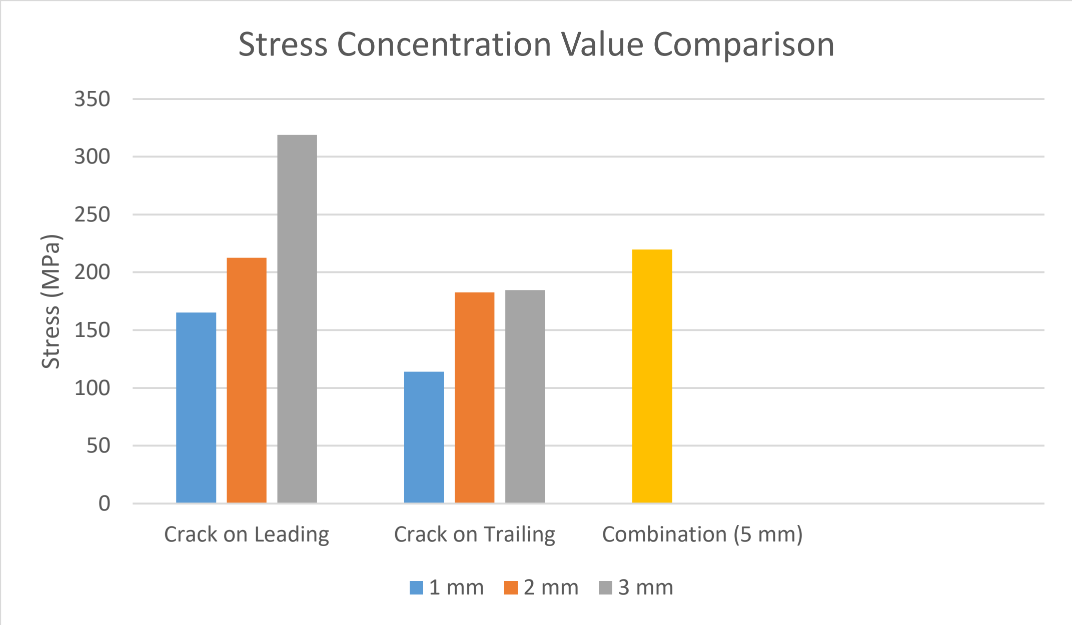

Figure 72 Stress Concentration Value Comparison

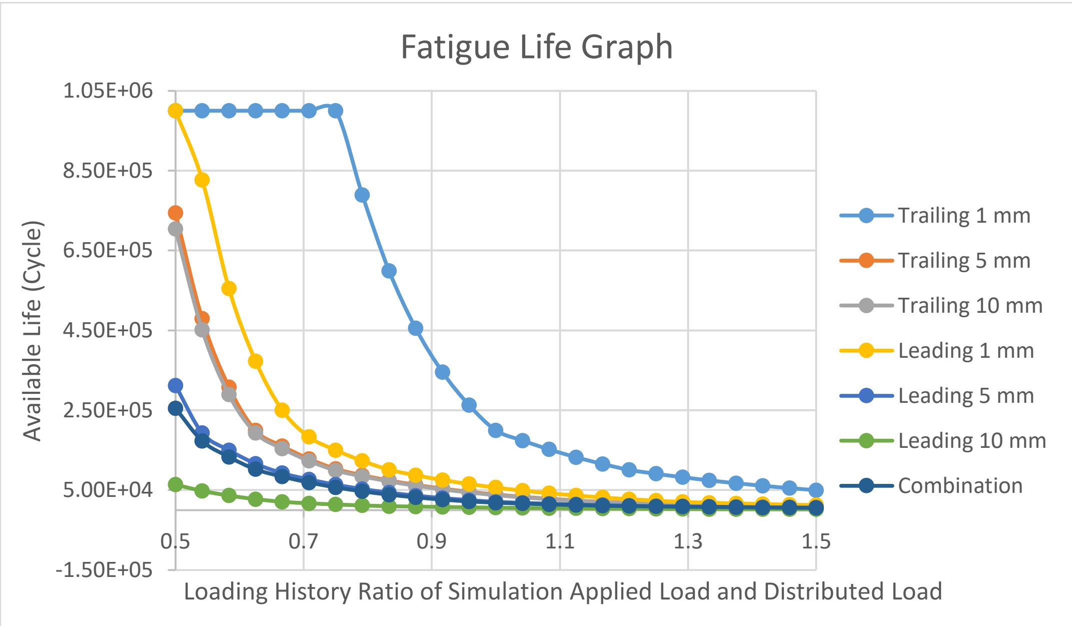

Figure 73 Fatigue Life Graph of Flawed Blade

4.5 Crack Propagation Prediction Analysis

Crack propagation prediction simulation is perform on the last stage blade with certain initial cracks as the input value. This simulation done using the Paris' Law theory. The highest crack dimension of the both side leading and trailing is selected for this simulation to see greater propagation result. Simulation done in five substeps due to computer specification limitation.

Table 17 Analysis Result of Crack Propagation

Quantities	Leading Tip 10 mm	Trailing Edge 10 mm
Max. Equivalent Stress on 1 substep (MPa)	306.24	165.26
Max. Equivalent Stress on 2 substep (MPa)	783.82	201.65
Max. Equivalent Stress on 3 substep (MPa)	713.5	197.16
Max. Equivalent Stress on 4 substep (MPa)	561.4	249.79
Max. Equivalent Stress on 5 substep (MPa)	540.91	188.26
Total Crack Extension (mm)	2.179	1.501
Total Number of Cycles	12	79
Crack Growth Rate (mm/cycle)	0.186	0.019

Based on both result, it can be observe that value of stress concentration is relatively increasing as the crack dimension grow. The total crack growth in mm of crack on leading tip is comparably higher than on the trailing edge, this statement can observe in the **Table 17**. **Figure 76** shows the crack growth comparison of both model. The visual crack growth of both model can observe in the

In trailing edge, crack grows from 10 mm to 11.501 mm in 79 cycles with highest recorded stress value of 249.79 MPa in substep 4th. In leading edge, crack grows from 10 mm to 12.179 mm in 12 cycles with highest recorded stress value of 783.82 MPa in substep 2nd. The stress concentration near crack edge can be observed in **Figure 74** and **Figure 75**.

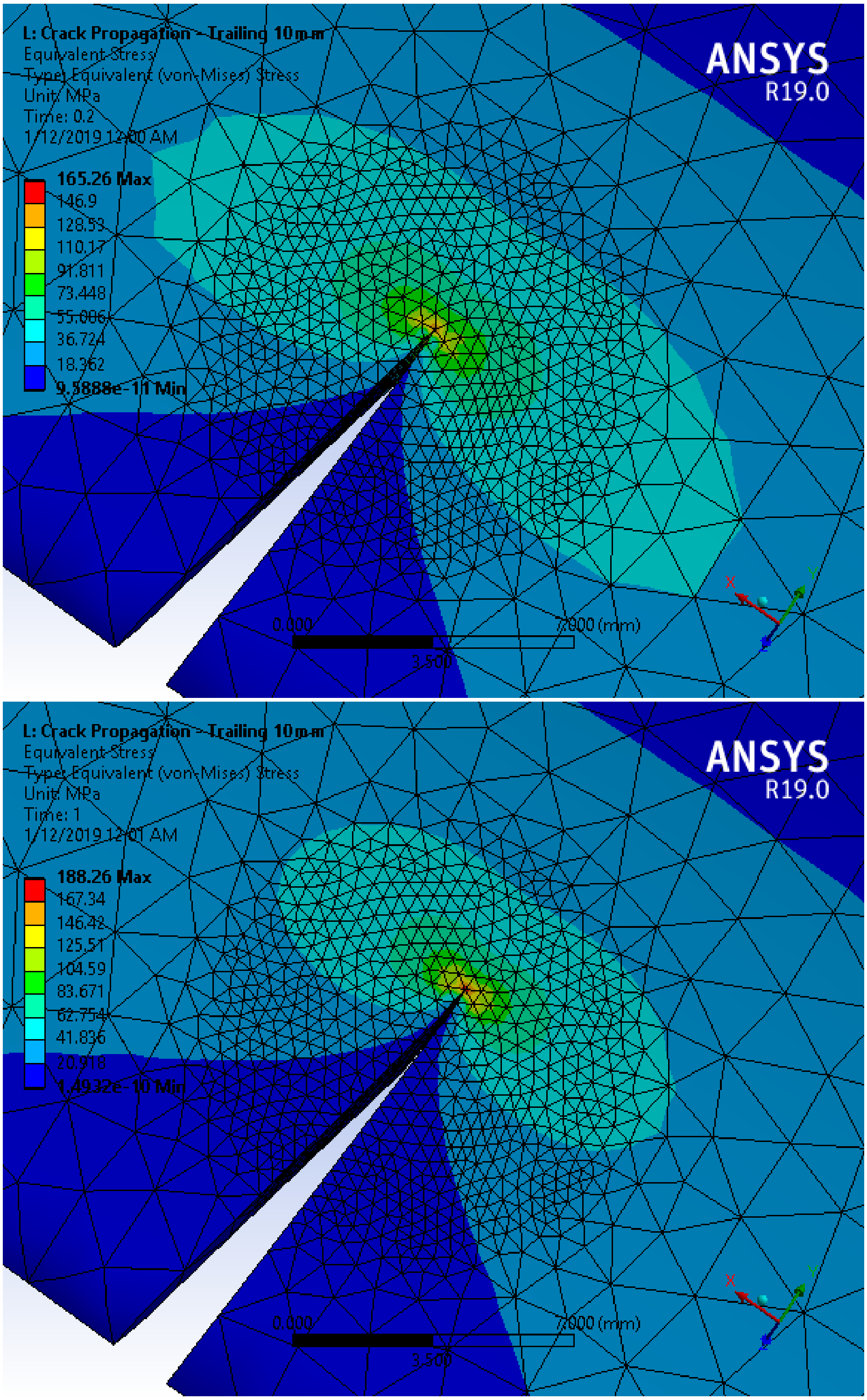

Figure 74 Stress Concentration on Crack Edge of Blade with Crack in Trailing Edge

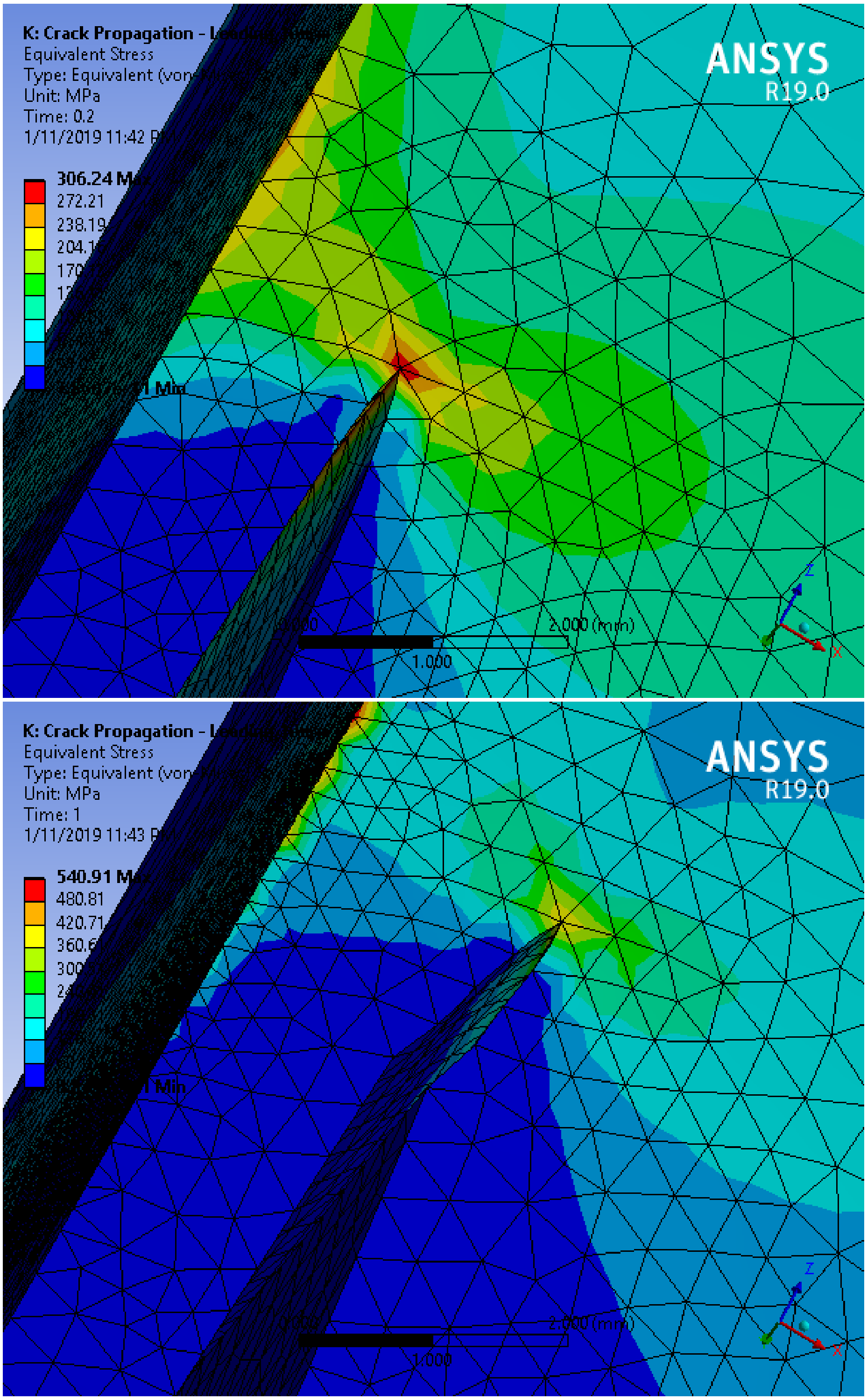

Figure 75 Stress Concentration on Crack Edge of Blade with Crack in Leading Edge

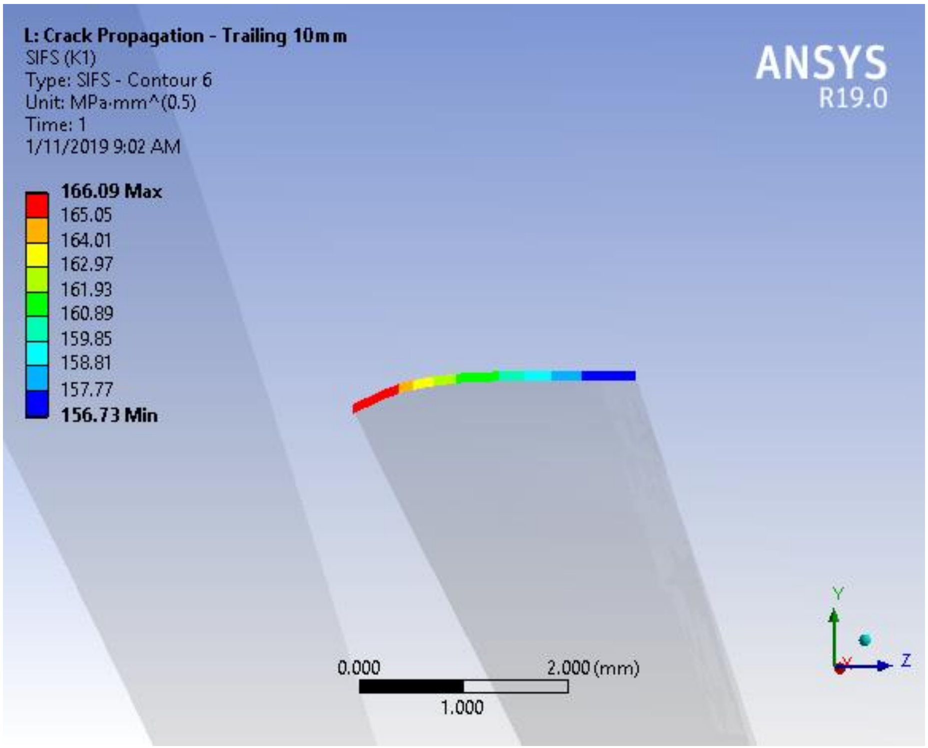

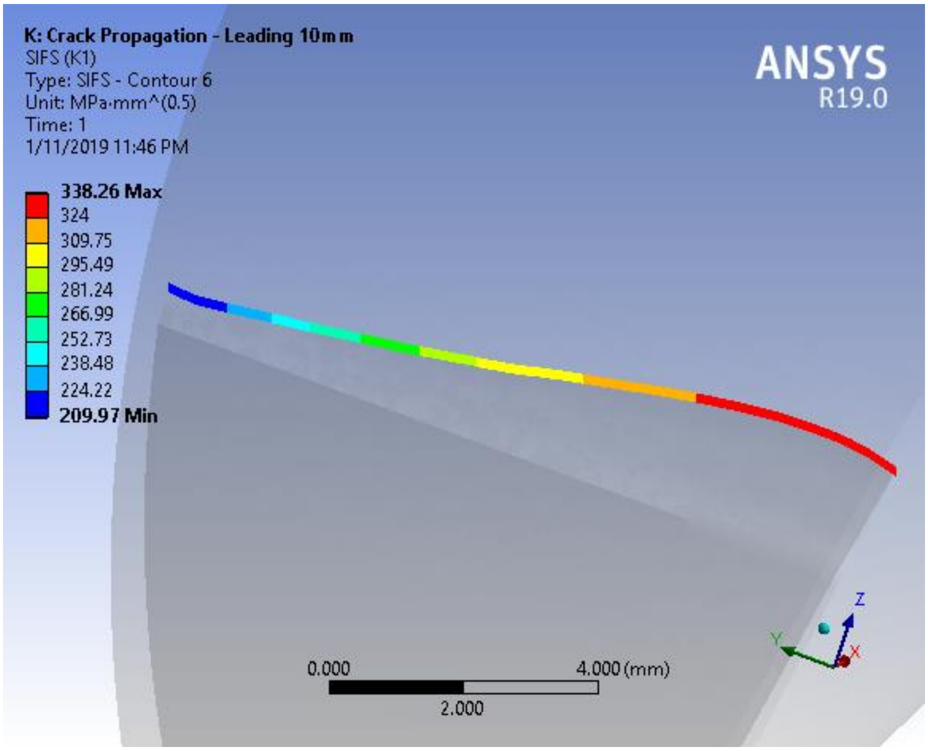

Figure 76 Stress Intensity Factor (SIF) on Both Model

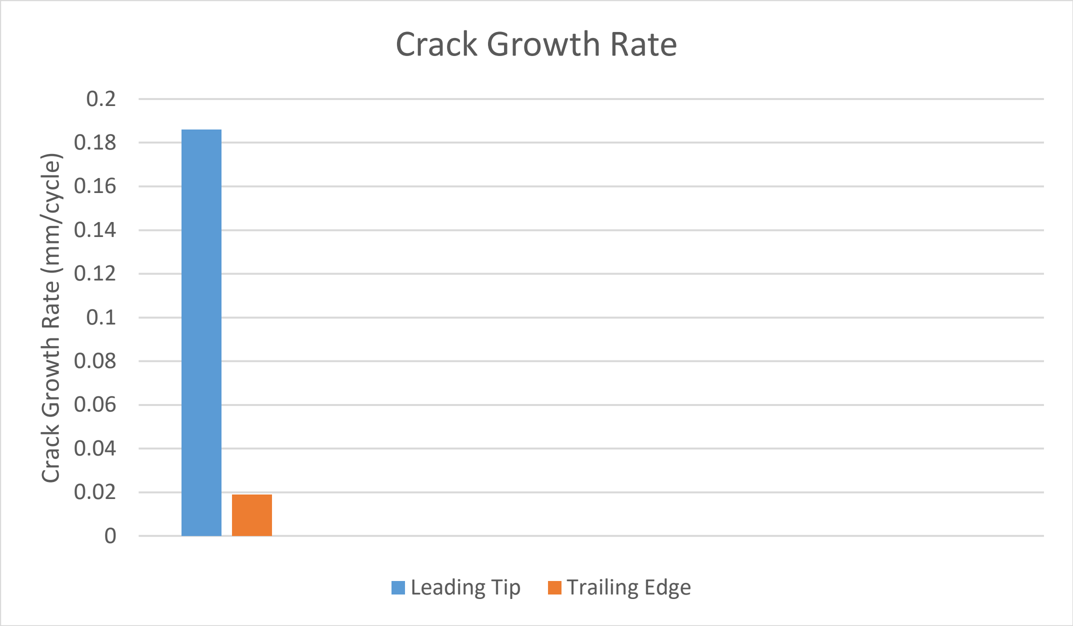

Figure 77 Crack Growth Rate Comparison of Both Model

In **Figure 76** shows that on the blade with crack on trailing edge tend to grows uniformly to the direction of crack front. However, on the blade with crack on leading edge, crack tend to grows toward surface where steam flow hit the body of blade.

From **Figure 77**, it can be understood that the crack growth rate on the blade with crack on leading tip tend to has greater value than the other model. The difference is huge which possibly caused by stress intensity factor (SIF) as it is the input value of crack propagation formula of Paris' Law.

“This page intentionally left blank”

CHAPTER V

CONCLUSION AND SUGGESTION

5.1 Conclusion

Based on the result of data analysis which have been done, it conclude as follows:

1. The stress concentration value on the last stage blade with normal condition is comparably higher than the first stage blade with the highest value of 91.925 MPa. The highest stress concentration is located in the bottom tip of leading edge and this value is below the yield and ultimate tensile strength of the material.
   The blade with 1 mm crack depth located on the trailing edge has lowest value of stress concentration among other model with value of 114.06 MPa and the blade with 10 mm depth crack located on the leading tip has highest value of stress concentration with value of 318.89 MPa. The blade with combination of crack on the both leading tip and trailing edge with depth of 5 mm has stress concentration value of 219.62 and it located in the leading tip crack front.

2. In normal condition blade, minor damage prediction with size less than 0.2 mm appear in bottom tip of leading edge and has an available life of 7.179×10^5 cycles. Flawed blade with crack size of 1 mm on trailing edge has the longest life with recorded available life of 199,700 cycles and blade with crack size of 10 mm on leading tip has the shortest life with recorded available life of 5,995.7 cycles.

3. The crack growth rate in the blade with crack depth of 10 mm in leading tip is comparably greater than the blade with crack depth of 10 mm in trailing edge with value of 0.186 mm/cycle and 0.019 mm/cycle. In the blade with crack depth of 10 mm in leading tip, crack grows from 0 mm to 2.179 mm in 12 cycles. In the blade with crack depth of 10 mm in trailing edge, crack grows from 0 mm to 1.501 mm in 79 cycles.

5.2 Suggestion

1. The modelling process shall be done accurately according geometry data of related real steam turbine.
2. Further researches shall consider particle implosion or erosion phenomenon.
3. Further researches shall conduct analysis based on real case of crack occurrence.

"This page intentionally left blank"

BIBLIOGRAPHY

[1] P. Breeze, Power Generation Technologies, Elsevier, 2014

[2] S. Basu, A. Debnath, Power Plant Instrumentation and Control Handbook, Elsevier, 2015

[3] Country Comparison on Electricity Consumption, The Central Intelligence Agency, 2014

[4] International Energy Outlook 2013, U.S. Energy Information Administration

[5] Global Energy Statistical Yearbook 2017, Enerdata

[6] S.C. Parsons, The Steam Turbine, Univeristy of Cambridge, 1911

[7] T. Tanuma, Advance in Steam Turbines for Modern Power Plants, Elsevier, 2017

[8] https://en.wikipedia.org/wiki/Steam_turbine

[9] C.T. Sun, Z.H. Jin, Fracture Mechanics, Elsevier, 2012

[10] R.N.L. Smith, Basic Fracture Mechanics, Butterworth-Heinemann, 1991

[11] J.A. Segura, L. Castro, I. Rosales, J.A. Rodriguez, G. Urquiza, J.M. Rodriguez, Diagnostic and Failure Analysis in Blades of a 300 MW Steam Turbine, Elsevier, 2017

[12] A.A. Griffith, The Phenomena of Rupture and Flow in Solids, Philosophical Transactions of the Royal Society of London, 1921

[13] https://en.wikipedia.org/wiki/Fracture_mechanics

[14] https://en.wikipedia.org/wiki/Paris%27_law

[15] D. Roylance, Fatigue, Massachusetts Institute of Technology, Cambridge, 2001

[16] Z. Mazur, R. Garcia-Illescas, J. Porcayo-Calderon, Last Stage Blades Failure Analysis of a 28 MW Geothermal Turbine, Elsevier, 2008

[17] Z. Mazur, R. Garcia-Illecas, J. Aguirre-Romano, N. Perez-Rodriguez, Steam Turbine Blade Failure Analysis, Elsevier, 2006

[18] D.L. Logan, A First Course in the Finite Element Method, Cengage Learning, 2011

[19] W. Zhao, Y. Li, M. Xue, P. Wang, J. Jiang, Vibration Analysis for Failure Detection in Low Pressure Steam Turbine Blades in Nuclear Power Plant, Elsevier, 2017

[20] L.O.A. Affonso, Introduction to Failure Modes, Machinery Failure Analysis Handbook, Elsevier, 2006

[21] J. E. Shigley, Mechanical Engineering Design 10th Ed.

[22] C.F. Zorowski, Fluctuating Load Analysis, 2002

“This page intentionally left blank”

ATTACHMENT I

STEAM TURBINE SPECIFICATION & CAPACITY DATA

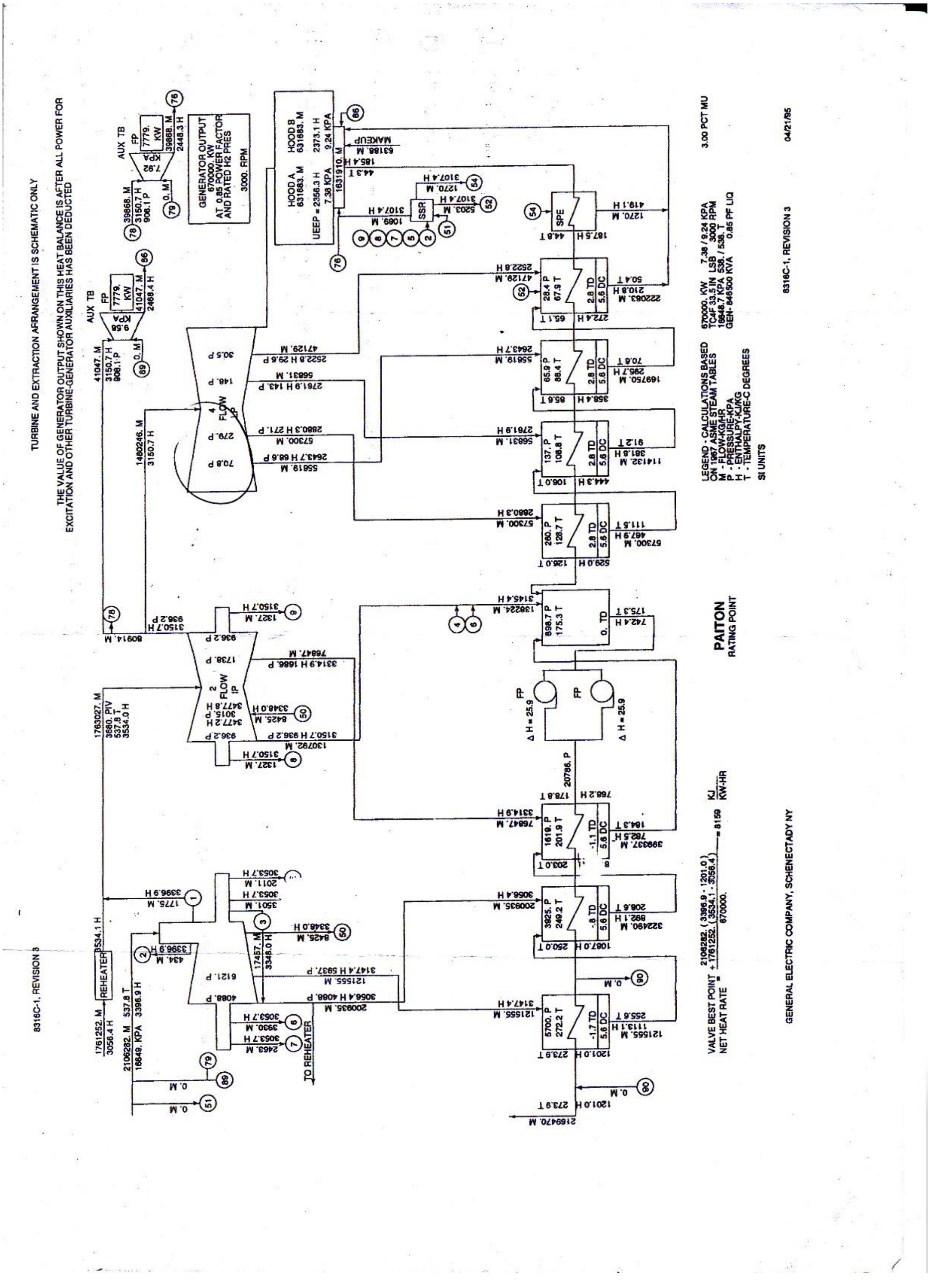

Figure (Attachment) 1 Energy Balance

TECHNICAL DATA SUPPLIED BY BIDDER FOR

STEAM TURBINE-GENERATOR(S)

Sheet 5 of 17

15. Mechanical-hydraulic logic cabinet overall size, ft - in. ____ NA ____

C. CONSTRUCTION

1. a) Nominal size of last stage buckets, in. 33.5 in.
   b) Last stage annulus area, sq. ft. 290.8
   c) Number of last stage exhausts 4

2. Casing materials (ASTM Specification and grade)
   a) Low pressure and up to 450 F A36
   b) From 451 F to 750 F A356 Gr6
   c) From 751 F to 900 F A356 Gr6
   c) Above 900 F A356 Gr6

3. Composition of steam chest (ASTM Specification and grade)

   ____

   Maximum allowable operating temperature in steam chest, F

   ____

4. Materials (ASTM Specification and grade)
   a) Turbine shaft LP Rotor – A470 C1.6 / HP Rotor – ASTM A470 C:
   b) Generator shaft ASTM A469 C1.7
   c) Turbine blading (HP) ASTM A479 Type 403 C2
      (IP) ASTM A479 Type 403 C2
      (LP) ASTM no equiv – 12% Cr 403SS
   d) Packing (HP) A439D – 2C
      (IP) A439D – 2C
      (LP) Lead Bronze
   e) Interstage packing See above
   f) Dummy packing NA

GE PROPRIETARY INFORMATION

RECEIVED
GSC TEC
DATE: 19 DEC 1996
BY: TIME:

Page 5 of 18

FOR INFORMATION ONLY
DATE: 10/08/96
ROBERT E. HALL
VICE PRESIDENT-ENG.
DUKE/FLUOR DANIEL

PT PAITON ENERGY COMPANY
PAITON PRIVATE POWER PROJECT PHASE
PAITON, EAST JAVA, INDONESIA
MITSUI & CO., LTD
DUKE FLUOR DANIEL
TOYO ENGINEERING CORP.
PROJECT DOC. NO.: P101-24-1700-00-0829 REV.: 00
ITEM NO.:
REQ. NO.:
PURCHASE ORDER NO.:

Figure (Attachment) 2 Material Information

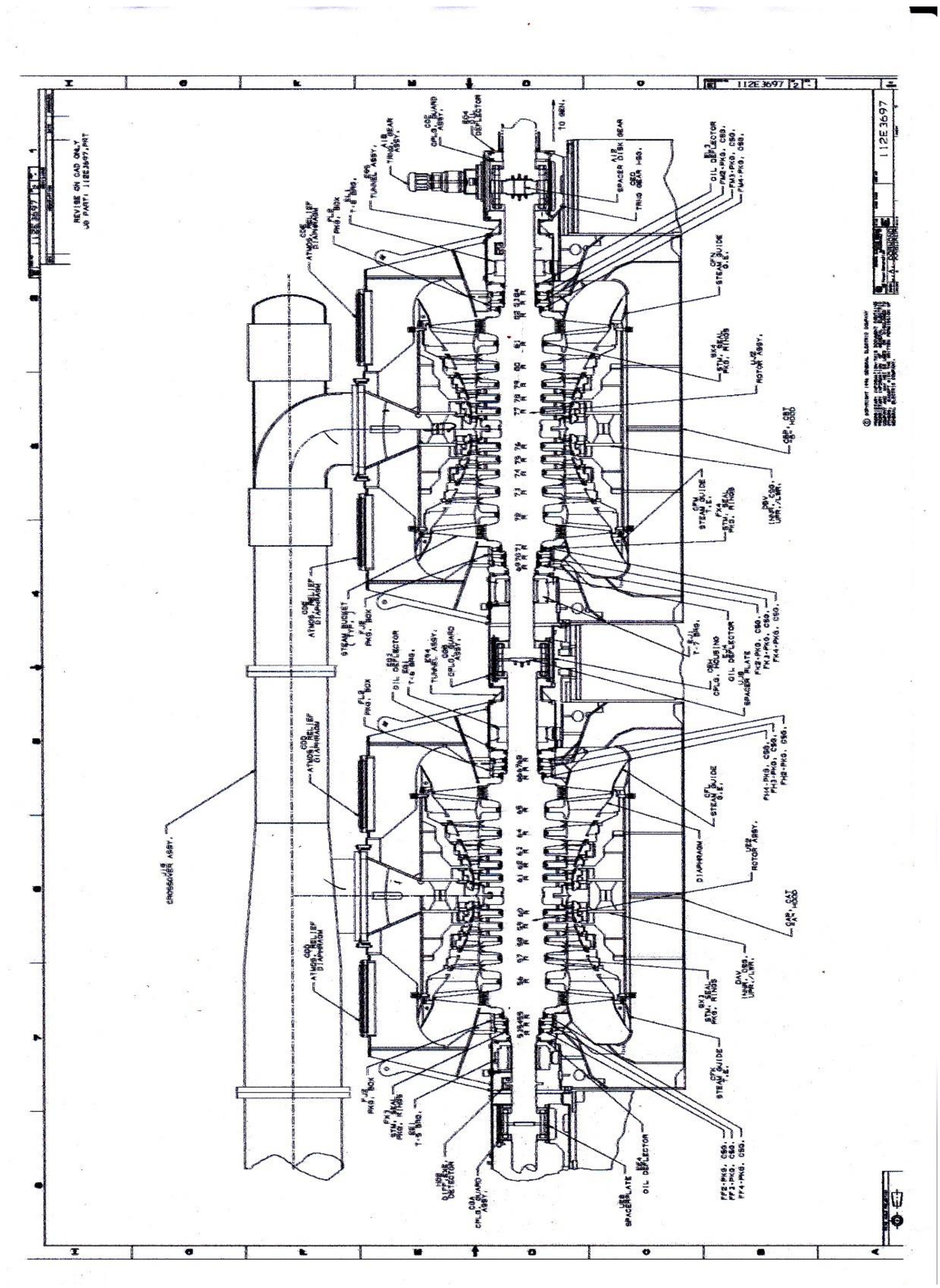

Figure (Attachment) 3 Steam Turbine Layout

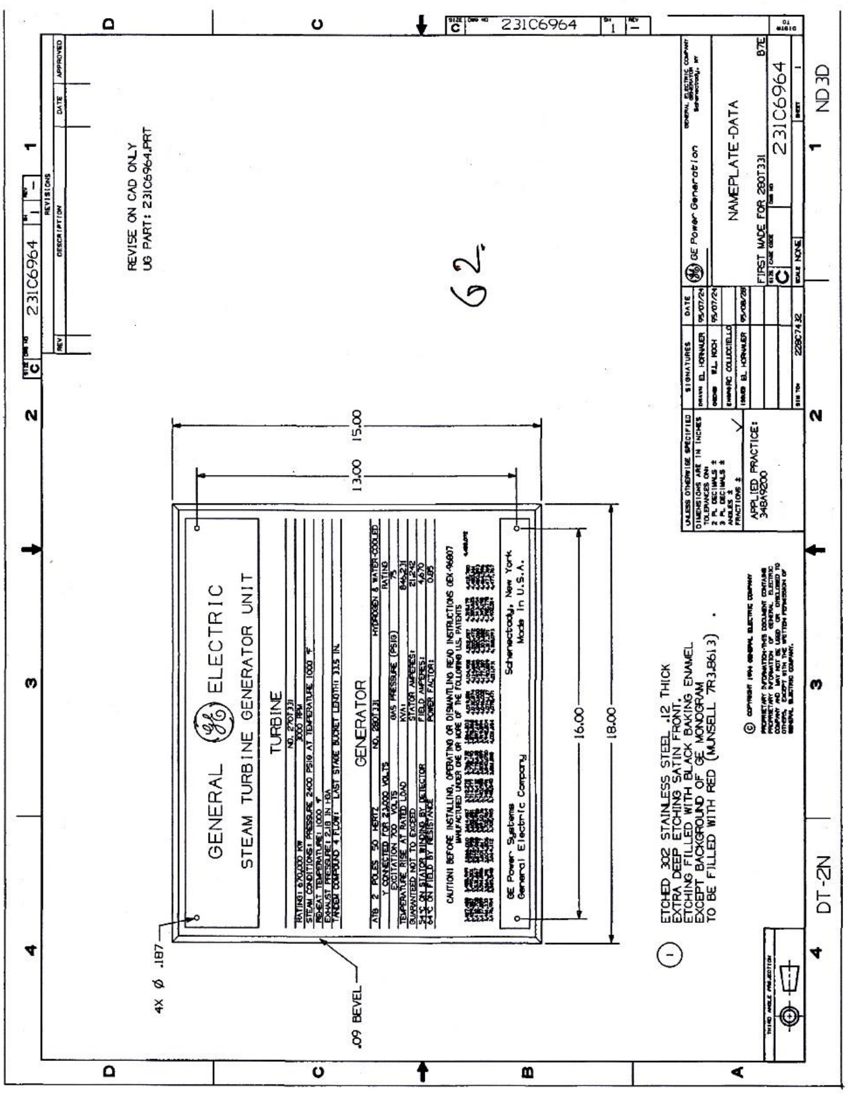

Figure (Attachment) 4 Steam Turbine LP General Information

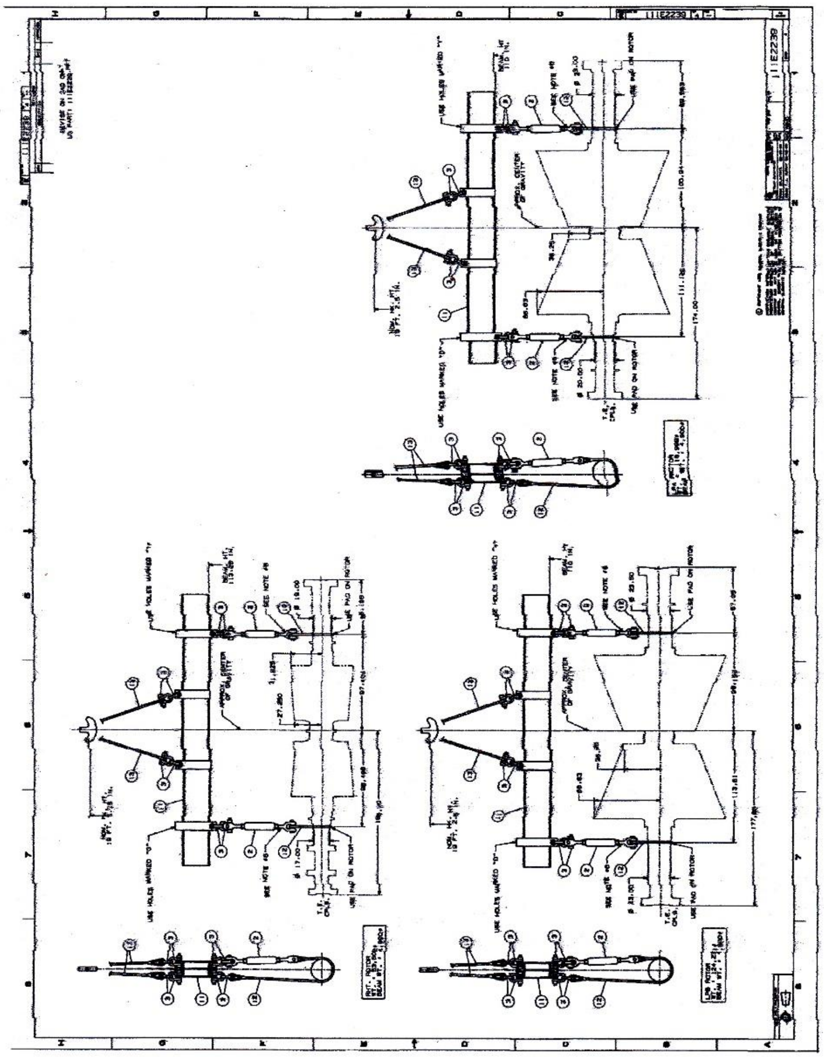

Figure (Attachment) 5 Steam Turbine Installation Procedure

Parts List

PREF XE00
BKTS,CVRS,&HDWR
0699L671G0051
QTY./TURBINE 1 CAT.NO.: LOC.:

PART NO.	ZONE	NOMENCLATURE	DRAWING I.D.	QTY.	CAT. NO.	LOC.	CAT. QTY.
1		BUCKET 33.5"	0962E740P0002	94			
2		SLEEVE TIE WIRE	224B1750P0001	94			
3		BKT COVER (INSRT)	187C4100P0002	94			
4		PIN,BUCKET–DOVETAIL	U766F938B0000	94			
5		PIN,BUCKET–DOVETAIL	U766F311B0000	94			
6		PIN,BUCKET–DOVETAIL	U766E686B0000	94			
7		BUCKET ASM	148D9823P0001	1			

Figure (Attachment) 6 Steam Turbine LP General Information

“This page intentionally left blank”

ATTACHMENT II

MATERIAL PROPERTIES (ASTM A479/A479M)

TABLE 2 *Continued*

UNS Designation	Type	Condition	Tensile Strength, min, ksi [MPa]	Yield Strength,^{A} min, ksi [MPa]	Elongation in 2 in. [50 mm] or 4D, min, %	Reduction of Area, min, %^{B,C}	Brinell Hardness, max
S40500	405	annealed	60 [415]	25 [170]	20	45	207
S43000, S43035	430, 439	annealed	70 [485]	40 [275]	20^{H}	45^{H}	192
S44627	XM-27	annealed	65 [450]	40 [275]		45^{H}	217
S44401	. . .	annealed	60 [415]	45 [310]	20^{I}	45^{I}	217
S44700	. . .	annealed	70 [485]	55 [380]	20	40	. . .
S44800	. . .	annealed	70 [485]	55 [380]	20	40	. . .
Martensitic Grades							
S40300, S41000	403, 410	annealed	70 [485]	40 [275]	20^{I}	45^{I}	223
		1	70 [485]	40 [275]	20^{I}	45^{I}	223
		2	110 [760]	85 [585]	15	45	269
		3	130 [895]	100 [690]	12	35	331
S41400	414	tempered	115 [795]	90 [620]	15	45	321
S41425	. . .	tempered	120 [825]	95 [655]	15	45	321
S41500	. . .	normalized and tempered	115 [795]	90 [620]	15	45	293
S43100	431^{J}	annealed	. . .	. . .	. . .	. . .	277
		tempered	115 [795]	90 [620]	15	45	321
S41040	XM-30	annealed	70 [485]	40 [275]	13^{H}	45^{H}	235
		quenched and tempered	125 [860]	100 [690]	13	45	302

^{A} See Section 7.
^{B} Reduction of area does not apply on flat bars 3⁄16 in. [4.80 mm] and under in thickness, as this determination is not generally made in this product size.
^{C} The material shall be capable of meeting the required reduction of area where listed, but actual measurement and reporting of the reduction of area are not required unless specified in the purchase order.
^{D} Cold-finished shapes require only 15 %, minimum, elongation.
^{E} American Welding Society designation.
^{F} Tensile strength 70 ksi [485 MPa] min permitted for extruded shapes.
^{G} For bars greater than 2 in. [51 mm], a cross section, 60 ksi [415 MPa] min, shall be permitted.
^{H} Elongation in 2 in. or 50 mm of 12 % min and reduction of area of 35 % min permitted for cold-finished bars.
^{I} Elongation in 2 in. of 12 % min and reduction of area of 35 % min permitted for cold-drawn or cold-rolled bars.
^{J} Annealed bars shall be capable of meeting the tempered condition requirements when heat treated.

TABLE 3 Response To Heat Treatment

Type^{A}	Heat Treatment Temperature^{B} °F (°C), min	Quenchant	Hardness HRC, min
403	1750 [955]	Air	35
410	1750 [955]	Air	35
414	1750 [955]	Oil	42

^{A} Samples for testing shall be in the form of a section not exceeding 3⁄8 in. [9.50 mm] in thickness.
^{B} Temperature tolerance is ±25°F [15°C].

SUPPLEMENTARY REQUIREMENTS

The following may be made requirements when the purchaser specifies them to be applicable.

S1. Materials for High-Temperature Service

S1.1 Unless an H grade has been ordered, this supplementary requirement shall be specified for ASME Code applications for service above 1000°F [540°C].

S1.2 The user is permitted to use an austenitic stainless steel as the corresponding H grade when the material meets all requirements of the H grade including chemistry, annealing temperature, and grain size (see Section 6).

S1.3 The user is permitted to use an L grade austenitic stainless steel for service above 1000°F [540°C], subject to the applicable allowable stress table of the ASME Code, when the material meets all requirements of this specification and the grain size is ASTM No. 7 or coarser as determined in accordance with Test Methods E112. The grain size shall be reported on a Certified Test Report.

Copyright ASTM International
Provided by IHS under license with ASTM
No reproduction or networking permitted without license from IHS

Licensee=BP International/5928366101
Not for Resale, 03/04/2013 10:13:32 MST

Figure (Attachment) 7 Material Properties

ATTACHMENT III

CRACK MODEL VARIATION

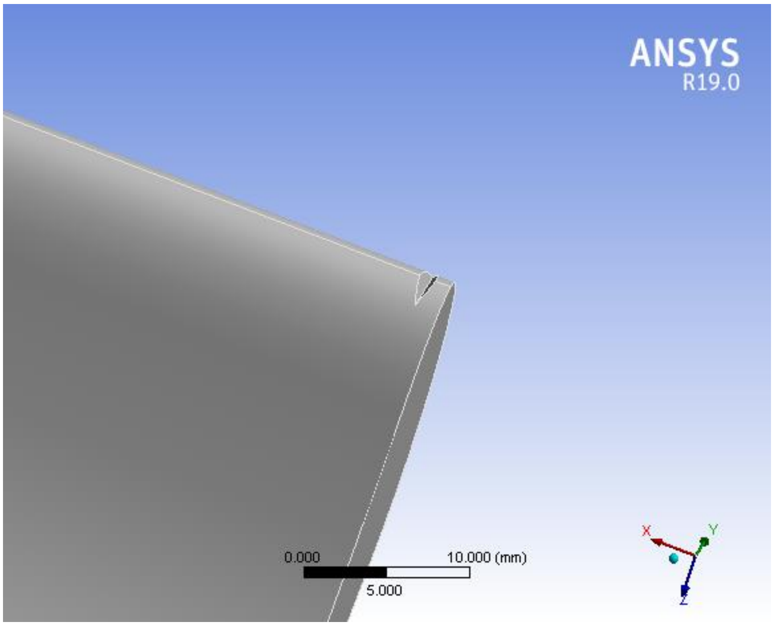

Crack Model with Depth of 1 mm Located on the Leading Tip

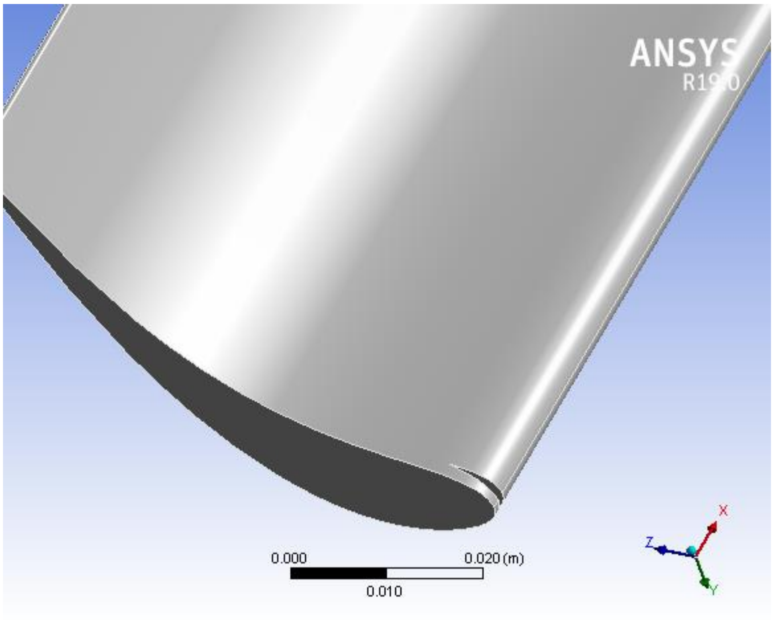

Crack Model with Depth of 5 mm Located on the Leading Tip

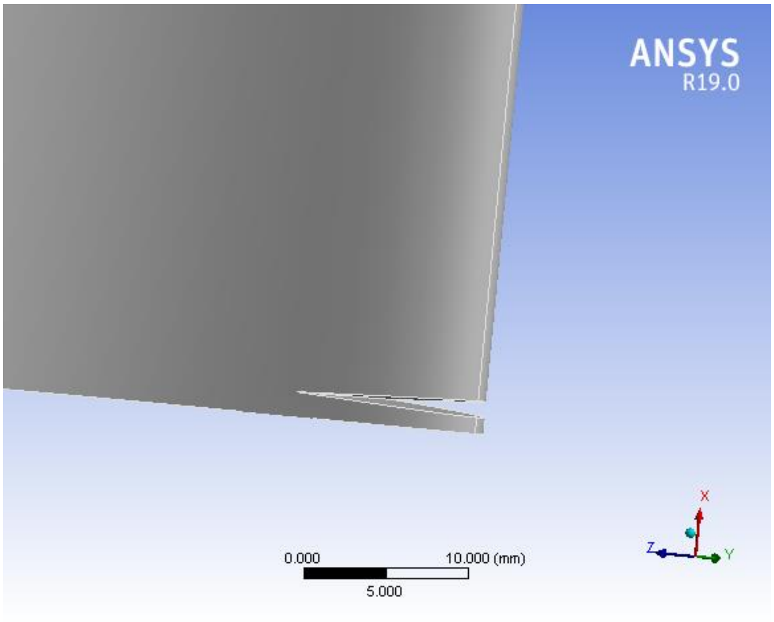

Crack Model with Depth of 10 mm Located on the Leading Tip

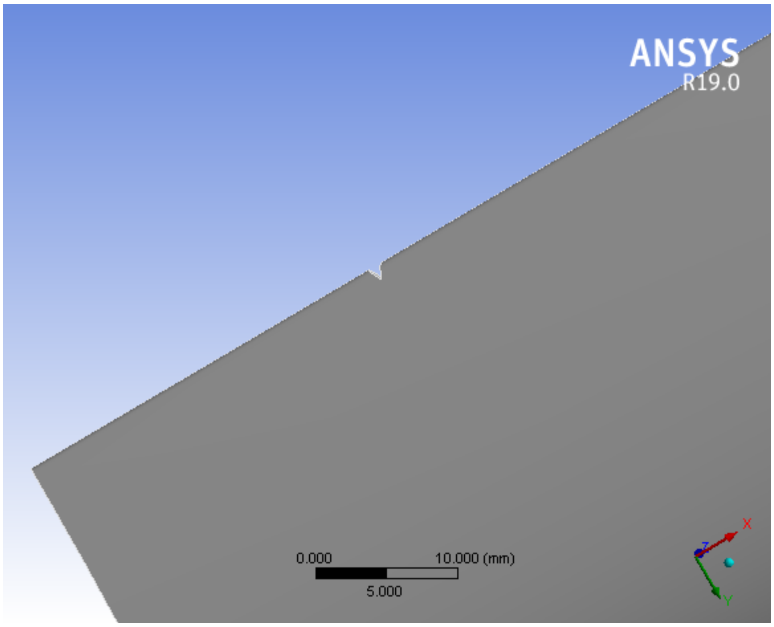

Crack Model with Depth of 1 mm Located on the Trailing Edge

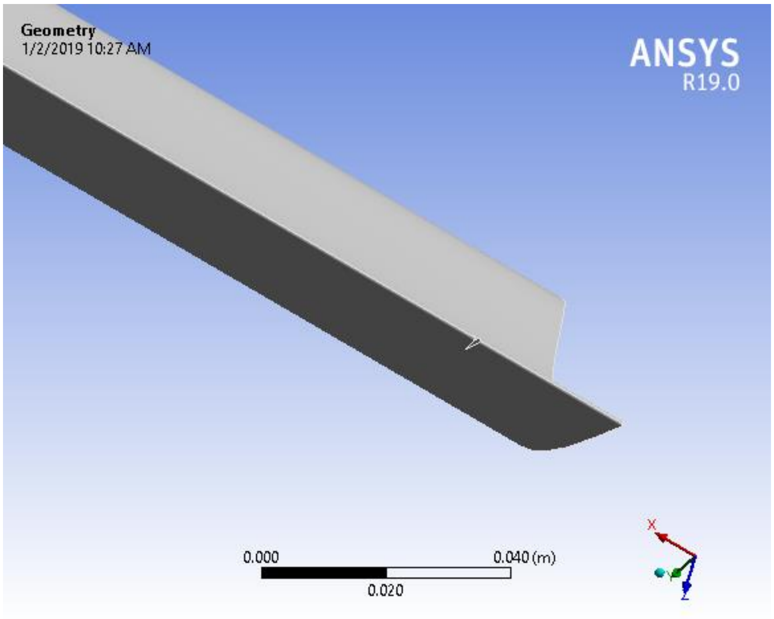

Crack Model with Depth of 5 mm Located on the Trailing Edge

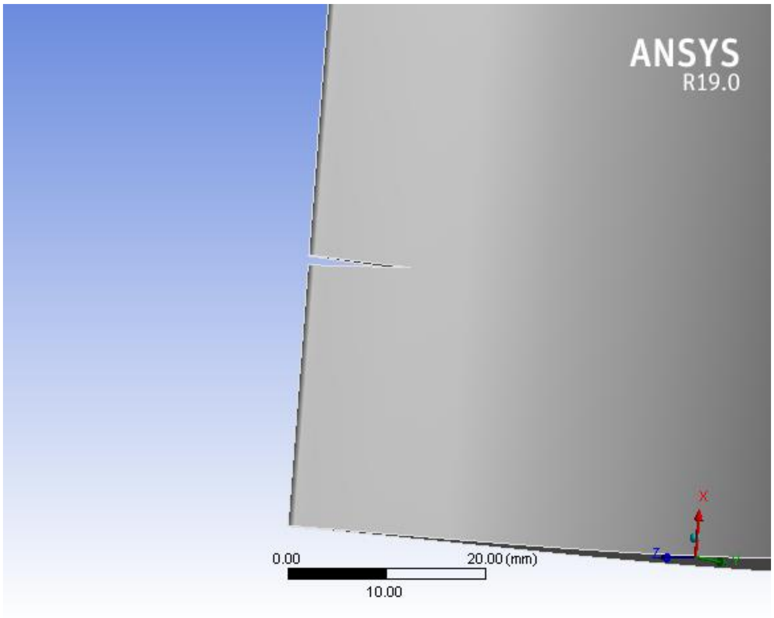

Crack Model with Depth of 10 mm Located on the Trailing Edge

ATTACHMENT IV

ANALYSIS RESULT

BLADE WITH 1 MM CRACK ON LEADING TIP

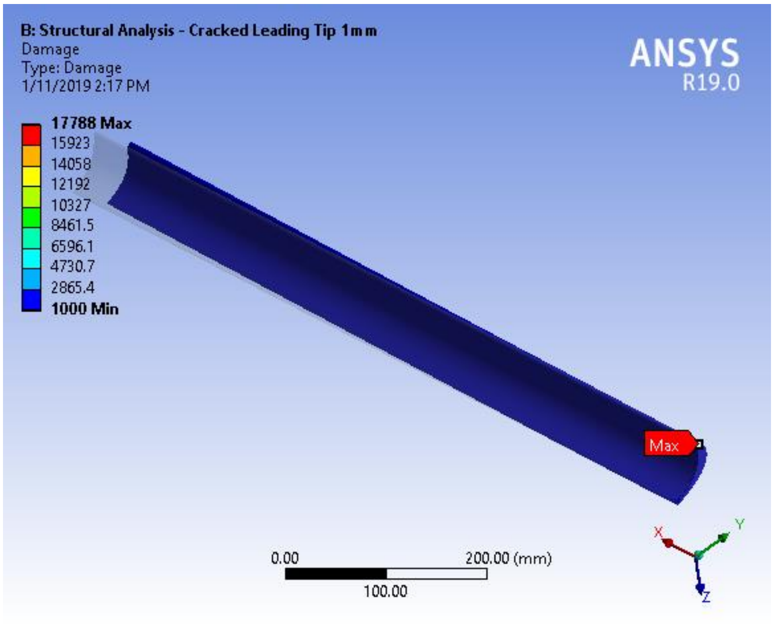

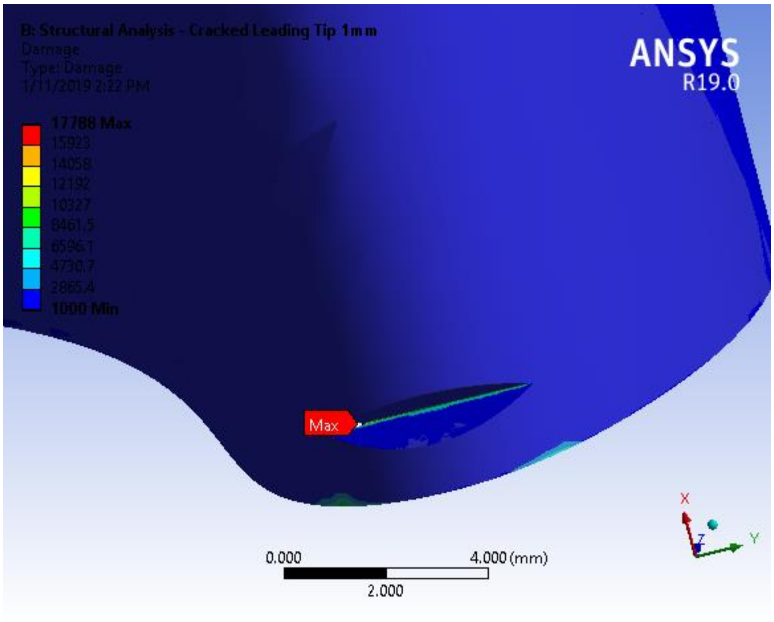

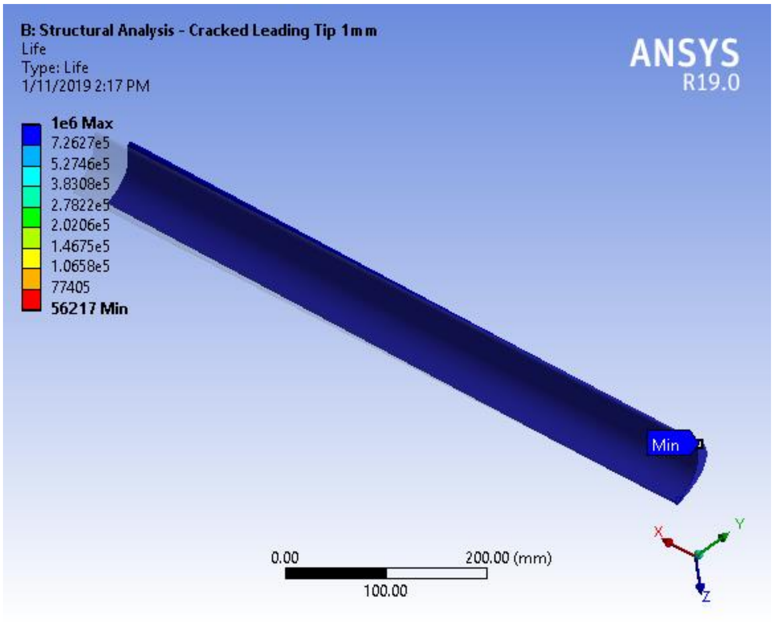
B: Structural Analysis - Cracked Leading Tip 1mm
Life
Type: Life
1/11/2019 2:17 PM
1e6 Max
7.2627e5
5.2746e5
3.8308e5
2.7822e5
2.0206e5
1.4675e5
1.0658e5
77405
56217 Min
ANSYS
R19.0
Min
0.00
200.00 (mm)
100.00
X
Y
Z

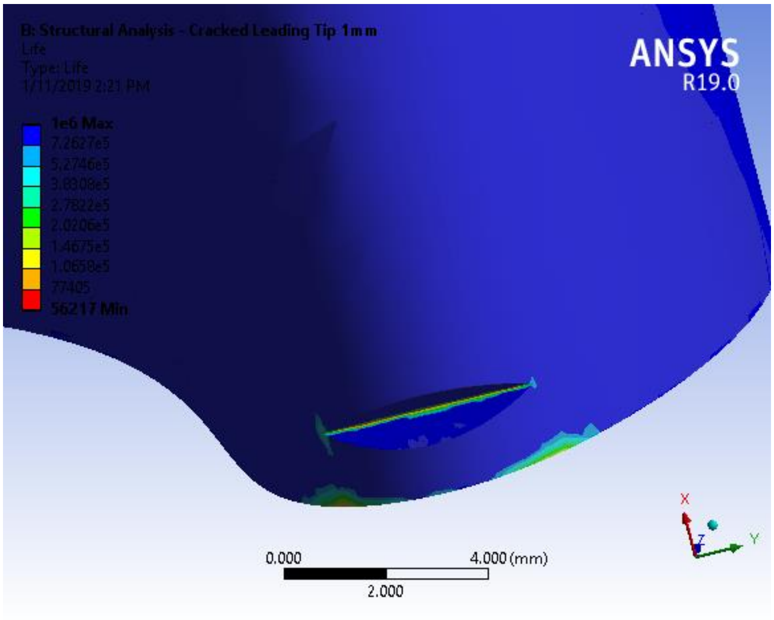
B: Structural Analysis - Cracked Leading Tip 1mm
Life
Type: Life
1/11/2019 2:21 PM
1e6 Max
7.2627e5
5.2746e5
3.8308e5
2.7822e5
2.0206e5
1.4675e5
1.0658e5
77405
56217 Min
ANSYS
R19.0
0.000
4.000 (mm)
2.000
X
Y
Z

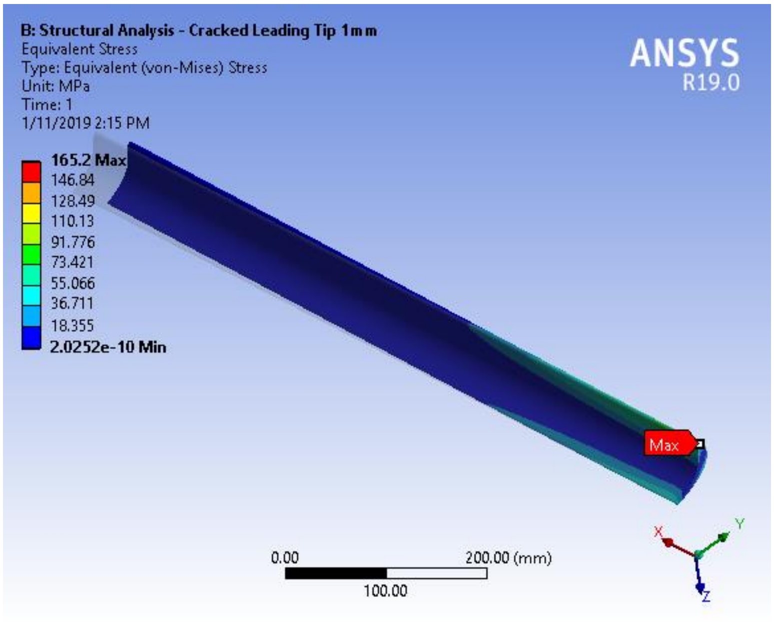
B: Structural Analysis - Cracked Leading Tip 1mm
Equivalent Stress
Type: Equivalent (von-Mises) Stress
Unit: MPa
Time: 1
1/11/2019 2:15 PM
ANSYS
R19.0
165.2 Max
146.84
128.49
110.13
91.776
73.421
55.066
36.711
18.355
2.0252e-10 Min
Max
0.00
200.00 (mm)
100.00
X
Y
Z

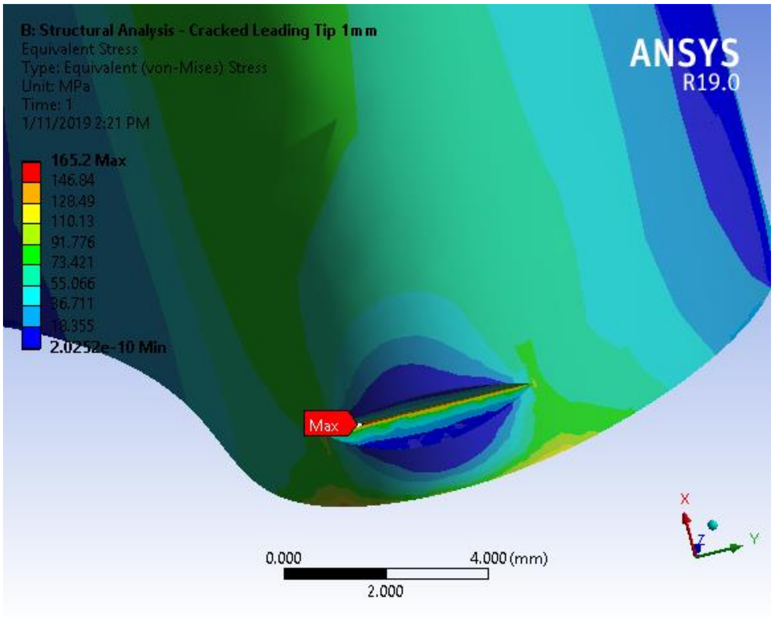
B: Structural Analysis - Cracked Leading Tip 1mm
Equivalent Stress
Type: Equivalent (von-Mises) Stress
Unit: MPa
Time: 1
1/11/2019 2:21 PM
ANSYS
R19.0
165.2 Max
146.84
128.49
110.13
91.776
73.421
55.066
36.711
18.355
2.0252e-10 Min
Max
0.000
4.000 (mm)
2.000
X
Z
Y

BLADE WITH 5 MM CRACK ON LEADING TIP

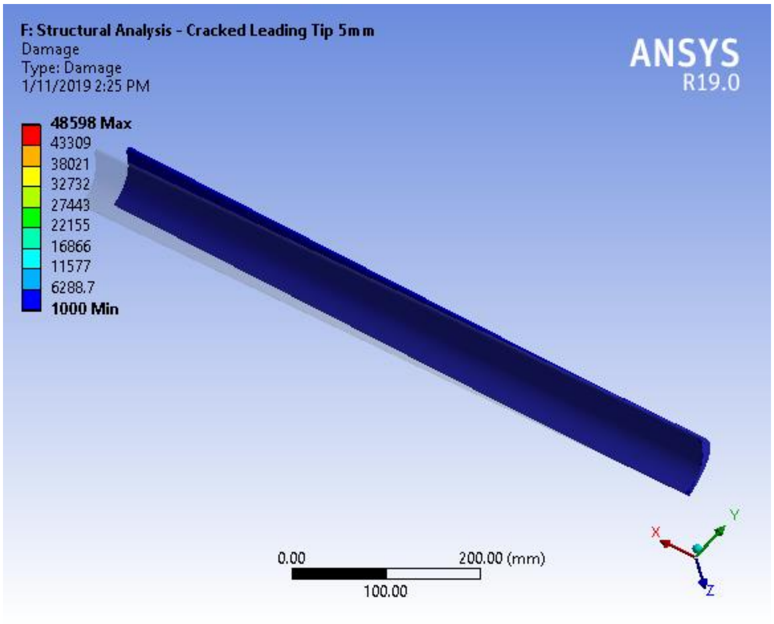

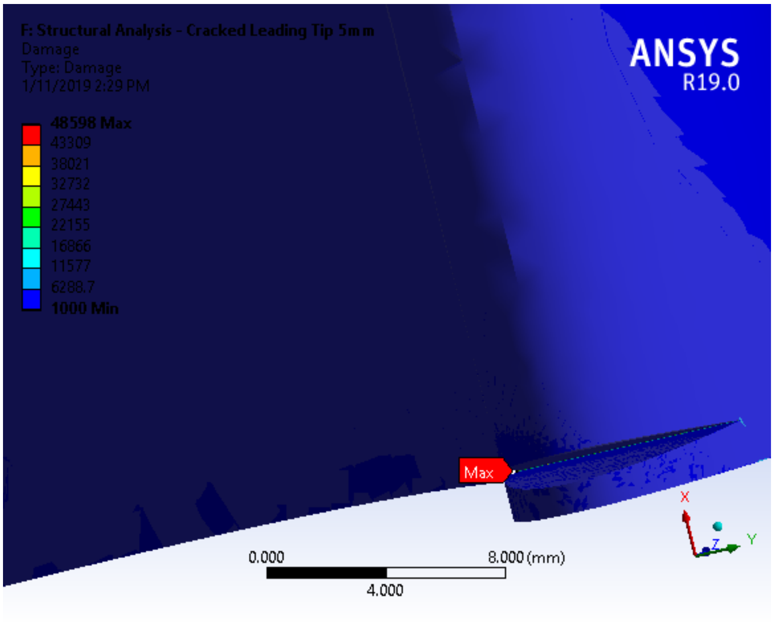

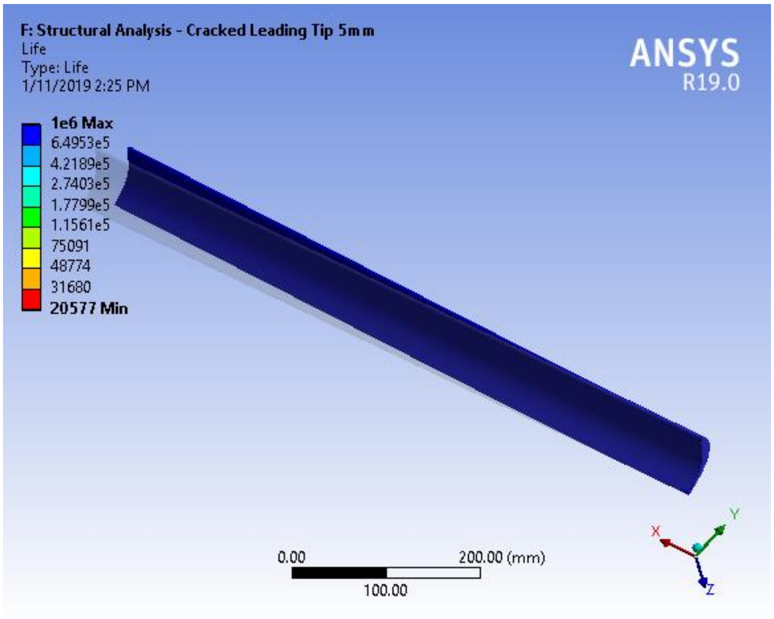
F: Structural Analysis - Cracked Leading Tip 5mm
Life
Type: Life
1/11/2019 2:25 PM
1e6 Max
6.4953e5
4.2189e5
2.7403e5
1.7799e5
1.1561e5
75091
48774
31680
20577 Min
ANSYS
R19.0
0.00
200.00 (mm)
100.00
X
Y
Z

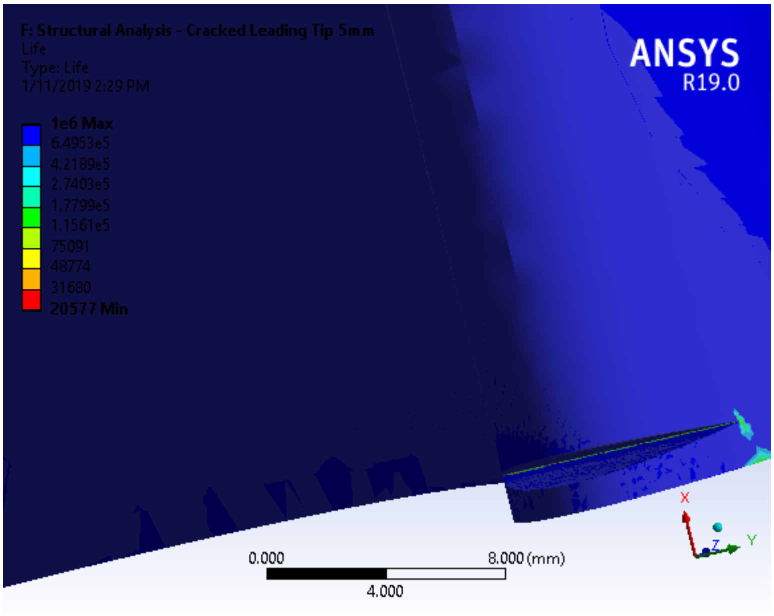
F: Structural Analysis - Cracked Leading Tip 5mm
Life
Type: Life
1/11/2019 2:29 PM
1e6 Max
6.4953e5
4.2189e5
2.7403e5
1.7799e5
1.1561e5
75091
48774
31680
20577 Min
ANSYS
R19.0
0.000
8.000 (mm)
4.000
X
Y
Z

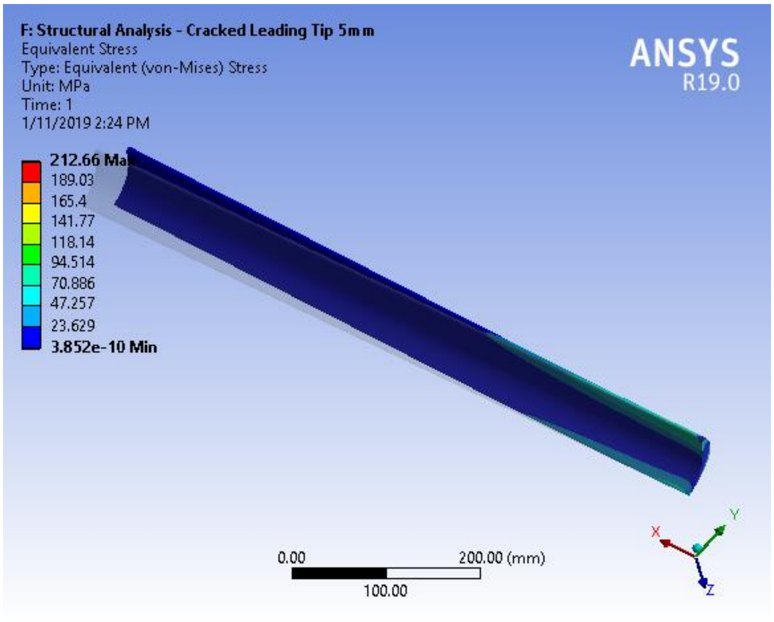
F: Structural Analysis - Cracked Leading Tip 5mm
Equivalent Stress
Type: Equivalent (von-Mises) Stress
Unit: MPa
Time: 1
1/11/2019 2:24 PM
212.66 Max
189.03
165.4
141.77
118.14
94.514
70.886
47.257
23.629
3.852e-10 Min
ANSYS
R19.0
0.00
200.00 (mm)
100.00
X
Y
Z

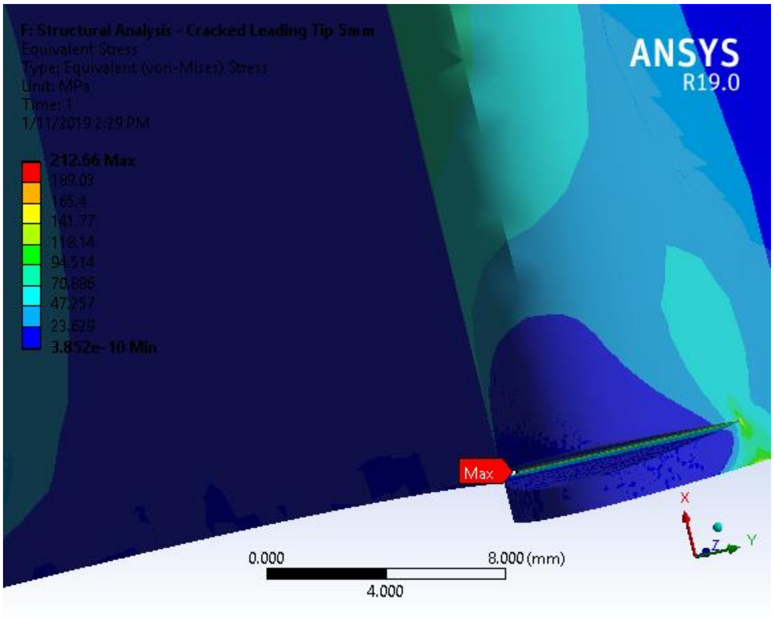
ANSYS
R19.0
Max
0.000
8.000 (mm)
4.000
X
Y

BLADE WITH 10 MM CRACK ON LEADING TIP

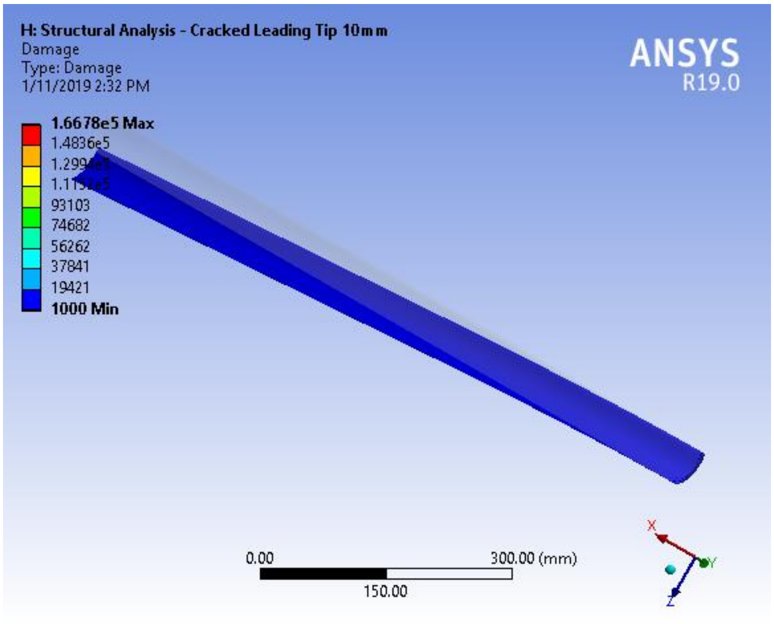

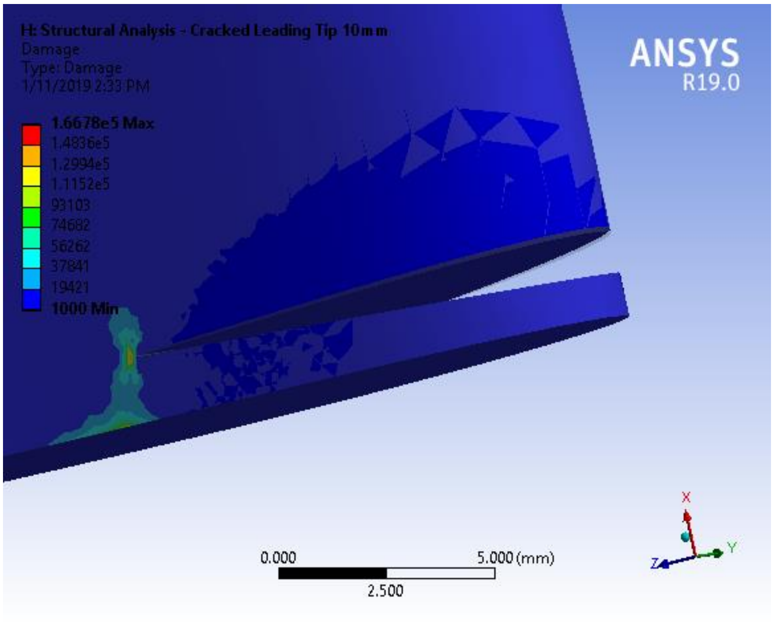

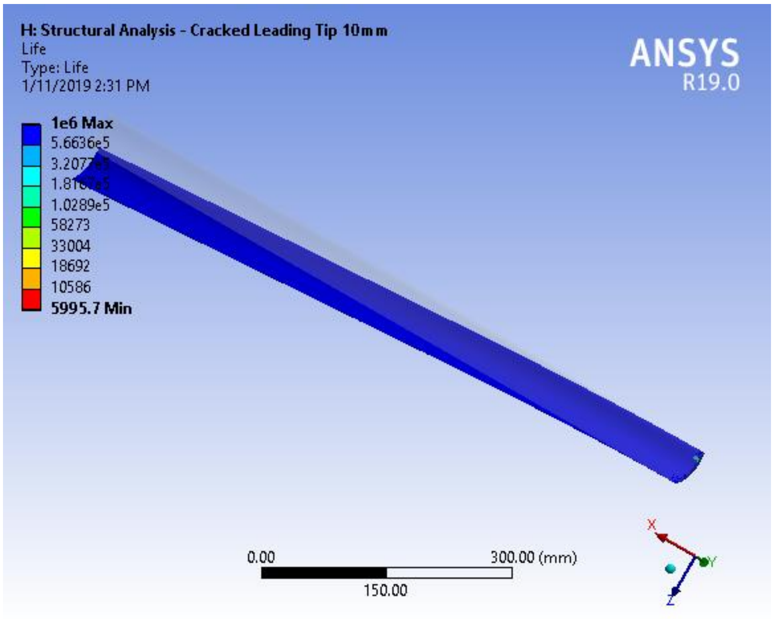
H: Structural Analysis - Cracked Leading Tip 10mm
Life
Type: Life
1/11/2019 2:31 PM
1e6 Max
5.6636e5
1.0289e5
58273
33004
18692
10586
5995.7 Min
ANSYS
R19.0
0.00
300.00 (mm)
150.00
X
Y
Z

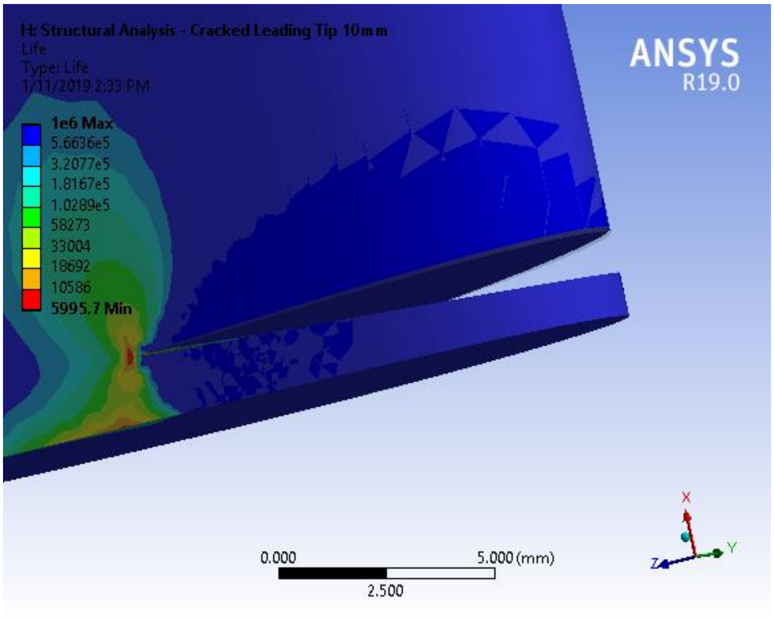
H: Structural Analysis - Cracked Leading Tip 10mm
Life
Type: Life
1/11/2019 2:33 PM
1e6 Max
5.6636e5
3.2077e5
1.8167e5
1.0289e5
58273
33004
18692
10586
5995.7 Min
ANSYS
R19.0
0.000
5.000 (mm)
2.500
X
Y
Z

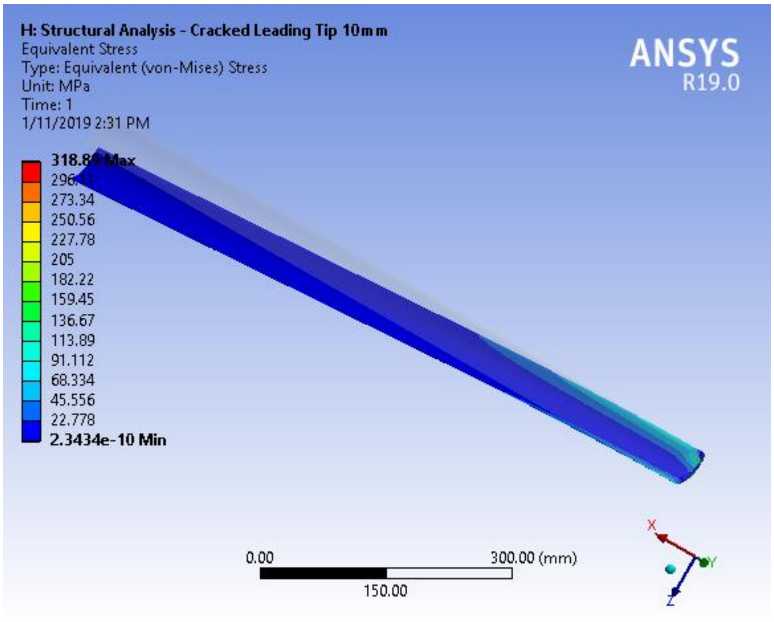
H: Structural Analysis - Cracked Leading Tip 10mm
Equivalent Stress
Type: Equivalent (von-Mises) Stress
Unit: MPa
Time: 1
1/11/2019 2:31 PM
318.89 Max
296.11
273.34
250.56
227.78
205
182.22
159.45
136.67
113.89
91.112
68.334
45.556
22.778
2.3434e-10 Min
ANSYS
R19.0
0.00
150.00
300.00 (mm)
X
Y
Z

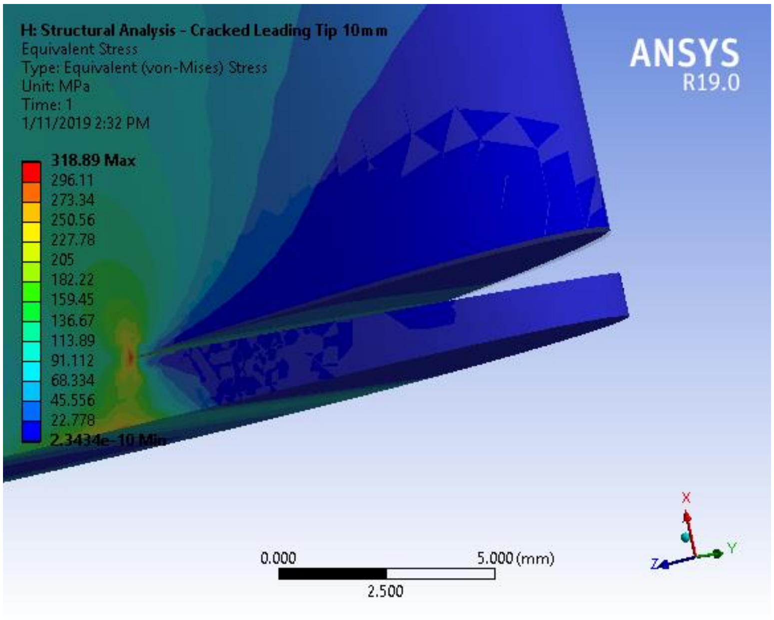
H: Structural Analysis - Cracked Leading Tip 10mm
Equivalent Stress
Type: Equivalent (von-Mises) Stress
Unit: MPa
Time: 1
1/11/2019 2:32 PM
318.89 Max
296.11
273.34
250.56
227.78
205
182.22
159.45
136.67
113.89
91.112
68.334
45.556
22.778
2.3434e-10 Min
ANSYS
R19.0
0.000
2.500
5.000 (mm)
X
Y
Z

BLADE WITH 1 MM CRACK ON TRAILING EDGE

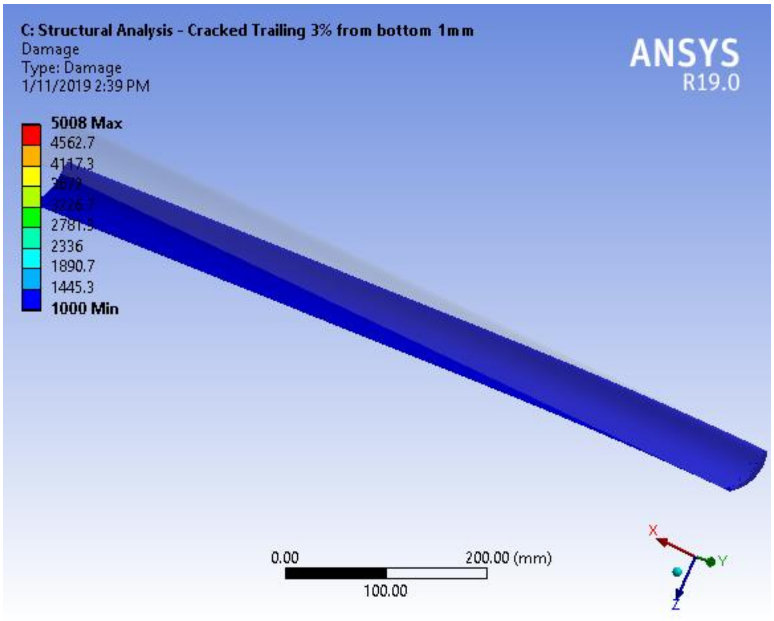

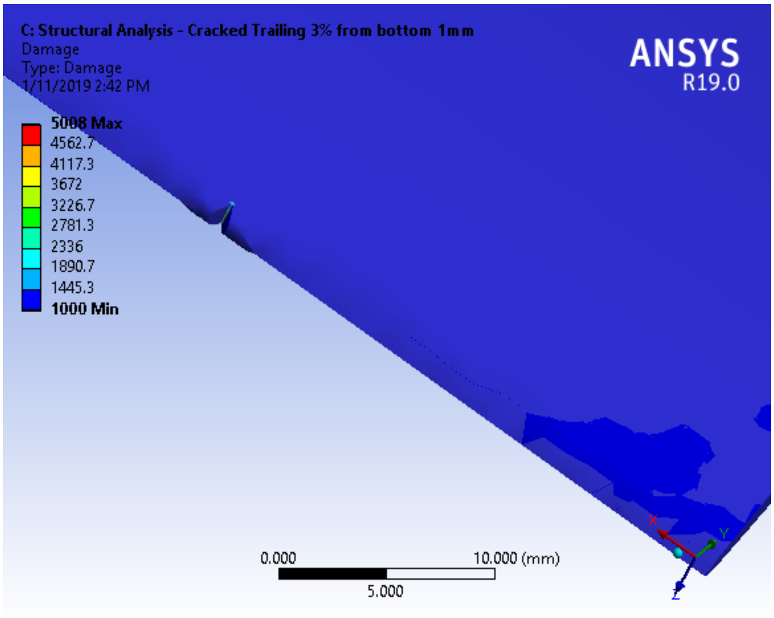

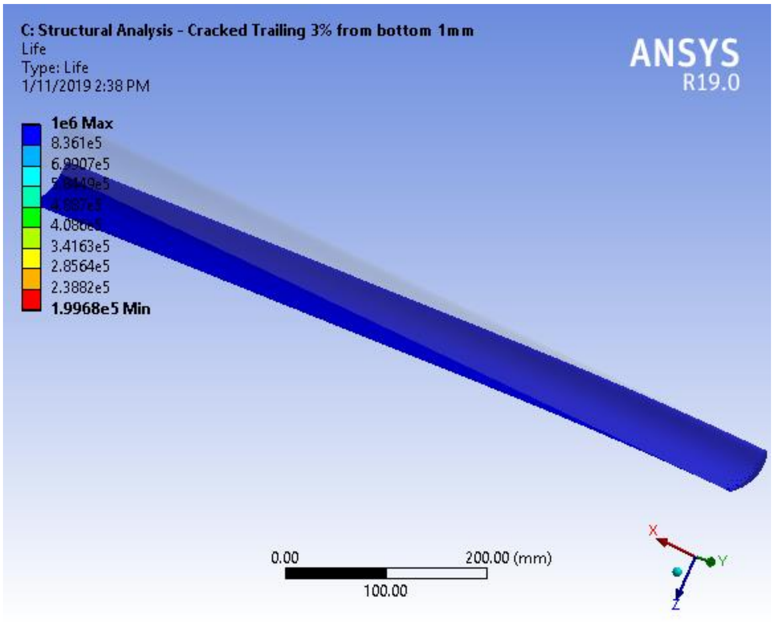
C: Structural Analysis - Cracked Trailing 3% from bottom 1mm
Life
Type: Life
1/11/2019 2:38 PM
ANSYS
R19.0
1e6 Max
8.361e5
6.9907e5
3.4163e5
2.8564e5
2.3882e5
1.9968e5 Min
0.00
200.00 (mm)
100.00

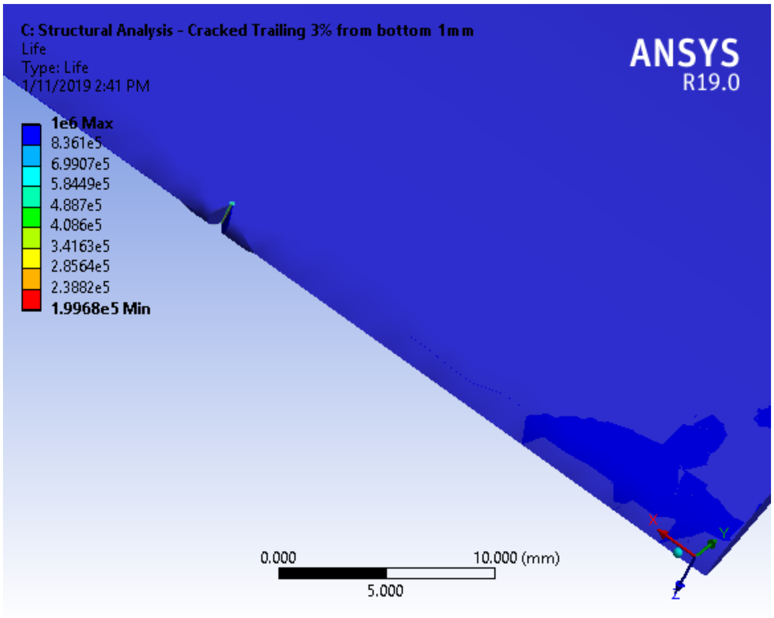
C: Structural Analysis - Cracked Trailing 3% from bottom 1mm
Life
Type: Life
1/11/2019 2:41 PM
ANSYS
R19.0
1e6 Max
8.361e5
6.9907e5
5.8449e5
4.887e5
4.086e5
3.4163e5
2.8564e5
2.3882e5
1.9968e5 Min
0.000
10.000 (mm)
5.000

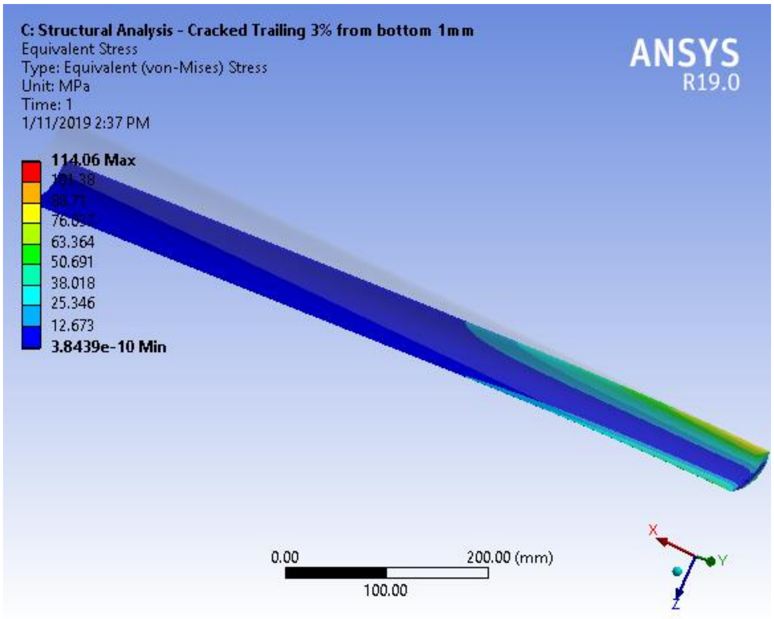
C: Structural Analysis - Cracked Trailing 3% from bottom 1mm
Equivalent Stress
Type: Equivalent (von-Mises) Stress
Unit: MPa
Time: 1
1/11/2019 2:37 PM
114.06 Max
63.364
50.691
38.018
25.346
12.673
3.8439e-10 Min
ANSYS
R19.0
0.00
200.00 (mm)
100.00

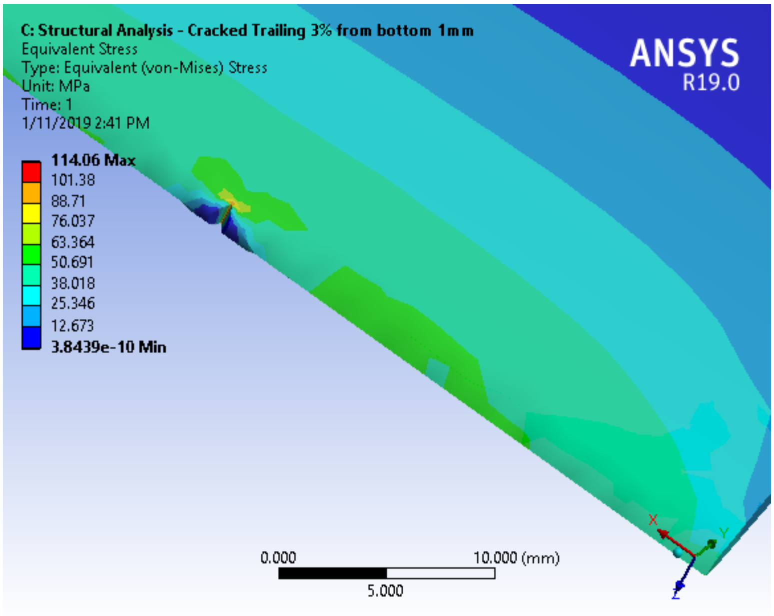
C: Structural Analysis - Cracked Trailing 3% from bottom 1mm
Equivalent Stress
Type: Equivalent (von-Mises) Stress
Unit: MPa
Time: 1
1/11/2019 2:41 PM
114.06 Max
101.38
88.71
76.037
63.364
50.691
38.018
25.346
12.673
3.8439e-10 Min
ANSYS
R19.0
0.000
10.000 (mm)
5.000

BLADE WITH 5 MM CRACK ON TRAILING EDGE

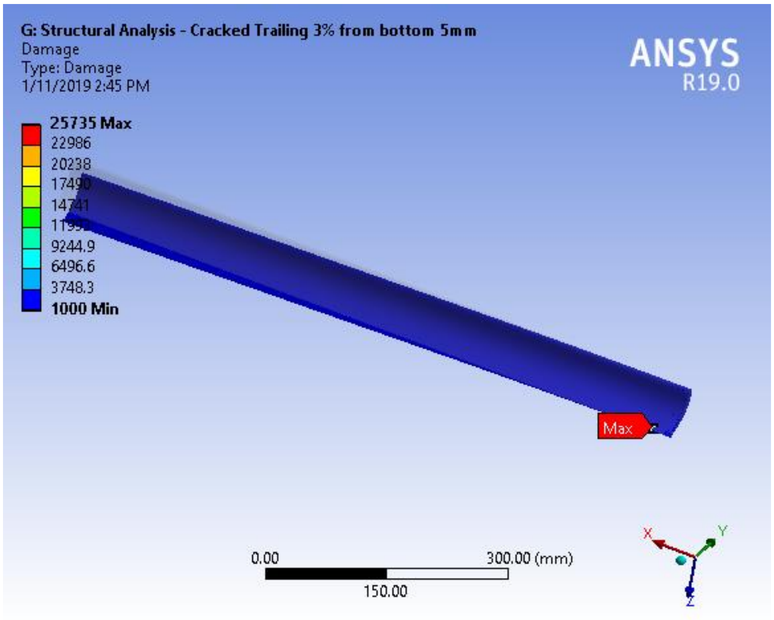

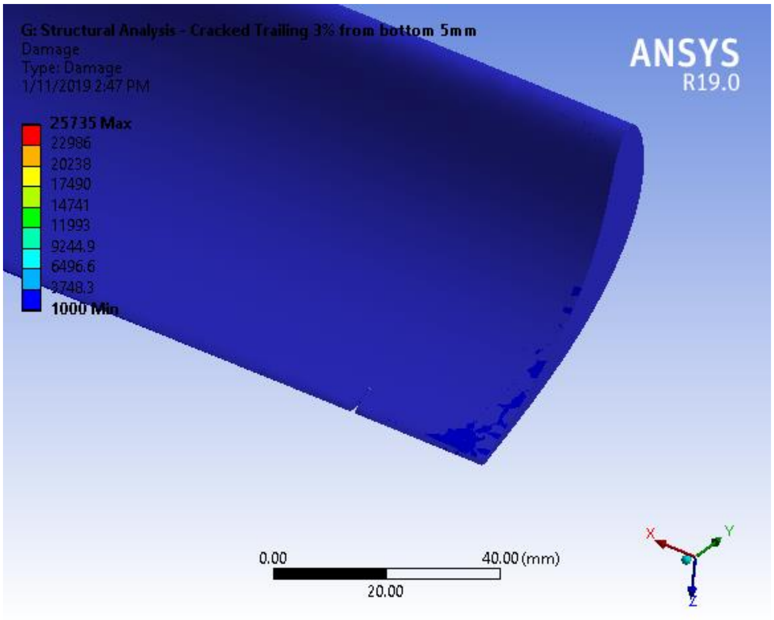

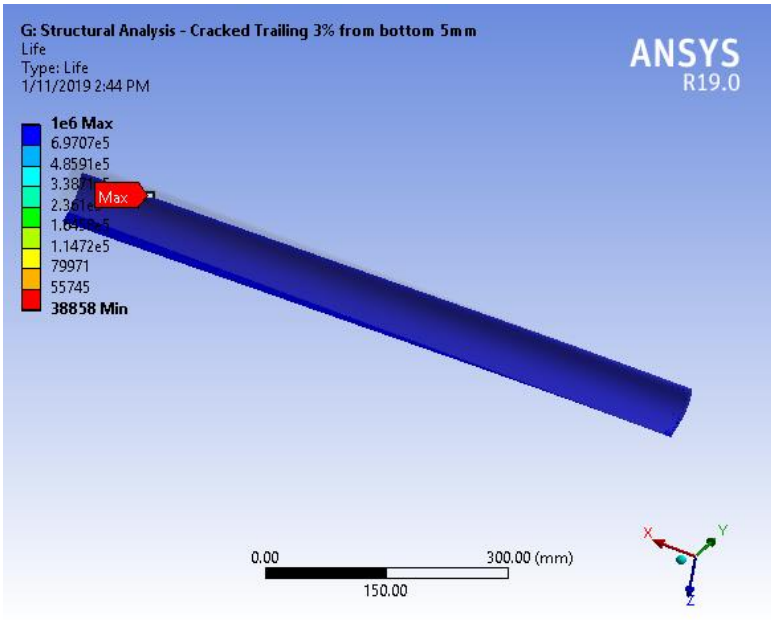
G: Structural Analysis - Cracked Trailing 3% from bottom 5mm
Life
Type: Life
1/11/2019 2:44 PM
ANSYS
R19.0
1e6 Max
6.9707e5
4.8591e5
1.1472e5
79971
55745
38858 Min
Max
0.00
300.00 (mm)
150.00
X
Y
Z

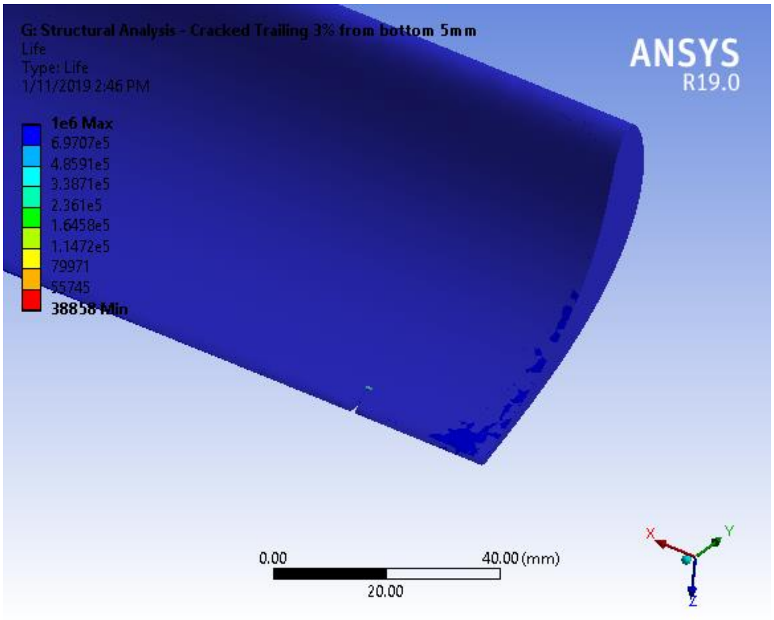
G: Structural Analysis - Cracked Trailing 3% from bottom 5mm
Life
Type: Life
1/11/2019 2:46 PM
ANSYS
R19.0
1e6 Max
6.9707e5
4.8591e5
3.3871e5
2.361e5
1.6458e5
1.1472e5
79971
55745
38858 Min
0.00
40.00 (mm)
20.00
X
Y
Z

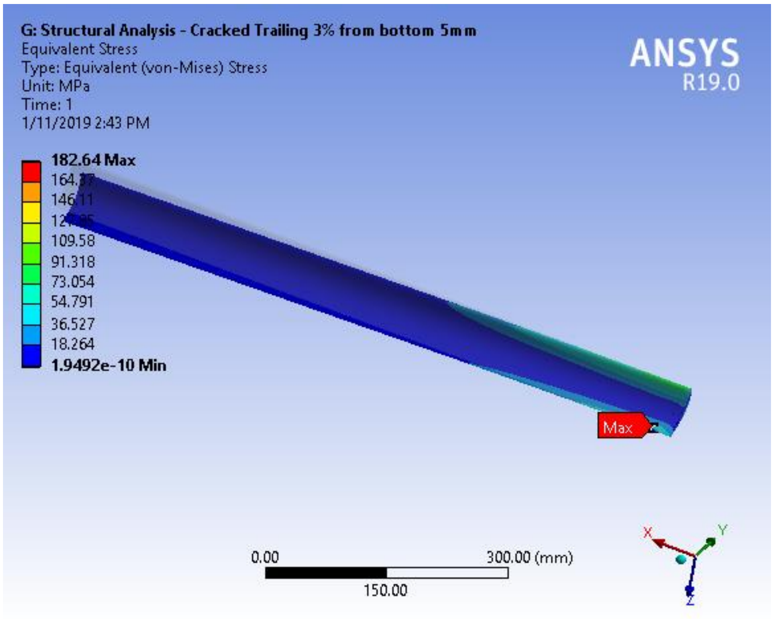
G: Structural Analysis - Cracked Trailing 3% from bottom 5mm
Equivalent Stress
Type: Equivalent (von-Mises) Stress
Unit: MPa
Time: 1
1/11/2019 2:43 PM
ANSYS
R19.0
182.64 Max
109.58
91.318
73.054
54.791
36.527
18.264
1.9492e-10 Min
Max
0.00
150.00
300.00 (mm)
X
Y
Z

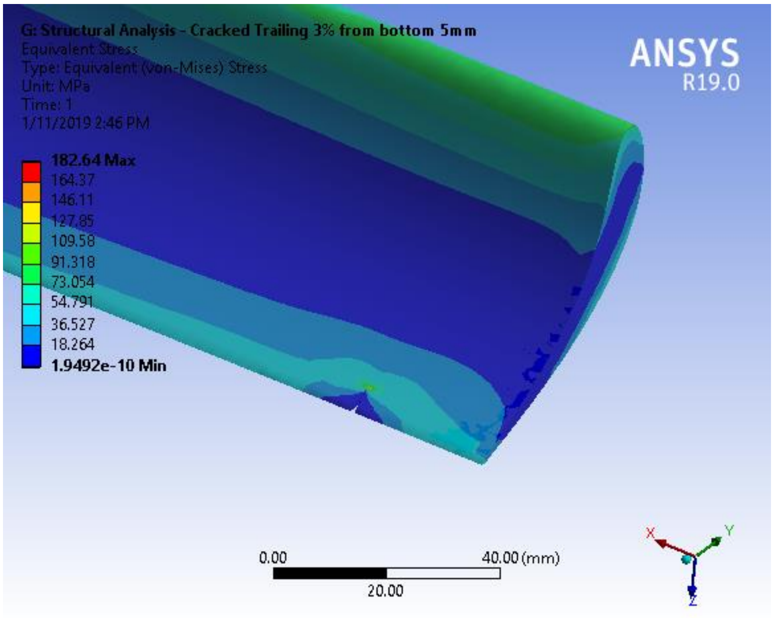
G: Structural Analysis - Cracked Trailing 3% from bottom 5mm
Equivalent Stress
Type: Equivalent (von-Mises) Stress
Unit: MPa
Time: 1
1/11/2019 2:46 PM
ANSYS
R19.0
182.64 Max
164.37
146.11
127.85
109.58
91.318
73.054
54.791
36.527
18.264
1.9492e-10 Min
0.00
20.00
40.00 (mm)
X
Y
Z

BLADE WITH 10 MM CRACK ON TRAILING EDGE

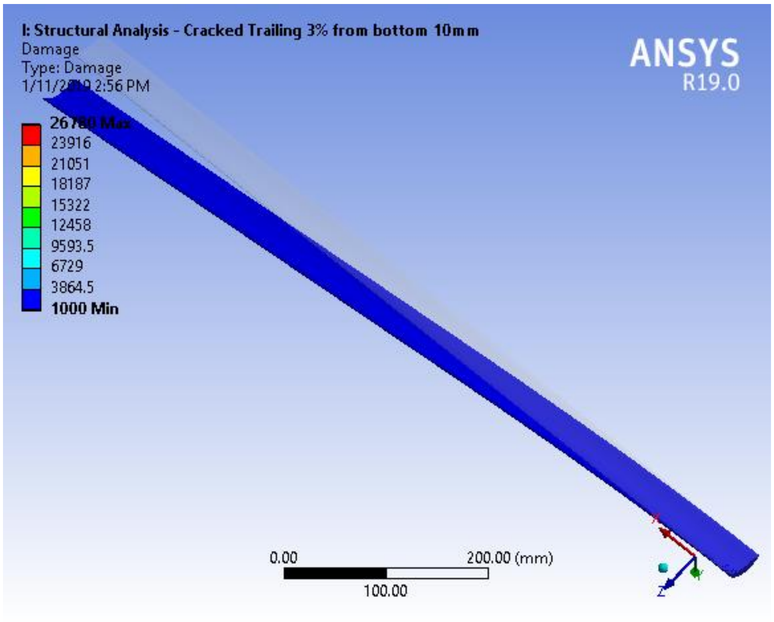

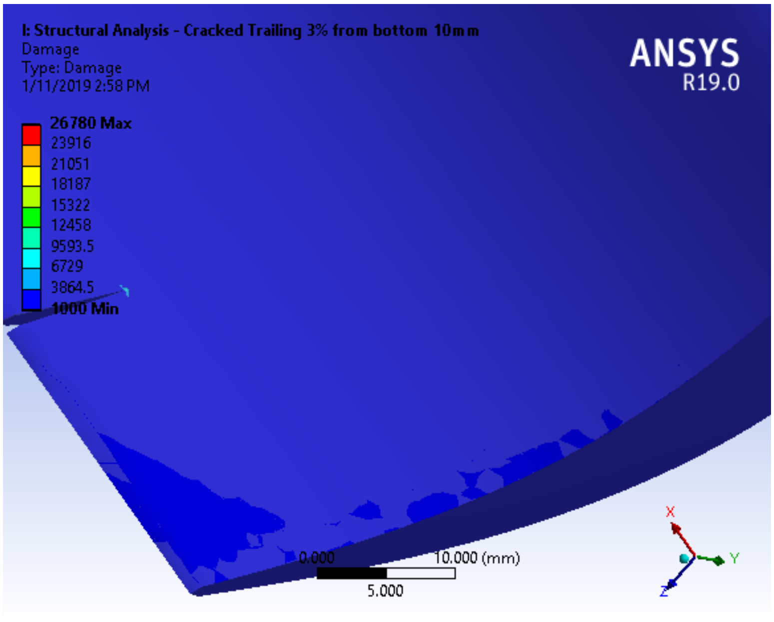

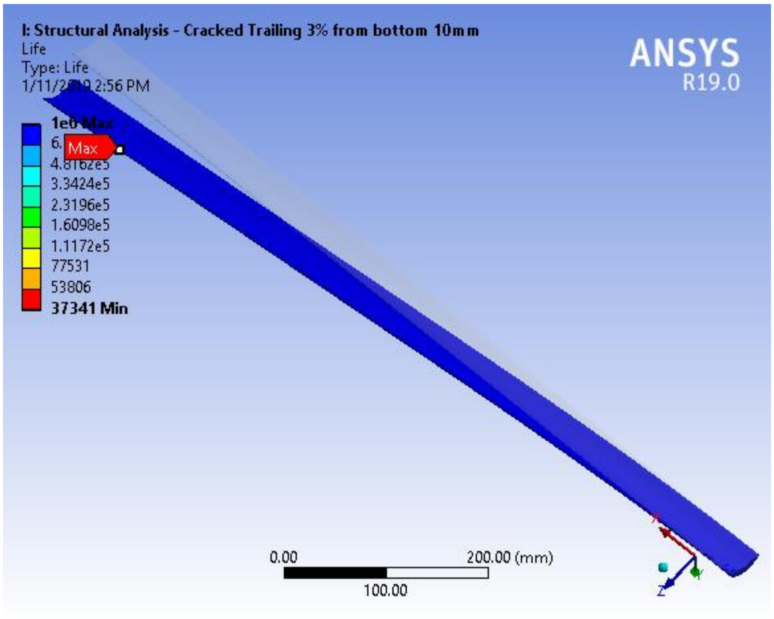
I: Structural Analysis - Cracked Trailing 3% from bottom 10mm
Life
Type: Life
1/11/2019 2:56 PM
1e6 Max
4.8162e5
3.3424e5
2.3196e5
1.6098e5
1.1172e5
77531
53806
37341 Min
Max
ANSYS
R19.0
0.00
200.00 (mm)
100.00

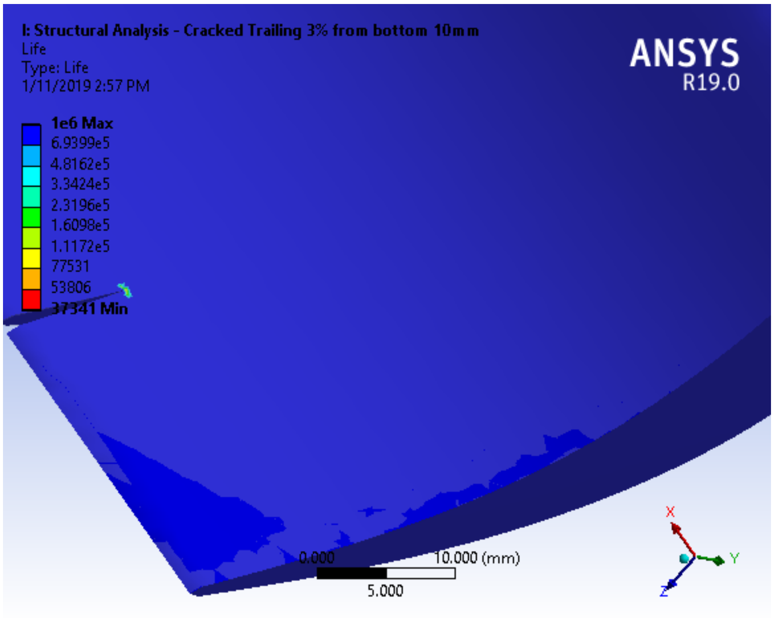
I: Structural Analysis - Cracked Trailing 3% from bottom 10mm
Life
Type: Life
1/11/2019 2:57 PM
1e6 Max
6.9399e5
4.8162e5
3.3424e5
2.3196e5
1.6098e5
1.1172e5
77531
53806
37341 Min
ANSYS
R19.0
0.000
10.000 (mm)
5.000

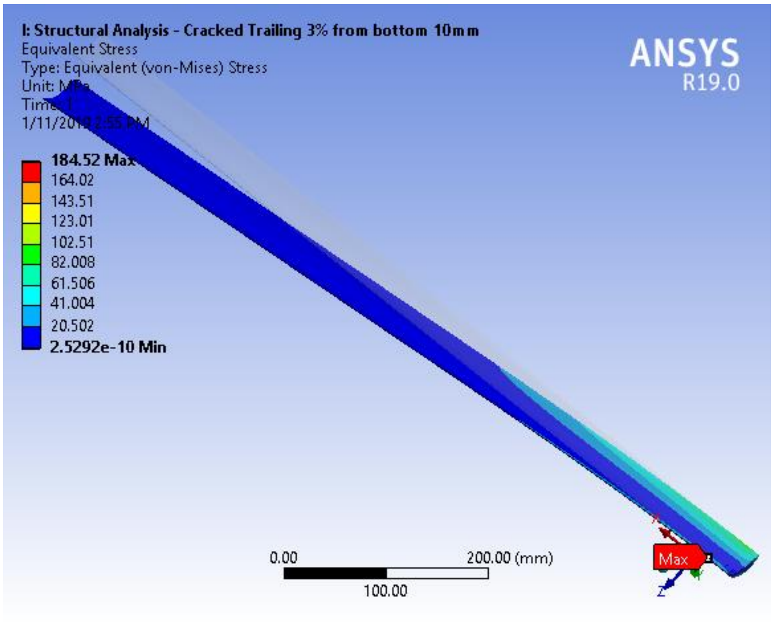
I: Structural Analysis - Cracked Trailing 3% from bottom 10mm
Equivalent Stress
Type: Equivalent (von-Mises) Stress
Unit: MPa
Time: 1
ANSYS
R19.0
184.52 Max
164.02
143.51
123.01
102.51
82.008
61.506
41.004
20.502
2.5292e-10 Min
0.00
200.00 (mm)
100.00
Max

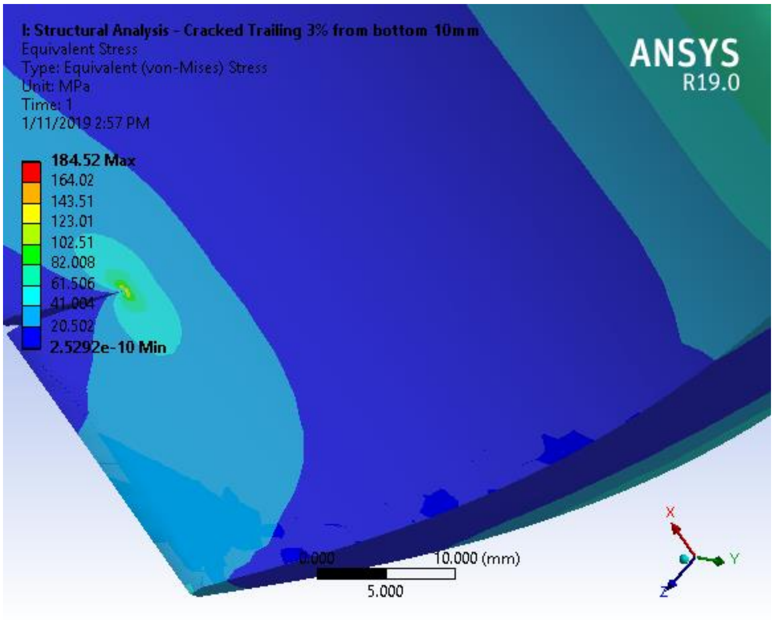
I: Structural Analysis - Cracked Trailing 3% from bottom 10mm
Equivalent Stress
Type: Equivalent (von-Mises) Stress
Unit: MPa
Time: 1
1/11/2019 2:57 PM
ANSYS
R19.0
184.52 Max
164.02
143.51
123.01
102.51
82.008
61.506
41.004
20.502
2.5292e-10 Min
0.000
10.000 (mm)
5.000
X
Y
Z

BLADE WITH 5 MM CRACK ON LEADING TIP & TRAILING EDGE

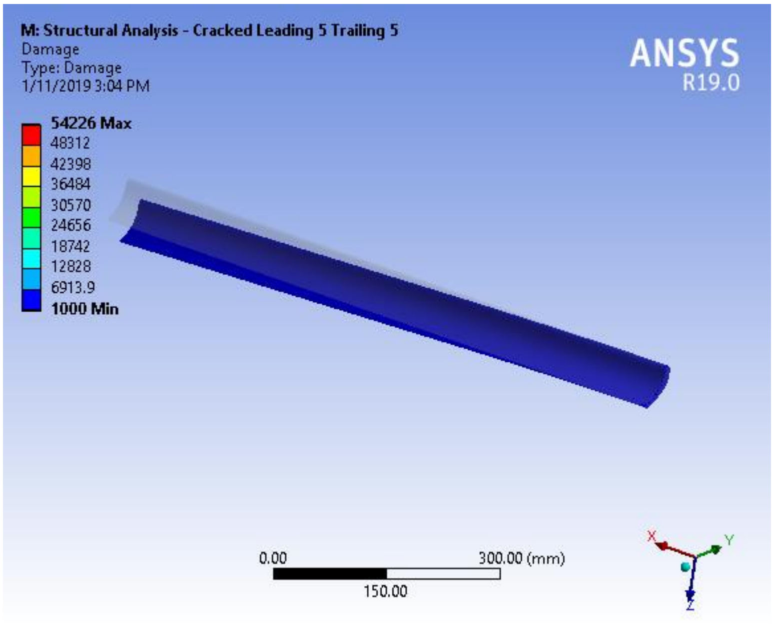

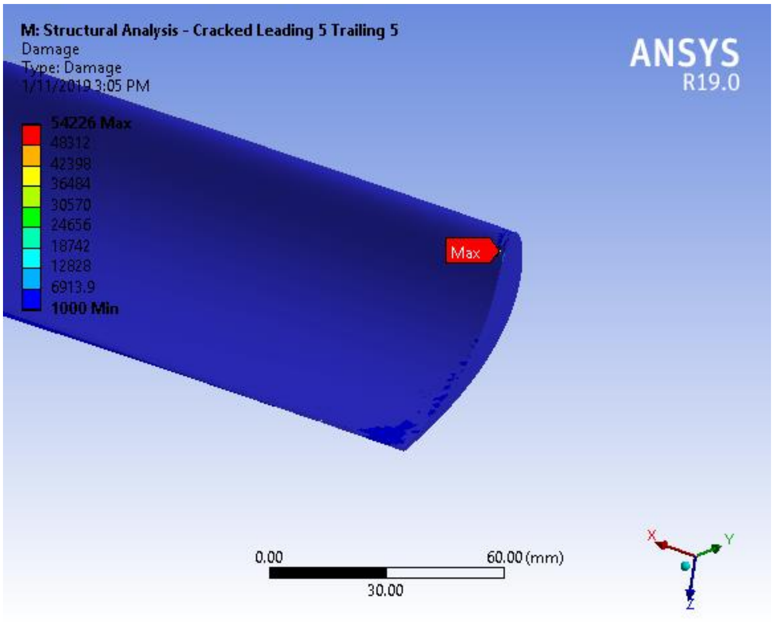

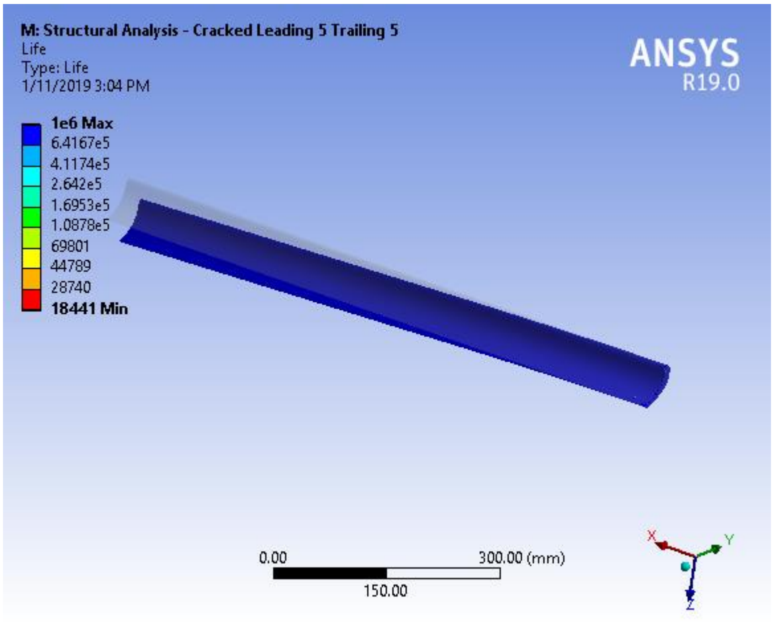
M: Structural Analysis - Cracked Leading 5 Trailing 5
Life
Type: Life
1/11/2019 3:04 PM
1e6 Max
6.4167e5
4.1174e5
2.642e5
1.6953e5
1.0878e5
69801
44789
28740
18441 Min
ANSYS
R19.0
0.00
150.00
300.00 (mm)
X
Y
Z

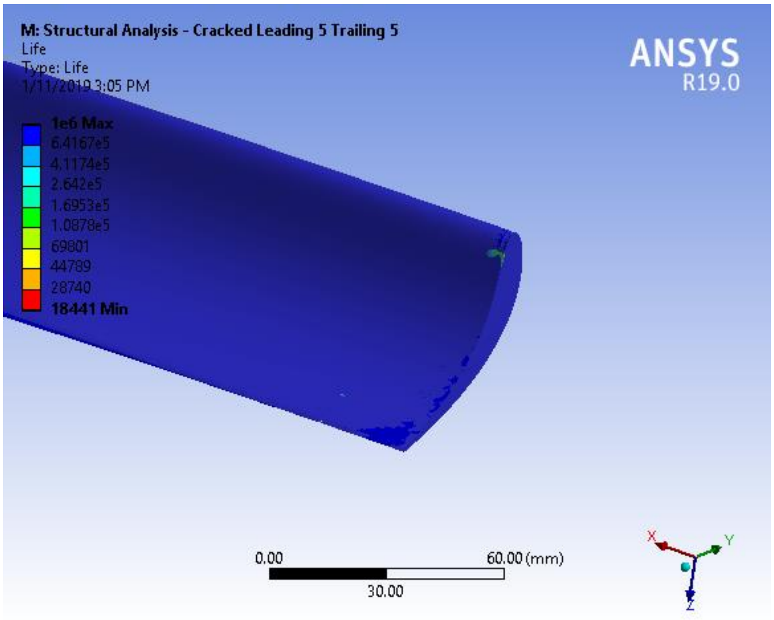
M: Structural Analysis - Cracked Leading 5 Trailing 5
Life
Type: Life
1/11/2019 3:05 PM
1e6 Max
6.4167e5
4.1174e5
2.642e5
1.6953e5
1.0878e5
69801
44789
28740
18441 Min
ANSYS
R19.0
0.00
30.00
60.00 (mm)
X
Y
Z

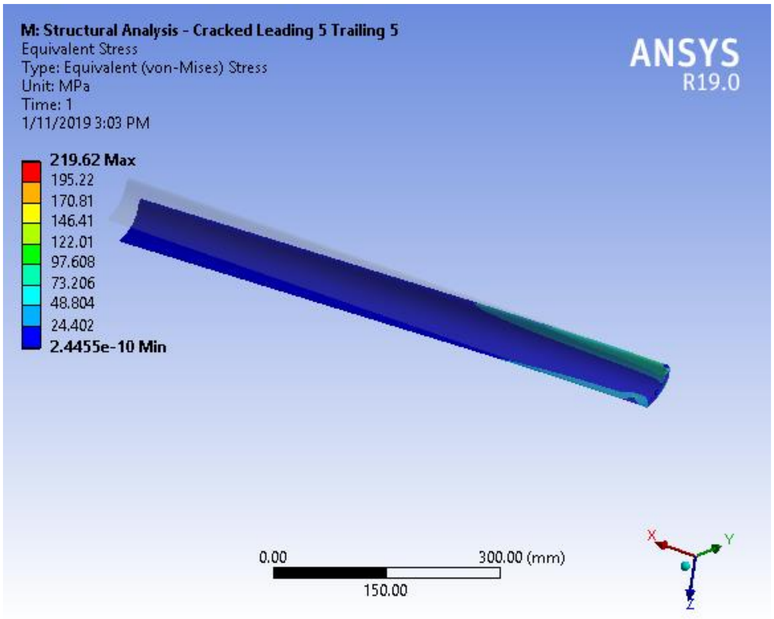
M: Structural Analysis - Cracked Leading 5 Trailing 5
Equivalent Stress
Type: Equivalent (von-Mises) Stress
Unit: MPa
Time: 1
1/11/2019 3:03 PM
ANSYS
R19.0
219.62 Max
195.22
170.81
146.41
122.01
97.608
73.206
48.804
24.402
2.4455e-10 Min
0.00
300.00 (mm)
150.00
X
Y
Z

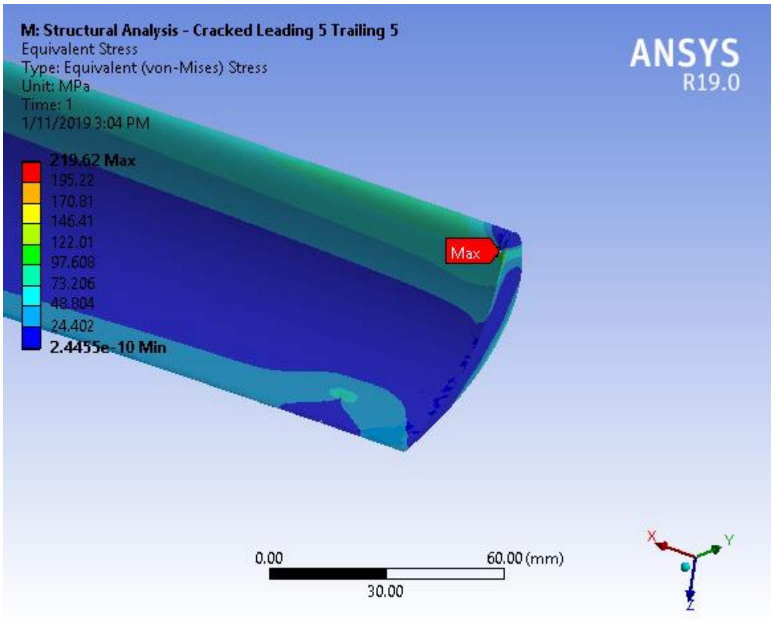
M: Structural Analysis - Cracked Leading 5 Trailing 5
Equivalent Stress
Type: Equivalent (von-Mises) Stress
Unit: MPa
Time: 1
1/11/2019 3:04 PM
ANSYS
R19.0
219.62 Max
195.22
170.81
146.41
122.01
97.608
73.206
48.804
24.402
2.4455e-10 Min
Max
0.00
60.00 (mm)
30.00
X
Y
Z

AUTHOR BIOGRAPHY

Fadilah Kurnia is a student of Marine Engineering Department (Joint Degree Wismar University of Applied Science, Germany) Faculty of Marine Technology, Institut Teknologi Sepuluh Nopember specialized in Marine Manufacturing and Design. He was born in Cilacap, Central Java on August 15th 1997. He completed his Senior High School at SMAN 1 Surabaya in 2015, Junior High School at SMP Ta'miriyah Surabaya in 2012 and Elementary School at SD Al-Irsyad 02 Cilacap in 2009. During his study in University he was active in several organizations and projects. He took the position as Team Manager of ITS Marine Solar Boat Team (Institutional Research Team) 2016/2018, Staff of Public Relation and Communication Department of Society of Petroleum Engineers (SPE) Student Chapter ITS 2016/2017, Coordinator of Sponsorship Division of Petrolida 2018, Coordinator of Liaison Officer of Petrolida 2017, Staff of Publication and Documentation of Petrolida 2016, and Staff of Fundraising Division of Marine Icon 2016. He also has speaking experiences on LKMM TD 2018 by Himpunan Mahasiswa Mekatronika PENS, Basic Media Schooling 2018 by Himpunan Mahasiswa Teknik Sistem Perkapalan ITS, and Public Relation Training 2018 by Badan Eksekutif Mahasiswa Fakultas Teknologi Kelautan ITS. He participated in Winter University Program 2018 in Darmstadt University of Applied Science, Germany and Solar Sport One 2018 Competition in Netherland. He holds internship certificates in PT Industri Kapal Indonesia, Makassar, Indonesia and PT Samudera Indonesia, Jakarta, Indonesia. For further discussion and suggestion regarding this bachelor thesis, the author can be reached through his email: fadilkurnia15@gmail.com